Fibrations in CICY threefolds

Lara B. Anderson,[a] Xin Gao,[a] James Gray[a] and Seung-Joo Lee[a,b]

[a]*Physics Department, Robeson Hall, Virginia Tech,*
Blacksburg, VA 24061, U.S.A.

[b]*European Organization for Nuclear Research (CERN),*
CH-1211 Genève 23, Switzerland

E-mail: lara.anderson@vt.edu, xingao@vt.edu, jamesgray@vt.edu,
seungsm@vt.edu

Abstract: In this work we systematically enumerate genus one fibrations in the class of $7,890$ Calabi-Yau manifolds defined as complete intersections in products of projective spaces, the so-called CICY threefolds. This survey is independent of the description of the manifolds and improves upon past approaches that probed only a particular algebraic form of the threefolds (i.e. searches for "obvious" genus one fibrations as in [1, 2]). We also study K3-fibrations and nested fibration structures. That is, K3 fibrations with potentially many distinct elliptic fibrations. To accomplish this survey a number of new geometric tools are developed including a determination of the full topology of all CICY threefolds, including triple intersection numbers. In $2,946$ cases this involves finding a new "favorable" description of the manifold in which all divisors descend from a simple ambient space. Our results consist of a survey of obvious fibrations for all CICY threefolds and a complete classification of all genus one fibrations for $4,957$ "Kähler favorable" CICYs whose Kähler cones descend from a simple ambient space. Within the CICY dataset, we find $139,597$ obvious genus one fibrations, $30,974$ obvious K3 fibrations and $208,987$ nested combinations. For the Kähler favorable geometries we find a complete classification of $377,559$ genus one fibrations. For one manifold with Hodge numbers $(19, 19)$ we find an explicit description of an infinite number of distinct genus-one fibrations extending previous results for this particular geometry that have appeared in the literature. The data associated to this scan is available here [3].

Contents

1 Introduction: fibrations in Calabi-Yau threefolds

Calabi-Yau manifolds admitting fibrations have long played a central role in the study of string compactifications. This has included bringing to light remarkable string dualities including heterotic/Type IIA duality, heterotic/F-theory duality and F-/M-theory duality, among others. Crucially, because F-theory arises from a "geometrization" of the axio-dilaton of Type IIB string theory [4], the structure of effective theories in this context is intrinsically linked to the geometry of elliptically (or more generally, genus one) fibered Calabi-Yau (CY) manifolds. In addition, genus one fibered CY geometries are significant because they provide an important foothold into attempts to classify *all compactification geometries* since the set of all genus one fibered CY 3-folds has been proven to be finite [5]. Recent progress [6] has given evidence of finiteness for genus one fibered CY 4- and 5-folds as well. From a mathematical perspective, these classifications [5, 7] were motivated by the hope that they could provide tools which might be used to establish the finiteness of the set of all CY n-folds. However, despite these hopes, and the manifest utility of CY fibrations for string dualities, for many years it was generally thought that CY manifolds which admit fibrations (i.e. genus-one, $K3$, or abelian surface fibrations) would likely be rare within the set of all CY geometries.

Recent work has made clear that, in fact, the vast majority of all known Calabi-Yau manifolds are genus-one fibered [1, 2, 8–11]. Further, these manifolds also appear to be generically multiply fibered, that is that they can be written in more than one way as a genus-one fibration, over topologically distinct bases [1, 2, 8, 12]. More explicitly, a *multiply elliptically fibered* (or genus one fibered in the case without section) CY n-fold admits multiple descriptions of the form $\pi_i : X_n \longrightarrow B_{n-1}^{(i)}$ with elliptic fiber $\mathbb{E}_{(i)b} = \pi^{-1}(b \in B_{n-1}^{(i)})$ (denoted succinctly by $\pi_i : X_n \xrightarrow{\mathbb{E}_{(i)}} B_{n-1}^{(i)}$). That is,

$$
\begin{array}{ccc}
 & X_n & \\
\mathbb{E}_{(1)} \swarrow & \downarrow \mathbb{E}_{(2)} & \searrow \mathbb{E}_{(i)} \\
B_{n-1}^{(1)} & B_{n-1}^{(2)} \cdots & B_{n-1}^{(i)}
\end{array}
\tag{1.1}
$$

For each fibration, π_i, the form of the associated Weierstrass model [13], the structure of the singular fibers, discriminant locus, fibral divisors and Mordell-Weil group can all be different, as can the topology of the base manifolds $B_{n-1}^{(i)}$. Initial steps to explore such

prolific fibration structures were taken for CICY four-folds in [1] and some examples were studied for three-folds in [2].

In this work, we will be focused on *systematically enumerating such fibration structures* for a simple dataset of CY threefolds. To begin, we will consider a dataset that is sufficiently large in scope to be interesting, but small enough to be tractable — the set of 7890 CY manifolds constructed as complete intersections in products of projective spaces (CICYs) [1, 14–16]. However many of the tools and observations could equally well be applied to complete intersections in toric varieties [8, 17, 18] or the recently constructed gCICY manifolds [19–23].

A CICY manifold can be described by a so-called "configuration matrix" which encodes the data essential to the algebraic definition of the manifold. In general, a three-fold X can be defined as the complete intersection of K polynomials, p_α where $\alpha = 1, \cdots, K$, in an ambient space, $\mathcal{A} = \mathbb{P}^{n_1} \times \cdots \times \mathbb{P}^{n_m}$. The polynomials p_α are sections of appropriate line bundle $\mathcal{O}_\mathcal{A}(a_\alpha^1, \cdots, a_\alpha^m)$, with $a_\alpha^r \geq 0$ specifying the non-negative homogeneous degree of p_α in the r-th projective piece. Here the indices $r, s, \cdots = 1, \cdots, m$ are used to label the projective ambient space factors $\mathbb{P}^{n_r}$, and the indices $\alpha, \beta, \cdots = 1, \cdots, K$, to label the polynomials, p_α. A family of such geometries can be characterized by a configuration matrix of the form,

$$
X = [\mathcal{A} \,||\, \{\mathbf{a}_\alpha\}] = \begin{bmatrix} \mathbb{P}^{n_1} & a_1^1 & \cdots & a_K^1 \\ \mathbb{P}^{n_2} & a_1^2 & \cdots & a_K^2 \\ \vdots & \vdots & \ddots & \vdots \\ \mathbb{P}^{n_m} & a_1^m & \cdots & a_K^m \end{bmatrix} \tag{1.2}
$$

where

$$
\dim_\mathbb{C} X = \sum_{r=1}^m n_r - K = 3 \,, \tag{1.3}
$$

and the Calabi-Yau condition leads to the degree constraints,

$$
n_r + 1 = \sum_{\alpha=1}^K a_\alpha^r \,, \tag{1.4}
$$

for each $r = 1, \cdots, m$.

Within this dataset, *many fibration structures are "obvious" from the form of the configuration matrix above*. It should be noted that it is possible to perform arbitrary row and column permutations on a configuration matrix without changing the geometry that is described. These operations simply correspond to reordering the $\mathbb{P}^{n_r}$ ambient factors and the hypersurface equations, respectively. Thus, we can ask whether the configuration matrix can be put in the following form by row and column permutations:

$$
X = \begin{bmatrix} \mathcal{A}_1 & 0 & \mathcal{F} \\ \mathcal{A}_2 & \mathcal{B} & \mathcal{T} \end{bmatrix} \,. \tag{1.5}
$$

where $\mathcal{A}_1$ and $\mathcal{A}_2$ are both products of projective spaces, while $\mathcal{F}, \mathcal{B}$ and $\mathcal{T}$ are block sub-matrices. Such a configuration matrix describes a fibration of the manifold described by

$[\mathcal{A}_1|\mathcal{F}]$ over the base $[\mathcal{A}_2|\mathcal{B}]$ where the "twisting" of the fibre over the base is determined by the matrix $\mathcal{T}$. Therefore, as long as the number of columns of $\mathcal{F}$ and the dimension of $\mathcal{A}_1$ are such that $\mathcal{F}$ is of complex dimension 1, (1.4) guarantees that the fibers will be Calabi-Yau one-folds: that is genus-one curves. It follows that the base of the fibration will then be of complex dimension $n-1$.

As a simple example, consider the following configuration matrix defining the tetra-quadric threefold:

$$X_{\{4,68\}} = \left[\begin{array}{c|c} \mathbb{P}^1 & 2 \\ \mathbb{P}^1 & 2 \\ \mathbb{P}^1 & 2 \\ \mathbb{P}^1 & 2 \end{array} \right] \tag{1.6}$$

as a single hypersurface of multi-degree $\{2,2,2,2\}$ in a product of four $\mathbb{P}^1$ factors. By choosing a point in a surface defined by any two ambient $\mathbb{P}^1$ factors, it is clear that the defining equation takes the form of a genus one curve defined via a $\{2,2\}$ hypersurface in the remaining $\mathbb{P}^1 \times \mathbb{P}^1$ factors. Thus, this manifold can be described as a genus one fibration $\pi : X \to \mathbb{P}^1 \times \mathbb{P}^1$. There are 6 distinct (but equivalent) fibrations of this type. Likewise, there are 4 manifest $K3$ fibrations, $\rho : X \to \mathbb{P}^1$, in which the $K3$ fiber is itself genus one fibered and is described as a $\{2,2,2\}$ hypersurface in a product of three $\mathbb{P}^1$ factors.

Fibers of the type described above — evident from the algebraic description of the manifold — have been referred to as Obvious Genus-One Fibrations (OGFs). As noted above, nearly all CICYs admit multiple fibrations of this kind. Of the 7,890 CICY threefold configuration matrices it was noted in [2] that 7,837 admit at least one such fibration, with the average number of inequivalent obvious fibrations per manifold being 9.85. For the CICY four-folds, the percentage of obviously fibered manifolds is even higher with 921,420 out of 921,497 cases admitting such a fibration (here the average manifold can be described as OGF in 54.6 different ways [1]).

It is important to note however, that the existence of such obvious fibration structures can be dependent on the algebraic form of the manifold and hence, potentially incomplete. For example, consider the following CY threefold with Hodge numbers $(h^{1,1}, h^{1,2}) = (6, 51)$.

$$X_{\{6,51\}} = \left[\begin{array}{c|ccc} \mathbb{P}^2 & 2 & 0 & 1 \\ \mathbb{P}^1 & 1 & 1 & 0 \\ \mathbb{P}^3 & 0 & 1 & 3 \end{array} \right] \tag{1.7}$$

By inspection, this manifold admits two obvious genus one fibrations of the form described in (1.5), $\pi_1 : X_{\{6,51\}} \to \mathbb{P}^2$ and $\pi_2 : X_{\{6,51\}} \to dP_4$ where dP_4 denotes the fourth del Pezzo surface ($\mathbb{P}^2$ blown up at four generic points). These can be seen by splitting the configuration matrix up into two pieces, one describing the base and the other the fiber.

$$\left[\begin{array}{c|ccc} \mathbb{P}^1 & 1 & 1 & 0 \\ \mathbb{P}^3 & 0 & 1 & 3 \\ \hline \mathbb{P}^2 & 2 & 0 & 1 \end{array} \right] \quad , \quad \left[\begin{array}{c|ccc} \mathbb{P}^3 & 0 & 1 & 3 \\ \hline \mathbb{P}^1 & 1 & 1 & 0 \\ \mathbb{P}^2 & 2 & 0 & 1 \end{array} \right] . \tag{1.8}$$

In the first case, the rows of the configuration matrix have been reordered to separate the $\mathbb{P}^2$ base from the fiber and in the second case, the base surface

$$dP_4 = \left[\begin{array}{c|c} \mathbb{P}^1 & 1 \\ \mathbb{P}^2 & 2 \end{array} \right] \tag{1.9}$$

has been made clear. In each case if any point is selected on the base manifold, substituting the coordinates of this point into the remaining defining relations leads to (a specific complex structure and) equations which now depend only upon the coordinates in the first projective space factors (given above the dotted horizontal line in the two cases above). The degrees of the equations in the remaining variables satisfy (1.4) thus, these equations describe a Calabi-Yau one-fold — a torus. If the choice of point in the base is varied, the complex structure describing the associated torus fiber will change, and so it is clear that each of the configuration matrices in (1.8) is a non-trivial fibration of a genus-one curve over that base. However, it must be noted that the description given in (1.7) is not unique. The *same CY manifold* can also be described by the configuration matrix:

$$\tilde{X}_{\{6,51\}} = \left[\begin{array}{c|ccccc} \mathbb{P}^3 & 0 & 0 & 0 & 1 & 3 \\ \mathbb{P}^1 & 0 & 0 & 1 & 1 & 0 \\ \hline \mathbb{P}^2 & 1 & 1 & 1 & 0 & 0 \\ \mathbb{P}^2 & 1 & 1 & 0 & 0 & 1 \end{array} \right]. \tag{1.10}$$

This description makes evident yet another fibration $\pi_3 : \tilde{X}_{\{6,51\}} \to dP_3$ given by

$$dP_3 = \left[\begin{array}{c|cc} \mathbb{P}^2 & 1 & 1 \\ \mathbb{P}^2 & 1 & 1 \end{array} \right]. \tag{1.11}$$

The existence of OGF structures has also been observed in other constructions of CY manifolds (e.g. toric [17], gCICY constructions [19] and CY quotient geometries [24, 25]) and its ubiquitous nature is suggestive of the fact that most CY manifolds with large enough topology may admit a genus one fibration. However, the above example illustrates that any characterization of fibrations that relies on one algebraic description of a given CY manifold is destined to be incomplete and that a *full classification can only be possible via criteria that rely only on the fundamental topology of the CY manifold*. Fortunately, just such a tool exists for CY 3-folds and we will employ it in this work.

1.1   Criteria for the existence of a genus one fibration

Throughout this work we will refer to a fibration in which the generic fiber is a complex curve of genus one as a *genus one fibration*.[1] The existence of a genus-one fibration in a Calabi-Yau n-fold has been conjectured by Kollár [26] to be determined by the following criteria:

---

[1]Sometimes in the literature the terms "elliptic fibration" and "genus one fibration" are used interchangeably. Here we will follow the convention that an elliptic fibrations is a genus one fibration with section. In the present work we do not attempt to identify sections in our classification of genus one fibrations (although tools to do this for CICYs have recently been developed in [29]).

Conjecture [26]: *let X be a Calabi-Yau n-fold. Then X is genus-one fibered iff there exists a $(1,1)$-class D in $H^2(X, \mathbb{Q})$ such that $D \cdot C \geq 0$ for every algebraic curve $C \subset X$, $D^{\dim(X)} = 0$ and $D^{\dim(X)-1} \neq 0$.*

In the case that X is a Calabi-Yau threefold this conjecture has been proven by Oguiso and Wilson subject to the additional constraints that D is effective or $D \cdot c_2(X) \neq 0$ [27, 28]. Phrased simply these criteria are characterizing the existence of a fibration by *characterizing a particular divisor in the base manifold of that fibration*. In particular, the role of the divisor D above is that of a pull-back of an ample divisor in the base, B, where the fibration of X is written $\pi : X \to B$. Such a divisor in X is sometimes referred to as *semi-ample* [26]. The existence of $D = \pi^*(D_{base})$ makes it possible to define the form dual to points on the base (i.e. $D^{\dim(X)-1}$) which in turn determines the class of the genus-one fiber itself.[2] While Kollár's conjecture has yet to be proven for CY manifolds in arbitrary dimensions, for threefolds, this is a well-established if and only if condition that can be used to determine whether or not fibrations exist. In this paper we will employ the criteria above to enumerate all genus one fibrations in a set of CICY 3-folds ($K3$ fibrations will also be enumerated using different means in section 3). Throughout this work, we will refer to an effective divisor satisfying the criteria in the conjecture above to be a "Kollár divisor".

Before beginning such an enumeration, it should be noted that there can in fact be many divisors D of the form above for a single fibration structure in X. Thus, to count fibrations using this tool, the question of redundancy must be addressed. For a given fibration $\pi : X \to B$ there are in general, an infinite number of divisors $D \subset X$ satisfying the criteria above. For example, for a fibration $\pi : X \to \mathbb{P}^2$ not only will the pull-back of the hyperplane class, H, of the base $\mathbb{P}^2$, satisfy $D^2 \neq 0$ and $D^3 = 0$, but also any multiple of it, aH for $a \in \mathbb{Z}_{>0}$. This is not surprising since for any value of a, D^2 defines both a good volume form for $\mathbb{P}^2$ and the class of one or more fibers (i.e. a^2 fibers) of $\pi : X \to B$.

To eliminate this redundancy of counting, we will consider two divisors $D, D' \subset X$ to define *generically the same fibration* if the fiber classes they define are proportional curves within X. That is,

$$D^2 \sim D'^2 \quad \text{as curves in } X \tag{1.12}$$

If this proportionality is satisfied, there are two immediate possibilities that are likely to arise: a) The fibers are proportional as in (1.12) and as in the $\pi : X \to \mathbb{P}^2$ example above, are associated to the same base and hence, the same fibration (in this case D and D' just count multiple copies of the same fundamental fiber class) or b) The two fibrations differ at non-generic points over the base. This case would be expected in cases where the two base geometries (associated to D and D') are birational. We will study such possibilities in detail in sections 5 and appendix A.2. Throughout this work, the criteria in (1.12) will be most useful to us to establish that when proportionality fails, the two possible fibrations are definitely distinct (and not even birational).

---

[2]It should be noted that the existence of a fibration structure within a smooth Calabi-Yau n-fold with $n > 2$ is a deformation invariant quantity (i.e. given a fibered manifold, every small deformation is also fibered) [26, 28, 30]. Indeed this must clearly be the case if the above conjecture is to make sense.

Finally, we note that since triple intersection numbers of divisors in CY threefolds are generally easier to compute than double intersection numbers, we will frequently apply this test as

$$D \cdot D \cdot D_r = aD' \cdot D' \cdot D_r \qquad (1.13)$$

for some a and every divisor D_r, $r = 1, \ldots h^{1,1}$ in the basis.

With these results in hand, we turn now to a brief summary of our approach and key results.

1.2 Enumeration of fibrations and key results

The goal of this work is to systematically count genus one fibrations in the dataset of CICY threefolds. There are two distinct ways that we undertake this study:

1. By enumerating obvious fibrations (OGFs as defined in section 1) that are apparent from the given algebraic (in this case complete intersection) form of the CY geometry.

2. By utilizing the criteria in section 1.1 to scan for possible base divisors D and thereby to systematically enumerate all fibrations.

Since all surveys in the literature to date have involved the first approach, we will be interested in undertaking both and comparing the totals where possible. In addition, we would like to probe other fibration structures (i.e. $K3$- or Abelian Surface fibrations). It should also be noted that at present the "obvious" fibration approach is our only tool to count $K3$ fibrations or to consider compatible (i.e. nested) $K3$ and genus-one fibrations.

It is clear from the Kollár-Oguiso-Wilson criteria laid out in section 1.1 that a systematic search for genus-one fibrations must begin with a clear determination of all intersection numbers in the CY geometry as well as the structure of the Kähler and Mori cones. Despite the fact that the CICY dataset has existed for nearly 30 years, this information was still incomplete for the majority of manifolds in the list. In the following sections we compute the triple intersection numbers of all CICY threefolds and provide a description of the Kähler and Mori cones for the subset of "Kähler Favorable" geometries whose Kähler/Mori cones descend in a simple way from an ambient space. For this subset of 4957 manifolds out of 7890, we are able to completely classify all genus one fibrations.

Thus our first results, laid out in section 2 are,

- Algorithmic tools are developed to systematically replace CICY configuration matrices with new descriptions that provide an easy determination of their topological data (i.e. Hodge numbers, $c_2(X)$ and triple intersection numbers, d_{rst}, $r = 1, \ldots h^{1,1}$). We construct this complete topological data for *all CICY threefolds*.[3]

- For the 4957 Kähler favorable geometries their Kähler and Mori cones are constructed explicitly. 4874 of these geometries are Kähler favorable with respect to an ambient

---

[3]It would be interesting to use this data to investigate the number of distinct Calabi-Yau threefolds described by the CICY configuration matrices, in line with the work in [31]. We thank the referee for making this suggestion.

product of projective spaces and 83 are Kähler favorable with respect to an ambient space defined as the product of two almost del Pezzo surfaces.

With these tools available, we then undertake the fibration surveys described above. In section 3 we enumerate obvious fibration structures extending the tools developed in [1, 2, 20, 29]. These are applied to all 7868 CICY threefolds which are not direct products. We find

- 139, 597 obvious genus one fibrations.

- 30, 974 obvious K3 fibrations.

- 208, 987 distinct nestings of these fibrations.

In section 4 we complete a scan for Kollár divisors of the type described in section 1.1 for the 4874 Kähler favorable geometries descending from an ambient space of the form $\mathbb{P}^{n_1} \times \ldots \times \mathbb{P}^{n_m}$ and compare this to the OGF count for these manifolds. We find that here

- The number of OGF fibrations exactly matches the exhaustive list of fibrations (obtained by counting Kollár divisors). In these cases the (special) chosen algebraic form of the manifold has captured all relevant fibration structures.

Finally, there remains to consider the 83 CICY configurations which are Kähler favorable with respect to an ambient space of the form $S \times S'$ where S, S' are almost del Pezzo surfaces (i.e. $\mathbb{P}^1 \times \mathbb{P}^1$, dP_r with $r = 0, \ldots 7$ or the smooth rational elliptically fibered surface denoted as dP_9 in the physics literature). This class of geometries is studied in sections 5 and 6. For these CY geometries

- For the 83 CICYs defined as hypersurfaces in a product of almost del Pezzo surfaces, the criteria given in section 1.1 produce vastly more fibrations than the OGF count.

- More precisely, for the CYs defined as an anticanonical hypersurface in a product of two del Pezzo surfaces, we find 327, 340 fibrations, of which at most 1, 289 are OGFs.

- Combining the counts of genus-one fibrations classified in all Kähler favorable geometries (with ambient spaces consisting of products of projective spaces and almost del Pezzo surfaces) we provide a complete classification of 377, 559 fibrations in total on 4, 957 manifolds.

- For one manifold — the threefold[4] with Hodge numbers $(h^{1,1}, h^{2,1}) = (19, 19)$ — our survey yields an infinite number of genus-one fibrations.

Finally, in sections 7 we provide an overview of our conclusions and future applications of this work. The appendices provide a collection of useful technical results. All of the data outlined above, including a new augmented CICY list (with complete topological data), and all the fibration data described is publicly available at [3] and in part through an arXiv

---

[4]Sometimes referred to as the "Schoen" manifold (due to its study in [33]) or the "split bi-cubic" (from its original inclusion in [16]).

attachment associated to this work. The exception to this are the intersection numbers of the CICYs which can quickly be computed in all cases using the results of this paper. The size of the data associated to these invariants means that it is more efficient to compute them as needed rather than tabulate their values.

2 Completing the topological data of the CICY 3-folds: intersection numbers and Kähler cones

As described in the Introduction, in any attempt to systematically classify all genus one fibrations within a dataset of Calabi-Yau manifolds, it must first be possible to fully determine, for each manifold, X:

- The Kähler and Mori Cones of X.

- The triple intersection numbers of all effective divisors on X.

In this section we attempt to characterize both of these structures as far as possible for the entire CICY threefold dataset using all available tools. We will begin with a systematic approach to determining the Picard groups of CICY threefolds.

2.1 Splitting configuration matrices to produce favorable descriptions

In the context of this work, when all divisors (equivalently the Picard group) of a Calabi-Yau three-fold X descend from the simple ambient space $\mathcal{A}$, we refer to it as a "favorable" geometry [32]. To determine explicitly when this occurs, consider the adjunction sequence and its dual:

$$0 \to TX \to T\mathcal{A}|_X \to \mathcal{N}|_X \to 0, \tag{2.1}$$

$$0 \to \mathcal{N}^*|_X \to T\mathcal{A}^*|_X \to TX^* \to 0.$$

The latter induces the long exact sequence in cohomology,

$$\cdots \longrightarrow H^1(X,\mathcal{N}|_X^*) \xrightarrow{\ \alpha\ } H^1(X,T\mathcal{A}|_X^*) \longrightarrow H^1(X,TX^*) \longrightarrow$$

$$\hookrightarrow H^2(X,\mathcal{N}^*|_X) \xrightarrow{\ \beta\ } H^2(X,T\mathcal{A}|_X^*) \longrightarrow H^2(X,TX^*) \longrightarrow \cdots . \tag{2.2}$$

It follows that the Kähler moduli of X can be decomposed as $H^1(X,TX^*) \cong H^{1,1}(X) \cong$ coker(α) $\oplus$ ker(β). These two contributions correspond to the descent of the Kähler moduli on $\mathcal{A}$ to Kähler moduli on X and Kähler forms that arise on X only (i.e. non-toric divisors) . If the contribution from ker(β) is zero, the only divisors on X are those descending from $\mathcal{A}$ (possibly with additional linear relations) and we say the geometry is "favorable". In such a case we see that $h^{1,1}(X) = \dim(H^{1,1}(X)) \leq \dim(\text{Pic}(\mathcal{A}))$. The simplest case of a favorable geometry is when $h^2(X,\mathcal{N}|_X^*) = 0$ (or by Serre duality, when $h^1(X,\mathcal{N}|_X) = 0$). Of the original 7890 configuration matrices in the CICY three-fold dataset [16], there are 4896 favorable geometries (including 22 direct product geometries) and 2994 unfavorable geometries.

For 2994 manifolds then, there are non-toric divisors present from the point of view of the given configuration matrix and it is clear that the standard tools (see for example [34]) will not suffice to determine the required data for a fibration scan. We turn next to one approach to remedying this deficit.

2.1.1 A review of CICY splitting/contraction

To improve this situation, in this work, we make systematic use of a known approach to exchanging one configuration matrix with another that *describes the same CY threefold*. This process, known as "splitting" or "contracting" a CICY has long been utilized in the context of this dataset of manifolds [16]. It was noted early on to be useful in computing Hodge data for example [35]. The original generating algorithm of the CICY threefold dataset was designed to remove many such redundancies from the list.

The notion of splitting/contracting first arose naturally in the context of conifold transitions [36]. For example the famous conifold of the quintic:

$$\left[\, \mathbb{P}^4 \,\middle|\, 5 \,\right]^{1,101} \quad (\text{Def}) \quad \Leftrightarrow l_1 q_2 - l_2 q_1 = 0 \quad (\text{sing.locus}) \quad \Leftrightarrow \quad \begin{bmatrix} \mathbb{P}^1 \\ \mathbb{P}^4 \end{bmatrix} \begin{bmatrix} 1 & 1 \\ 1 & 4 \end{bmatrix}^{2,86} \quad (\text{Res}) \;.$$

Here the left and right configuration matrices form the deformation and resolution sides of the conifold, respectively. The two topologically distinct geometries share a common *singular* locus in their moduli space — in this case the nodal quintic (given in the center above, where l_i and q_i, $i = 1, 2$ are linear and quartic polynomials in the coordinates of $\mathbb{P}^4$). See [36] for a review. An example of a CICY topology changing transition such as this is called an "effective splitting" of the initial manifold (in this case the quintic). However, there is another possibility in that the shared locus in moduli space between two configuration matrices need not be singular. For example, the singularities arise from the nodal quintic above for the 16 points where $l_1 = l_2 = q_1 = q_2 = 0$. On $\mathbb{P}^4$ there exists a common solution to the four equations, however, if the ambient space had been say, $\mathbb{P}^3$, no such solution would exist. When the shared locus in moduli space is *smooth* the splitting operation on the configuration matrix is referred to as an *ineffective splitting*. Because the manifolds described by the initial configuration matrix and its split then share a common smooth locus in moduli space, they are topologically equivalent.

In the remainder of this section, we will use this observation and the technique of "ineffective splitting" to try to determine when it is possible to split an unfavorable configuration matrix of a CICY three-fold to a favorable one. It is clear in principle that such ineffective splittings in general increase the number of rows/columns of the configuration matrix and as a result, will likely change the number of "obvious" genus one fibrations available.

More precisely, a $\mathbb{P}^n$-splitting of a CICY configuration matrix (corresponding to the manifold, X) can be written as follows:

$$X = [\mathcal{A} \,|\, \mathbf{c}\, \mathcal{C}] \longrightarrow X' = \begin{bmatrix} \mathbb{P}^n \\ \mathcal{A} \end{bmatrix} \begin{bmatrix} 1 & 1 & \dots & 1 & \mathbf{0} \\ \mathbf{c}_1 & \mathbf{c}_2 & \dots & \mathbf{c_{n+1}} & \mathcal{C} \end{bmatrix}, \quad \mathbf{c} = \sum_{\alpha=1}^{n+1} \mathbf{c}_\alpha \;. \tag{2.3}$$

We begin with an initial CICY three-fold, X, defined above by a starting configuration matrix of the form $[\mathcal{A} \,|\, \mathbf{c}\, \mathcal{C}]$ where $\mathcal{A} = \mathbb{P}^{n_1} \times \dots \mathbb{P}^{n_m}$ and $\mathbf{c}$ and $\mathcal{C}$ form an $m \times K$ matrix

of polynomial degrees for the K equations defining the complete intersection hypersurface. The first column of this matrix, $\mathbf{c}$, has been explicitly separated from the remainder of the columns, denoted by $\mathcal{C}$, to facilitate the rest of our discussion. Since X is a three-fold, $\sum_{r=1}^{m} n_r - K = 3$. We can "split" X by introducing the new configuration matrix X' where the vector $\mathbf{c}$ has been partitioned as the sum of $n+1$ column vectors $\mathbf{c}_i$ (of dimension m) with nonnegative components, as indicated. Since X' is still a three-fold, the new configuration matrix is $(m+1) \times (K+n)$ dimensional.

While the process of going from X to X' is called "splitting", the reverse process, in which $X' \to X$, is called a "contraction" [16] (see [37] for some work related to tracking bundles through this process). As described above, in some cases, a splitting of the form (2.3) will not produce a new (i.e. topologically distinct) Calabi-Yau three-fold, but rather a new description of the same manifold. As in the case of the quintic above, in either an effective or ineffective splitting, two manifolds X and X' related as in (2.3) share common loci in their complex structure moduli space — the so-called "determinental variety". It is defined as follows. Take the subset of the defining relations of X' corresponding to the first $n+1$ columns on the right hand side of (2.3).

$$
\begin{pmatrix}
f_1^1 & f_2^1 & \cdots & f_{n+1}^1 \\
f_1^2 & f_2^2 & \cdots & f_{n+1}^2 \\
\vdots & \vdots & \ddots & \vdots \\
f_1^{n+1} & f_2^{n+1} & \cdots & f_{n+1}^{n+1}
\end{pmatrix}
\begin{pmatrix}
x_0 \\
x_1 \\
\vdots \\
x_n
\end{pmatrix}
= 0 \,,
\tag{2.4}
$$

Here f_α^k is of degree $\mathbf{c}_\alpha$ for all k. The determinental variety (i.e. shared locus in moduli space) is found by taking the determinant of the matrix in (2.4) and combining it with the remaining equations whose degree is governed by $\mathcal{C}$.

We can thus state more clearly the observation made above: if the two configurations X and X' can be smoothly deformed into each other and hence represent the same topological type of Calabi-Yau manifolds, the splitting is called "ineffective" [16]. Otherwise it is an "effective" splitting. Thus, the question of whether a given splitting is effective or ineffective is decided by whether or not the determinental variety defined via (2.4) is smooth. For all CICY three-fold splittings, the singular locus of the determinental variety is a zero-dimensional space. That is, it can either be the empty set or a collection of points. It turns out that the number of singular points is counted by the difference in Euler characteristic between the original and the split configuration (the 16 singular points lead to $\Delta\chi = 32$ in the example above). This leads to the simple rule that two three-fold configurations, related by splitting as in (2.3), are equivalent if and only if they have the same Euler characteristic. In this case, the splitting is ineffective.

2.1.2 Finding favorable splitting chains

With these definitions in hand, we now turn to the question of when can a chain of ineffective splittings of a configuration matrix take a non-favorable configuration matrix to a favorable one? An important tool in this regard was provided by a small lemma in [38] which we re-state here for completeness:

Lemma 2.1 *Suppose that X and X' are two Calabi-Yau three-folds realized as complete intersections in products of projective spaces and related by a splitting of the type described in (2.3). Let $\mathcal{L} = \mathcal{O}_X(a^1, \ldots, a^m)$ be a "favorable" line bundle on X-that is, a line bundle corresponding to a divisor $D \subset X$ such that $D = D_{\mathcal{A}}|_X$ is the restriction of a divisor $D_{\mathcal{A}}$ in the ambient space. Then the calculation (and dimension) of the cohomology of $\hat{\mathcal{L}} = \mathcal{O}_{X'}(0 \ldots, 0, a^1, \ldots, a^m)$ on X' (defined by (2.3)) is identical to that of $\mathcal{L}$ on X on the locus in complex structure moduli space shared by X and X'.*

See [38] for a proof/discussion.

Returning to the adjunction sequence (2.1) above, we see that a CICY configuration matrix will be potentially non-favorable whenever $h^1(X, \mathcal{N}_X) > 0$ (denoting $\mathcal{N}_X = \mathcal{N}|_X$ as a sum of line bundles on X). Thus, in the process of splitting, we would like to know when it is possible to generate a new configuration matrix such that $h^1(X', \mathcal{N}'_{X'})$ goes to zero? For any CICY configuration matrix, $\mathcal{N}_X$ is simply a sum of line bundles and from the lemma above, it is clear that the line-bundle cohomology of any line bundle, $\mathcal{L} \subset \mathcal{N}_X$, on X does not change if we *do not split* the elements (i.e. partition the multi-degree) of the column in X associated to that component of the normal bundle (i.e. $\mathcal{L}$).

As a result, to find an ineffective split that changes an unfavorable to a favorable manifold, it is not necessary to split any part of $\mathcal{N}_X$ — i.e. column of the configuration matrix — in which the associated line bundle cohomology gives $h^1(X, \mathcal{L}) = 0$. Instead, we will systematically consider splitting only those columns for which the associated line bundle cohomology is non-vanishing and determine whether splitting reduces that number.

To make the somewhat opaque description above more clear, it is useful to illustrate this with an explicit CICY configuration matrix. One example of a non-favorable CICY is given by the following configuration matrix.

$$X = \left[\begin{array}{c|ccc} & \mathcal{L}_1 & \mathcal{L}_2 & \mathcal{L}_3 \\ \hline \mathbb{P}^2 & 2 & 0 & 1 \\ \mathbb{P}^1 & 1 & 1 & 0 \\ \mathbb{P}^3 & 0 & 1 & 3 \end{array} \right]. \tag{2.5}$$

where $(h^{1,1}(X), h^{1,2}(X)) = (6, 51)$ and $\chi(X) = -90$. Since $h^{1,1}(X) = 6$, but only three Kähler forms descend from the ambient projective spaces, this configuration matrix is clearly unfavorable in the original CICY list.

To begin, it can be verified that only one line bundle in $\mathcal{N}_X$ has a non-zero h^1. That is, denoting $\mathcal{N}_X = \mathcal{L}_1 \oplus \mathcal{L}_2 \oplus \mathcal{L}_3$ (with multi-degree given by the columns in (2.5) above), we find the cohomology dimensions: $h^{\bullet}(X, \mathcal{L}_1) = (11, 3, 0, 0)$, $h^{\bullet}(X, \mathcal{L}_2) = (7, 0, 0, 0)$, $h^{\bullet}(X, \mathcal{L}_3) = (59, 0, 0, 0)$. Overall, the dimension of the cohomology of the normal bundle is $h^{\bullet}(X, \mathcal{N}_X) = (77, 3, 0, 0)$. Since $h^1(X, \mathcal{L}_1) \neq 0$, in order to find a favorable description we must begin with a splitting which partitions the column associated to the line bundle $\mathcal{L}_1$.

For this column there is only one split available which will non-trivially partition the entries and add a $\mathbb{P}^1$ factor to the ambient space as:

$$X' = \left[\begin{array}{c|ccc} & \mathcal{L}'_1 & \mathcal{L}_4 & \hat{\mathcal{L}}_{2,3} \\ \hline \mathbb{P}^1 & 1 & 1 & \mathbf{0} \\ \mathcal{A} & \mathbf{c_1} & \mathbf{c_2} & \mathcal{C} \end{array} \right] = \left[\begin{array}{c|cccc} & \mathcal{L}'_1 & \mathcal{L}_4 & \hat{\mathcal{L}}_2 & \hat{\mathcal{L}}_3 \\ \hline \mathbb{P}^1 & 1 & 1 & 0 & 0 \\ \mathbb{P}^2 & 1 & 1 & 0 & 1 \\ \mathbb{P}^1 & 1 & 0 & 1 & 0 \\ \mathbb{P}^3 & 0 & 0 & 1 & 3 \end{array} \right] \tag{2.6}$$

For this new configuration matrix, $h^\bullet(X', \mathcal{L}_1') = (9, 2, 0, 0)$ and $h^\bullet(X', \mathcal{L}_4) = (5, 0, 0, 0)$, while due to the lemma above, the cohomology of $\hat{\mathcal{L}}_{2,3}$ stays the same. It is easy to verify that this splitting is ineffective with $\chi(X') = -90$. Moreover, by performing this $\mathbb{P}^1$-split, the dimension of the first cohomology of the normal bundle decreases from $h^1(X, \mathcal{N}_X) = 3$ to $h^1(X', \mathcal{N}_{X'}') = 2$ while $h^2(X', \mathcal{N}_{X'}') = 0$. It is clear that this splitting has produced a potentially slightly more favorable configuration matrix and furthermore, that this process can be continued — that is, there are still further splittings of the configuration available to us.

Starting again from the configuration X', we can proceed to split the first column in $\mathcal{L}_1' \in X'$ with a $\mathbb{P}^2$ in a way that the new submatrix $\mathbf{c_i}$ has the maximal rank:

$$X'' = \begin{bmatrix} \mathbb{P}^2 & \mathcal{L}_1'' & \mathcal{L}_6 & \mathcal{L}_5 & \hat{\mathcal{L}}_{2,3,4} \\ \hline \mathbb{P}^2 & 1 & 1 & 1 & \mathbf{0} \\ \mathcal{A} & \mathbf{c_1'} & \mathbf{c_2'} & \mathbf{c_3'} & \mathcal{C} \end{bmatrix} = \begin{bmatrix} & \mathcal{L}_1'' & \mathcal{L}_6 & \mathcal{L}_5 & \hat{\mathcal{L}}_4 & \hat{\mathcal{L}}_2 & \hat{\mathcal{L}}_3 \\ \hline \mathbb{P}^2 & 1 & 1 & 1 & 0 & 0 & 0 \\ \mathbb{P}^1 & 0 & 0 & 1 & 1 & 0 & 0 \\ \mathbb{P}^2 & 1 & 0 & 0 & 1 & 0 & 1 \\ \mathbb{P}^1 & 0 & 1 & 0 & 0 & 1 & 0 \\ \mathbb{P}^3 & 0 & 0 & 0 & 0 & 1 & 3 \end{bmatrix} \quad (2.7)$$

with $h^\bullet(X'', \mathcal{L}_1'') = (7, 1, 0, 0)$, $h^\bullet(X'', \mathcal{L}_{5,6}) = (5, 0, 0, 0)$. Once again, the remaining normal bundle cohomology and the overall Euler number of the manifold is unchanged. At this step in the splitting chain, the dimension of the first cohomology of the normal bundle decreases from $h^1(X', \mathcal{N}_{X'}') = 2$ to $h^1(X'', \mathcal{N}_{X''}'') = 1$ while the second cohomology group is still zero.

It is important to note at this stage, that even having identified a problematic element of the normal bundle (such as $\mathcal{L}_1$ above), not all splittings will cause the relevant cohomology, $h^1(X, \mathcal{L}_1)$ to decrease. In general, an analysis of the associated long exact sequences in cohomology demonstrates that the maximal change is possible when the new submatrix, $\mathbf{c_i}$, is of maximal rank. For example, an alternative splitting to (2.7) is

$$\hat{X} = \begin{bmatrix} & \mathcal{L}_1'' & \mathcal{L}_6 & \mathcal{L}_5 & \hat{\mathcal{L}}_4 & \hat{\mathcal{L}}_2 & \hat{\mathcal{L}}_3 \\ \hline \mathbb{P}^2 & 1 & 1 & 1 & 0 & 0 & 0 \\ \mathbb{P}^1 & 0 & 0 & 1 & 1 & 0 & 0 \\ \mathbb{P}^2 & 0 & 1 & 0 & 1 & 0 & 1 \\ \mathbb{P}^1 & 0 & 1 & 0 & 0 & 1 & 0 \\ \mathbb{P}^3 & 0 & 0 & 0 & 0 & 1 & 3 \end{bmatrix}$$

For this configuration, $h^\bullet(\hat{X}, \mathcal{L}_1'') = (2, 0, 0, 0)$ while $h^\bullet(\hat{X}, \mathcal{L}_6) = (9, 2, 0, 0)$, $h^\bullet(\hat{X}, \mathcal{L}_1'') = (3, 0, 1, 0)$. Unfortunately, $h^1(\hat{X}, \mathcal{N}_{\hat{X}})$ does not decease while $h^2(\hat{X}, \mathcal{N}_{\hat{X}})$ increases. Finally, it should be noted that *even with maximal rank splittings of a column* in some non-generic cases, the cohomology may not decrease in the desired manner. We will return to this in a moment, but for now it is enough to observe that in general there are only a few choices of maximal rank splittings available and thus this process is suitable for an automated, algorithmic search for ineffective, favorable splittings.

To conclude the example at hand, we have one further step to take from the configuration, X'', in (2.7). Once again, the final $\mathbb{P}^1$ splitting is performed on the first column in

the configuration matrix $\mathcal{L}_1''$ on X'' as

$$
X''' = \left[\begin{array}{c|ccc}
 & \mathcal{L}_1''' & \mathcal{L}_7 & \hat{\mathcal{L}}_{2,3,4,5,6} \\ \hline
\mathbb{P}^1 & 1 & 1 & \mathbf{0} \\
\mathcal{A} & \mathbf{c}_1'' & \mathbf{c}_2'' & \mathcal{C}
\end{array} \right] = \left[\begin{array}{c|ccccccc}
 & \mathcal{L}_1''' & \mathcal{L}_7 & \hat{\mathcal{L}}_6 & \hat{\mathcal{L}}_5 & \hat{\mathcal{L}}_4 & \hat{\mathcal{L}}_2 & \hat{\mathcal{L}}_3 \\ \hline
\mathbb{P}^1 & 1 & 1 & 0 & 0 & 0 & 0 & 0 \\
\mathbb{P}^2 & 0 & 1 & 1 & 1 & 0 & 0 & 0 \\
\mathbb{P}^1 & 0 & 0 & 0 & 1 & 1 & 0 & 0 \\
\mathbb{P}^2 & 1 & 0 & 0 & 0 & 1 & 0 & 1 \\
\mathbb{P}^1 & 0 & 0 & 1 & 0 & 0 & 1 & 0 \\
\mathbb{P}^3 & 0 & 0 & 0 & 0 & 0 & 1 & 3
\end{array} \right] \tag{2.8}
$$

with $h^\bullet(X''', \mathcal{L}_1''') = (5, 0, 0, 0)$, $h^\bullet(X'', \mathcal{L}_7) = (5, 0, 0, 0)$ and $\chi(X''') = -90$. Now at last, after a three-step chain of splittings, a configuration matrix has been obtained with $H^1(X''', \mathcal{N}_{X'''}) = 0$. Thus, the procedure outlined above has produced a new, equivalent description of the same CY manifold, but one for which we have complete control of the divisors/line bundles via restriction from a simple ambient space.

In summary, it is clear that for a given CICY configuration matrix, there are a finite number of such splitting chains that have the potential to lead to a new, favorable description of the manifold via ineffective splitting. In practice, a computer search can easily be implemented. The algorithm we employed consists of the following steps:

1. Begin by computing the line-bundle cohomology for each component of the normal bundle (i.e. column of the matrix) and split (in any order) those with non-zero $h^1(X, \mathcal{L})$ cohomology. Due to the Lemma, other line-bundle cohomology groups will not change in the splitting process.

2. If the maximal size of the degree entries in the chosen column/line bundle $\mathcal{L} = \mathcal{O}_X(a^1, \ldots, a^m)$ is 2, split it with $\mathbb{P}^1$ as:[5]

$$
\left[\begin{array}{c|cc}
\mathbb{P}^n & 2 & \mathbf{b} \\
\mathcal{A} & \mathbf{c} & \mathcal{C}
\end{array} \right] = \left[\begin{array}{c|ccc}
\mathbb{P}^1 & 1 & 1 & \mathbf{0} \\
\mathbb{P}^n & 1 & 1 & \mathbf{b} \\
\mathcal{A} & \mathbf{c_1} & \mathbf{c_2} & \mathcal{C}
\end{array} \right] \tag{2.9}
$$

and at the same time choose degree partitions such that the submatrix $[\mathbf{c_{i,j}}]$ is maximal rank. If the largest degree entry in the chosen line bundle $\mathcal{L}$ is 1, then perform a $\mathbb{P}^n$-split, where $n = \sum_i^m a^i - 1$ and choose the submatrix $[\mathbf{c_{i,j}}]$ to be of maximal rank.

3. For each step of splitting, verify that the split is ineffective by computing the Euler number of the new configuration matrix.

4. Repeat these procedures whenever $h^1(X, \mathcal{N}_X)$ decreases while $h^2(X, \mathcal{N}_X)$ is unchanged. Finish the procedure when $h^1(X, \mathcal{N}_X) = 0$ and a favorable description of the manifold has been obtained.

---

[5]In the original CICY list with unfavorable descriptions, 2 is the largest degree/entry for the line-bundle involved in the splitting.

Implementing this search in the original CICY database [16], there are 2994 unfavorable configuration matrices to be analyzed. A search as described above readily provides a new, favorable description of 2946 of them. For the remaining 48 configuration matrices an exhaustive search demonstrates that no chain of splittings/contractions will lead to a favorable description. The remaining 48 configuration matrices will be dealt with separately in section 5 where we will demonstrate that this set of 48 geometries in fact contains 15 descriptions of the same CY threefold (the so-called "Schoen manifold" with Hodge numbers $(19, 19)$) and 33 others. Of these latter manifolds, we find a further 9 redundancies and observe that the remaining 24 distinct geometries can all be simply described as hypersurfaces defined in an ambient product of two del Pezzo surfaces.

For now, we see that the simple process of splitting has allowed to generate a new version of the CICY list in which we have dramatically increased the number of favorable configurations to 7842 in total. For each of these new descriptions, we can employ existing tools [34, 39] to fully specify the topological data of the manifold, including the triple intersection numbers, line bundle cohomology, etc. By combining these results with those from section 5 for the remaining 48 manifolds we have produced a new version of the CICY list with all topological data fully specified. It is available at [3] and in an attachment to the arXiv submission of this work.

2.2 Kähler favorable manifolds

As observed in section 1.2, a fibration scan crucially relies on the characterization of the Kähler and nef cones. Although the Kähler cone of a hypersurface in a Fano variety descends simply from the ambient space, in general, few tools exist to characterize the Kähler cones of complete intersection Calabi-Yau manifolds (even those defined in simple ambient spaces). In this section, we review two useful tools that together help us to determine the Kähler and Mori cones of 4957 out of 7890 configuration matrices in the list of CICY threefolds. This set has the simple property that their Kähler cones descend from the ambient space in which they are embedded. We will refer to such manifolds as *"Kähler Favorable"* configurations (see [40] for earlier related ideas). For these, we will provide a complete classification of all genus one fibrations in the CY geometries.

To begin, let us review two simple results about Kähler and Mori cones of CICYs. The first is the following result for the cone of curves (denoted $\overline{NE}(X)$) of CY hypersurfaces in Fano fourfolds proved in [41]:

Lemma 2.2 *(Kollár) Let Y be a smooth Fano variety with $\dim(Y) \geq 4$. Let $X \subset Y$ be a smooth divisor in the class $-K_Y$ (in fact X can have arbitrary singularities). Then the natural inclusion*

$$i_* : \overline{NE}(X) \to \overline{NE}(Y) \tag{2.10}$$

is an isomorphism.

Thus, a CY hypersurface in any *smooth* Fano fourfold has a cone of algebraic curves that descends simply from its ambient space. Moreover, from the simple form of intersection numbers on a hypersurface, it follows that the (dual) Kähler cone also descends from the

ambient space (for a careful set of arguments on the descent of the effective, nef and ample cones of divisors see [42, 43]). We will utilize this, and one additional result, to describe the Kähler cones of 83 CICYs described as hypersurfaces in a product of two almost del Pezzo surfaces in sections 5 and 6.

For more general complete intersections $X \subset \mathcal{A}$, the first observation to be made is that every Kähler form on $\mathcal{A}$ restricts to a Kähler form on X. For the CICY threefolds defined in products of projective spaces considered here, the Kähler cone of $\mathbb{P}^{n_1} \times \ldots \mathbb{P}^{n_m}$ is simply the positive orthant (see [16] for details). Thus, for all the favorable manifolds in the CICY list, it is clear that the Kähler cone of X is at least as big as the positive orthant. In general, however, it could be larger. To illustrate this, consider the following example:

$$
X = \left[\begin{array}{c|ccc:c}
\mathbb{P}^2 & 0 & 0 & 0 & 3 \\ \hdashline
\mathbb{P}^1 & 1 & 0 & 0 & 1 \\
\mathbb{P}^1 & 0 & 1 & 0 & 1 \\
\mathbb{P}^1 & 0 & 0 & 0 & 1 \\
\mathbb{P}^2 & 1 & 1 & 1 & 0
\end{array} \right] .
\tag{2.11}
$$

This manifold (with Hodge numbers $(h^{1,1}, h^{2,1}) = (5, 59)$) is an anti-canonical hypersurface in $\mathbb{P}^2 \times dP_3$. It is also a manifest genus one fibration over dP_3 (with a $\mathbb{P}^2[3]$ fiber). Although it is favorable in the sense that its Picard group descends from the ambient product of 5 projective spaces, it is *not Kähler favorable* since the Kähler cone of X is actually larger than the positive orthant! To see this, note that by Lemma 2.2 above the Kähler cone of X is simply that of $\mathbb{P}^2 \times dP_3$. However, the Kähler cone of dP_3 is non-simplicial (with 5 generators [44]). Written in terms of a basis of the 5 restricted hyperplanes (D_i, $i = 1, \ldots 5$), the six generators of the Kähler cone of X are

$$
\{ D_1, D_2, D_3, D_4, D_5, D_2 + D_3 + D_4 - D_5 \}
\tag{2.12}
$$

This last generator, $D_2 + D_3 + D_4 - D_5$, is manifestly not in the Kähler cone of the ambient space.

How, then, are we to determine when the Kähler cone of a CICY, X is "enhanced" in this way relative to the Kähler cone of the ambient space? It is clear that whenever the Kähler cone expands (as in the example above), the dual (i.e. Mori) cone must shrink. Thus, one simple way to determine when the Kähler cone of X descends from that of $\mathcal{A}$ is to determine when *the Mori cone remains the positive orthant*.

More precisely, consider the basis of curves dual to the Kähler forms J_i (i.e. basis of $H^{1,1}$ restricted from the ambient space in a favorable CICY), defined via

$$
\int_{C_i} J_j = \delta_j^i
\tag{2.13}
$$

A general curve can be written in terms of this basis as $C = a^i C_i$. The claim for a favorable CICY then is

> If C_i are in the (closure of the) Mori cone for all i then the Kähler cone
> is exactly the positive orthant.

The expectation then is that if all C_i (i.e. all the boundaries of the dual positive orthant) are in the Mori cone then it is clear that the Mori cone cannot be smaller than that orthant (as would be the case if the Kähler cone expanded as in (2.12)). For the example above, it is clear that because of the presence of the last Kähler generator, $D_2 + D_3 + D_4 - D_5$, the curve C_5 (dual to J_5) is not an element of the Mori cone.

It remains then to try to determine when can we establish that X contains effective curves in the class $[C_i]$? One simple (but certainly not exhaustive) approach[6] is to use existing tools to determine the existence of curves of a given class and genus in X — namely to compute the Gromov-Witten Invariants of X.

In the case at hand — that of complete intersection Calabi-Yau manifolds in smooth toric ambient spaces — techniques to compute the *genus zero* Gromov-Witten Invariants are well established in the literature using mirror symmetry [45–47]. In particular, the tools laid out in [46] provide a simple algorithmic way to enumerate simple, algebraic curves in genus zero. In general, caution must be used in interpreting a Gromov-Witten invariant as an actual count of algebraic curves, however for the CICYs in consideration here (defined in simple, smooth toric ambient spaces) the results of a mirror symmetry computation lead to positive integers which are expected to give a physically relevant, enumerative count (see [48–50] for mathematical conjectures in this regard).

We employ the method of [46] to determine the vector:

$$n(0, [C_i]) = (\#, \ldots, \#) \tag{2.14}$$

where $i = 1, \ldots h^{1,1}(X)$ for every favorable CICY in the augmented CICY list attached to this arXiv submission. We find that for 4874 out of 7820 non-product, favorable CICY configuration matrices (in the new list),

$$n(0, [C_i]) > 0 \quad \forall i = 1, \ldots h^{1,1}(X) \tag{2.15}$$

Thus, for this subset of CICY manifolds, every dual curve C_i in the positive orthant should in fact be effective and hence in the Mori cone. It follows from the logic above that the Kähler cones are in turn exactly the (dual) positive orthant. Since the Kähler cones for these manifolds descend exactly from the ambient product of projective spaces, they are Kähler favorable as defined above. Of course, a zero entry in the genus zero Gromov-Witten Invariant vector *does not* necessarily imply that the Mori cone is smaller than the positive orthant. However, the condition above should be sufficient (though not in general necessary) and for these geometries we will provide a complete classification of genus one fibrations. We leave it to future work to thoroughly explore the full curve enumeration on CICYs and their correspondence with Gromov-Witten invariants. In addition, we would also hope to search for other tools that might fully determine the Kähler cones of the remaining CICYs.

Summarizing the two approaches outlined above, we find that 4957 out of 7890 CI-CYs have Kähler cones that descend from a simple ambient space — either a product of

---

[6]We would like to thank Andre Lukas for helpful discussions on this topic and for pointing out the utility of Gromov-Witten Invariants for this question. See also the recent work [51] for alternative approaches to curve counting in CICY geometries.

projective spaces (with entirely non-vanishing $n(0, [C_i])$ as described above) or a product of two almost del Pezzo surfaces. Of this latter type, there are 83 geometries in the CICY list that can be written this way and we will analyze them in section 5.

In the augmented CICY list attached to this arXiv submission, there are simple flags added to each entry to denote the status of the Picard group ("Favorable $\rightarrow$ True" indicates the Picard group descends from the ambient space) and Kähler cone ("KahlerPos $\rightarrow$ True" denotes a Kähler cone that descends from the ambient product of projective spaces). In addition, the configuration matrix, second Chern class and Hodge numbers are also provided. A sample entry in the new CICY list, with all data annotated, is given in appendix E.

3 A search for "obvious" genus one fibrations

3.1 General comments on obvious Calabi-Yau fibrations

As was described in the introduction, row and column permutations can be applied to the configuration matrix of a CICY without affecting the geometries it describes. Permuting rows simply corresponds to writing the ambient projective space factors in a different order, and permuting columns corresponds to relabeling the defining equations. Consider a case where such row and column permutations can be used to put a configuration matrix in the following block form.

$$X = \left[\begin{array}{c|c} \mathcal{A}_1 & 0 \;\vdots\; \mathcal{F} \\ \hline \mathcal{A}_2 & \mathcal{B} \;\vdots\; \mathcal{T} \end{array} \right] \tag{3.1}$$

Here $\mathcal{A}_1$ is a product of m projective spaces and $\mathcal{A}_2$ is a product of $N-m$ projective spaces (where N is the total number of such factors in the initial configuration). The blocks 0 and $\mathcal{B}$ contain n columns while $\mathcal{F}$ and $\mathcal{T}$ contain $K-n$. We will include cases where $n=0$.

A configuration which can be put in the form (3.1) describes a fibration of the fiber $\left[\mathcal{A}_1 \big| \mathcal{F} \right]$ over the base $\left[\mathcal{A}_2 \big| \mathcal{B} \right]$ where the twisting of the fiber over the base is encoded by the matrix $\mathcal{T}$. To see this, consider the following line of reasoning. First, pick a solution to the first n equations by choosing a point in $\mathcal{A}_2$ which satisfies the equations whose degrees are encoded by $\mathcal{B}$. This furnishes us with a point in the base. Take this set of coordinates in $\mathcal{A}_2$ and substitute it into the remaining $K-n$ equations, whose multi-degrees are determined by the matrices $\mathcal{F}$ and $\mathcal{T}$. This results in a particular set of equations, whose degrees are described by the configuration matrix $\left[\mathcal{A}_1 \big| \mathcal{F} \right]$, associated to that base point. As we change the base point the complex structure of this fiber over that base point will change. Thus we end up with a non-trivial fibration of this type over the base.

Note that the fiber $\left[\mathcal{A}_1 \big| \mathcal{F} \right]$ is a Calabi-Yau manifold. This is a simple consequence of the Calabi-Yau condition applied to the original configuration matrix (1.4), together with the presence of a completely zero block in the top left of (3.1). For an initial configuration describing a Calabi-Yau p-fold, we can in general find Calabi-Yau q-fold fibers of this type for any $q < p$. For the case of $q = 1$ fibrations that can be seen in this manner have been referred to as Obvious Genus One Fibrations (OGFs) [1, 29].

In fact, as has been noted before [1], a given configuration will generically admit a multitude of different such fibrations. In other words, a given configuration matrix can often be put in the form (3.1) in several different ways. For example, the following are all rearrangements of the same configuration matrix.

$$
\left[\begin{array}{c|cccccc}
\mathbb{P}^2 & 0 & 0 & 0 & 0 & 2 & 1 \\
\mathbb{P}^3 & 0 & 0 & 1 & 1 & 1 & 1 \\
\hline
\mathbb{P}^1 & 1 & 0 & 1 & 0 & 0 & 0 \\
\mathbb{P}^2 & 1 & 2 & 0 & 0 & 0 & 0 \\
\mathbb{P}^1 & 0 & 1 & 0 & 1 & 0 & 0
\end{array}\right]
\left[\begin{array}{c|cccccc}
\mathbb{P}^1 & 0 & 1 & 1 & 0 & 0 & 0 \\
\mathbb{P}^2 & 0 & 0 & 0 & 0 & 2 & 1 \\
\mathbb{P}^3 & 0 & 0 & 1 & 1 & 1 & 1 \\
\hline
\mathbb{P}^1 & 1 & 0 & 0 & 1 & 0 & 0 \\
\mathbb{P}^2 & 2 & 1 & 0 & 0 & 0 & 0
\end{array}\right]
\left[\begin{array}{c|cccccc}
\mathbb{P}^1 & 0 & 0 & 1 & 1 & 0 & 0 \\
\mathbb{P}^2 & 0 & 0 & 0 & 0 & 2 & 1 \\
\mathbb{P}^3 & 0 & 1 & 0 & 1 & 1 & 1 \\
\hline
\mathbb{P}^1 & 1 & 1 & 0 & 0 & 0 & 0 \\
\mathbb{P}^2 & 1 & 0 & 2 & 0 & 0 & 0
\end{array}\right]
$$

$$
\left[\begin{array}{c|cccccc}
\mathbb{P}^2 & 0 & 0 & 0 & 0 & 2 & 1 \\
\mathbb{P}^2 & 1 & 0 & 2 & 0 & 0 & 0 \\
\mathbb{P}^3 & 0 & 1 & 0 & 1 & 1 & 1 \\
\hline
\mathbb{P}^1 & 1 & 1 & 0 & 0 & 0 & 0 \\
\mathbb{P}^1 & 0 & 0 & 1 & 1 & 0 & 0
\end{array}\right]
\left[\begin{array}{c|cccccc}
\mathbb{P}^1 & 1 & 1 & 0 & 0 & 0 & 0 \\
\mathbb{P}^1 & 0 & 0 & 1 & 1 & 0 & 0 \\
\mathbb{P}^2 & 0 & 0 & 0 & 0 & 2 & 1 \\
\mathbb{P}^3 & 0 & 1 & 0 & 1 & 1 & 1 \\
\hline
\mathbb{P}^2 & 1 & 0 & 2 & 0 & 0 & 0
\end{array}\right]
\left[\begin{array}{c|cccccc}
\mathbb{P}^1 & 1 & 1 & 0 & 0 & 0 & 0 \\
\mathbb{P}^1 & 0 & 0 & 1 & 1 & 0 & 0 \\
\mathbb{P}^2 & 1 & 0 & 2 & 0 & 0 & 0 \\
\mathbb{P}^3 & 0 & 1 & 0 & 1 & 1 & 1 \\
\hline
\mathbb{P}^2 & 0 & 0 & 0 & 0 & 2 & 1
\end{array}\right]
\tag{3.2}
$$

The block matrix form, as described in (3.1) has been denoted here with dotted lines. Computing the dimension of the fibers in this case the reader will find that these constitute six different torus fibrations of the CY manifold. Similarly we can find two different K3 fibrations in this case.

$$
\left[\begin{array}{c|cccccc}
\mathbb{P}^2 & 0 & 0 & 0 & 0 & 2 & 1 \\
\mathbb{P}^3 & 0 & 0 & 1 & 1 & 1 & 1 \\
\mathbb{P}^1 & 1 & 0 & 1 & 0 & 0 & 0 \\
\mathbb{P}^2 & 1 & 2 & 0 & 0 & 0 & 0 \\
\hline
\mathbb{P}^1 & 0 & 1 & 0 & 1 & 0 & 0
\end{array}\right]
\left[\begin{array}{c|cccccc}
\mathbb{P}^2 & 0 & 0 & 0 & 0 & 2 & 1 \\
\mathbb{P}^3 & 0 & 0 & 1 & 1 & 1 & 1 \\
\mathbb{P}^1 & 0 & 1 & 0 & 1 & 0 & 0 \\
\mathbb{P}^2 & 1 & 2 & 0 & 0 & 0 & 0 \\
\hline
\mathbb{P}^1 & 1 & 0 & 1 & 0 & 0 & 0
\end{array}\right]
\tag{3.3}
$$

Note that trivial redundancies have been removed in enumerating the fibrations in the (3.2) and (3.3) above. For example, column permutations that do not mix the first n and the last $K-n$ columns generate obviously identical fibrations and thus this redundancy has been removed. Similarly for row permutations that do not mix the fiber (first m) and base (last $N-m$) rows. In the results we present here, however, there are certain potential redundancies, which have been removed in the previous literature [1] which we will *not* be removing from our data. These are best illustrated with an example. Consider the bi-cubic.

$$
X_{\text{bicubic}} = \left[\begin{array}{c|c}
\mathbb{P}^2 & 3 \\
\mathbb{P}^2 & 3
\end{array}\right]
\tag{3.4}
$$

In past work this manifold would have been said to admit a single obvious fibration, a torus described as a cubic in $\mathbb{P}^2$ fibered over a $\mathbb{P}^2$ base. Here we will count both fibrations of this type that appear in the matrix - that is we will consider the two fibrations which arise by considering each of the two $\mathbb{P}^2$ factors in the ambient space to be the base in turn.

There are two main reasons for making this choice in our approach to redundancy removal, one physical and one mathematical. First, counting distinct but identical fibrations

like these will enable us to enumerate fibrations in a manner which agrees with the mathematics literature. After all, there are two fibrations in our example (3.4), albeit ones that are symmetric in structure. In particular, counting fibrations that appear with symmetry like this will make it easier to compare to the number of fibrations that are obtained by applying Kollár's criteria. Second, from a physical perspective, the fact that there are two distinct fibrations in the example (3.4) does have important physical consequences. One would not obtain two different F-theory models by compactifying on the two fibrations, of course, as the moduli space of the two F-theory geometries would be identical. Nevertheless, in considering dualities, the fact that there are two fibrations can be key. Picking a particular complex structure for the bi-cubic and performing a heterotic compactification, for example, one finds that the two fibrations present in (3.4) will lead to two very different F-theory duals [2] (see also [52] for related ideas in 6-dimensional heterotic/F-theory duality). This is due to the fact that at a given point in complex structure moduli space, the two torus fibers will be twisted over their $\mathbb{P}^2$ bases in distinct ways. Given the above discussion, we will not remove distinct but topologically isomorphic fibrations from our scans over the CICYs.

Another issue that must be addressed in enumerating obvious fibrations of the type being discussed in this section is that of multiple fibers. Consider, for example, the following configuration matrix and associated obvious fibration:

$$X_{\mathrm{multiple}} = \left[\begin{array}{c|cc} \mathbb{P}^2 & 0 & 3 \\ \mathbb{P}^1 & 2 & 0 \\ \hline \mathbb{P}^2 & 1 & 2 \end{array} \right] \quad . \tag{3.5}$$

This follows all of the rules to be considered an OGF but exhibits an obvious problem. The fiber in this case, as described by the configuration,

$$X_{\mathrm{fiber}} = \left[\begin{array}{c|cc} \mathbb{P}^2 & 0 & 3 \\ \mathbb{P}^1 & 2 & 0 \end{array} \right] , \tag{3.6}$$

is not a single genus one curve. Instead it describes two disjoint tori embedded in the $\mathbb{P}^2 \times \mathbb{P}^1$ ambient space. All such cases can be removed from consideration by imposing the additional condition that no fiber can be described by a configuration matrix that can be put in block diagonal form by row and column permutations. We shall impose this requirement in all of the fibrations, by Calabi-Yau of any dimension, that we discuss in the remainder of this paper.

As a last point in the general discussion of this section, we should note that the Calabi-Yau fibers of different dimensions discussed above can be nested within one another. For example, if we look at the first matrices in (3.2) and (3.3) above, we see that the torus fibration depicted in (3.2) is actually also a torus fibration of the $K3$ fibration in (3.3). Such nesting is rather common, with the vast majority of higher dimensional Calabi-Yau fibers also being fibered themselves. However, not every torus fibration need be nested in a $K3$ fibration in this manner. As an example of this, the final torus fibration presented in (3.2) clearly does not lie nested within a $K3$ fibration as its base is simply $\mathbb{P}^2$.
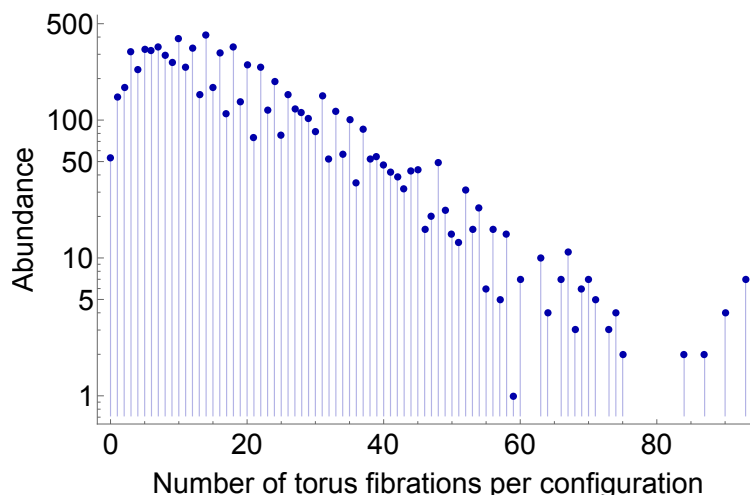
Figure 1. Distribution of obvious torus fibration abundance in the CICY threefold list (excluding product manifolds). The values lie in the range 0 - 93. We find $139,597$ fibrations in total and on average each CICY threefold configuration is elliptically fibered in 17.7 different ways.

3.2 Enumeration of obvious Calabi-Yau fibrations

Classifying the obvious fibrations, as discussed in the previous subsection, results in the following numbers of inequivalent structures of this type. For torus fibers, the CICY three-folds, using the new favorable configurations mentioned in section 2.1, admit an average of 17.7 fibrations per configuration matrix, for a total of $139,597$ such structures in the list. The maximum number of such torus fibrations admitted by any one configuration matrix is 93. Note that these figures are somewhat larger than those given in [2]. This is for three reasons. First, we have favorable configurations describing more of the CICY manifolds and thus can find more torus fibrations. Second, as described in the proceeding subsection, we are not removing what was considered a redundancy in that work. That is, we are keeping symmetric fibrations that are nevertheless distinct. A plot of the number of configurations admitting a given number of obvious torus fibrations is presented in figure 1.

For K3 fibrations, the threefolds in our data set admit an average of 3.9 fibrations per configuration matrix, for a total of $30,974$ such structures in total. The maximum number of such $K3$ fibrations admitted by any one configuration matrix is 9. A plot of the number of configurations admitting a given number of obvious K3 fibrations is presented in figure 2.

Finally, we can ask about the nesting of the torus fibrations inside K3 fibrations. Counting each different obvious torus fibration with a multiplicity determined by how many obvious K3 fibrations it appears nested inside, we find that the average CICY threefold admits 26.6 such structures. Note that this is bigger than the average number of obvious torus fibrations given above as a given torus fibration can be nested inside multiple different K3 fibrations. The total number of such nested fibrations is $208,987$ with the largest example admitting 174 such nested fibrations. A plot of the number of configurations admitting a given number of obvious torus fibrations nested inside obvious K3 fibrations is presented in figure 3.

The full data describing these fibration structure can be found at [3]. The data format is described in appendix E.
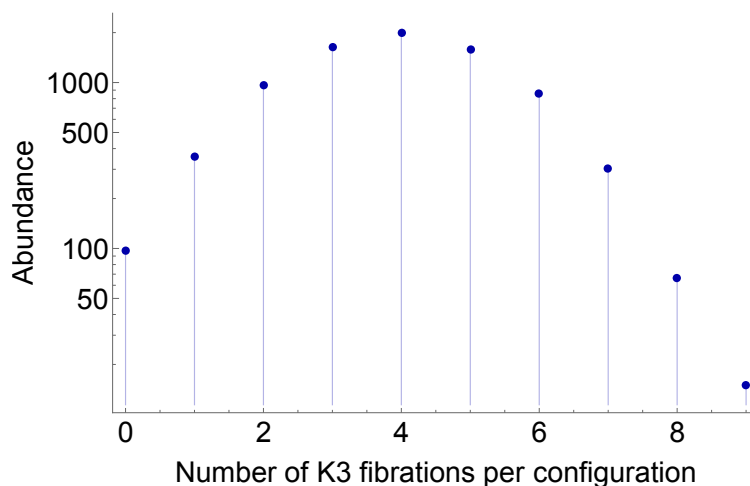
Figure 2. Distribution of obvious K3 fibration abundance in the CICY threefold list (excluding product manifolds). The values lie in the range 0 - 9. We find $30,974$ fibrations in total and on average each CICY threefold configuration is obviously K3 fibered in 3.9 different ways.
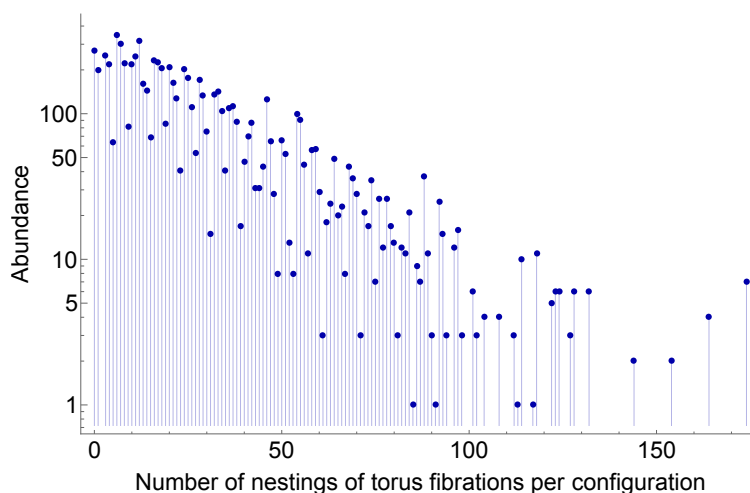
Figure 3. Distribution of the abundance of obvious torus fibrations nested inside obvious K3 fibrations in the CICY threefold list (excluding product manifolds). The values lie in the range 0–174. We find $208,987$ such nested fibrations in total and on average each CICY threefold configuration admits 26.6 different nested fibrations of this type.

4 A comparison of obvious fibrations vs. all fibrations for Kähler favorable manifolds

As discussed in section 1.1 (see the conjecture there), it has been established [26–28] that any effective divisor class D of a Calabi-Yau threefold, X, leads to a genus-one fibration if and only if it obeys the following criteria:

$$D \cdot C \geq 0 \quad \text{for all effective curves } C \text{ in } X \ ; \qquad D^2 \neq 0 \ ; \qquad D^3 = 0 \ . \qquad (4.1)$$

One is thus led to classify the solutions to (4.1) for

$$D = \sum_{r=1}^{h^{1,1}(X)} a_r J_r\,, \quad \text{with } a_r \in \mathbb{Z}\,, \tag{4.2}$$

where $\{J_r\}$ is a chosen basis of $H^{1,1}(X)$.

In this section we will compare the results of a scan for Kollár divisors of the form given above to the searches for OGFs described in section 3. It is of interest to see whether the total number of fibrations (as counted by the divisor criteria above) exceeds the number of "obvious" fibrations that are visible from the algebraic form of the CICY configuration matrix. To make this comparison however, full control of the Kähler cone of X is crucial. Thus, we will be able to make this comparison only for Kähler favorable manifolds as defined in section 2.2. For these, the Kähler cone of X descends directly from the ambient product of projective spaces.

Given such a Kähler favorable CICY threefold X embedded in $\mathcal{A} = \prod_r \mathbb{P}^{n_r}$, let us take the J_r to be the harmonic $(1,1)$-form of the ambient $\mathbb{P}^{n_r}$ pieces; we call $X \subset \mathcal{A}$ favorable if the J_r's form a basis[7] of $H^{1,1}(X)$. We begin by writing the conditions in (4.1) in terms of the explicit divisor in (4.2). These take the following forms in terms of a_r, respectively, as

$$a_r \geq 0 \text{ for all } r\,; \quad \sum_{s,t=1}^{h^{1,1}} d_{rst} a_s a_t \neq 0 \text{ for some } r\,; \quad \sum_{r,s,t=1}^{h^{1,1}} d_{rst} a_r a_s a_t = 0\,, \tag{4.3}$$

where $d_{rst} := \int_X J_r \wedge J_s \wedge J_t$ are the triple intersection numbers of X. We may then assume that a given solution to (4.3), $a_r = a_r^{(0)}$, is ordered as $0 = a_1 = \cdots a_\nu < a_{\nu+1} \leq \cdots \leq a_{h^{1,1}}$, upon an appropriate permutation of the $\mathbb{P}^{n_r}$'s in $\mathcal{A}$. Here, ν is the number of 0's appearing in the solution. Because all the triple intersections d_{rst} of a favorable CICY are nonnegative, it is then obvious that there is another solution, $a_r = a_r^{(1)}$:

$$a_r^{(1)} = \begin{cases} 0 & \text{if } r \leq \nu \\ 1 & \text{if } r > \nu\,, \end{cases} \tag{4.4}$$

which must represent the same genus-one fibration as the original solution (using the conditions of equivalence outlined in section 1.1). Thus, for Kähler favorable CICYs, in searching for Kollár divisors, we need only consider D as in (4.2) with $a_r = 0$ or 1 in classifying the solutions to (4.1). For each of the 4874 CICYs that are Kähler favorable with respect to an ambient space $\mathbb{P}^{n_1} \times \ldots \times \mathbb{P}^{n_m}$, such a search for minimal Kollár divisors (with $0 \leq a_r \leq 1$) was carried out.

Moreover, as described in section 3, a systematic scan for obvious genus-one fibrations (OGFs) has been completed for all the maximally favorable configuration matrices. In each case the classification proves to be finite and impressively, *a one-to-one correspondence between the two classification results can immediately be found.* In each case we find 50,219 fibrations in the set of 4874 manifolds and an exhaustive comparison shows that

---

[7]In general such a basis could be redundant but we will not need to consider such an eventuality here.

each Kollár divisor corresponds to an OGF (the converse is automatic). Thus, for Kähler favorable CICYs, the OGFs already provide a complete set of genus-one fibrations for these geometries. This result is not entirely surprising since the Kähler favorable form engineered in section 2 has been chosen to provide a description in which the ambient projective space factors encode the maximal amount of information about the Picard group and Kähler cone of X. It should be noted that this correspondence *does not persist for non-Kähler favorable CICY configurations.* For example, 2946 out of 7890 manifolds in the set described above have been described by new CICY configurations compared to the original CICY threefold data set. If the OGFs are counted for any non-favorable description of one of these geometries, many fibrations are missing. That is, the OGF count is found to be considerably less than the true count (based on (4.1)), as expected.

To conclude this comparison, it is worth making several remarks on the ubiquity of genus one fibrations within this dataset. Each of the 4874 CICY configurations studied yields a finite number of fibration structures. Moreover, the maximal number of fibrations observed from any one threefold in this set is 39 and the average number of fibrations is 10.3. Finally, it should be noted that this search yields 53 configuration matrices which do not admit any fibration structure (either via (4.1) or the OGF criteria). The CICY number of those 53 favorable configuration matrices are:

$$\{6771, 6803, 7036, 7208, 7242, 7530, 7563, 7566, 7571, 7578, 7588, 7626, 7631,$$
$$7635, 7636, 7638, 7644, 7647, 7648, 7679, 7717, 7721, 7726, 7734, 7747, 7759,$$
$$7761, 7781, 7799, 7806, 7809, 7816, 7817, 7819, 7822, 7823, 7840, 7842,$$
$$7858, 7861, 7863, 7867, 7869, 7873, 7878, 7879, 7882, 7885 - 7890\} \quad (4.5)$$

(labels refer to the dataset in [3]). Since this set are within the geometries for which we can scan exhaustively using the Kollár criteria, we are certain that they are not genus-one fibered. This is intriguing since it demonstrates that the largest value of $h^{1,1}$ for a non-fibered CY manifold in the CICY threefold list is $h^{1,1} = 4$ (note that for every other manifold in the CICY list, at least one OGF is present).

We will return to this point in section 7, but for now it suffices to note that all existing fibration studies within CY threefolds indicate that genus one fibered geometries seem to become ubiquitous as $h^{1,1}$ increases. For the CICY threefold data set it is clear that this bound on $h^{1,1}$ in order for the manifold to be guaranteed a genus-one fibration is quite low indeed.

5 Exceptional configurations

As described in section 2.1, the process of splitting/contraction yields a favorable description (in which a full basis for divisors is obtained via restriction from ambient projective space hyperplanes) for all but 48 configurations in the CICY list. In this section and the next, we turn our attention to these 48 seemingly non-favorable CICY threefold configurations. Fortunately, as we will see shortly, all 48 configurations in fact have a simple structure that will allow us to not only determine their Picard groups, but also their Kähler

and Mori cones and all their topological data, including the triple intersection numbers. We will thus analyze such topological properties and apply Kollár's criteria (4.1) to exhaustively search for the genus-one fibration structures. Unlike in the case of the favorable configurations studied in section 4, here we will see that *there exist many more fibration structures than are visible as OGFs.* We will enumerate these fully in the following sections.

To begin, it is worth considering the possible redundancy among the 48 configurations. We state the results here and leave the proofs of the equivalences to appendix D. First, the set contains 15 configurations with Hodge numbers $(h^{1,1}, h^{2,1}) = (19, 19)$ which are equivalent to one another and which all describe the Schoen manifold. Since our fibration analysis shows qualitatively different features for the Schoen manifold, we will elaborate on the Schoen manifold in section 6.

It turns out that each of the remaining 33 configurations is favorably embedded as an anticanonical hypersurface in a product of two del Pezzo surfaces of the form,

$$\mathcal{A}_{r,s} \equiv dP_r \times dP_s \quad \text{or} \quad \mathcal{A}_s \equiv \mathbb{P}^1 \times \mathbb{P}^1 \times dP_s \, . \tag{5.1}$$

Here, $r = 0, \ldots, 7$ and $s = 5, 6, 7$, leading us to a total of 24 geometries with $r \leq s$. This fact strongly suggests further redundancy and indeed some exists. Using equivalent descriptions of the ambient space surfaces and splittings/contractions, the 33 configurations can be grouped into the 24 distinct Calabi-Yau geometries as listed in table 1. In addition, there exist 35 favorable CICY configurations which are not Kähler favorable with respect to the ambient product of projective spaces, but which are still anticanonical hypersurfaces in ambient spaces of the form (5.1) with $r = 0, \ldots, 7$ and $s = 3, \ldots, 7$. All of these cases may be analyzed in the same fashion. Table 1 thus has total of 68 CICY configurations leading to 35 distinct Calabi-Yau geometries. In this section, we will analyze topological properties of these 35 anticanonical hypersurfaces,

$$X_{r,s} \subset \mathcal{A}_{r,s} \quad \text{and} \quad X_s \subset \mathcal{A}_s \, , \tag{5.2}$$

where $r = 0, \ldots, 7$ and $s = 3 \ldots, 7$ with $r \leq s$, and will classify genus one fibrations therein.

5.1 Favorable hypersurfaces in products of two del Pezzo surfaces

5.1.1 Topological data

It is fortunate that the configurations in table 1 all take the form of an anticanonical hypersurface in an ambient space consisting of the direct product $\mathcal{S} \times \mathcal{S}'$ of two smooth Kähler Fano surfaces. Such geometries[8] were systematically classified in [53]. Since the ambient space takes such a simple form, we have once again found a favorable description of the geometry in which the divisors on X descend simply from those on $\mathcal{A} = \mathcal{S} \times \mathcal{S}'$. In addition, thanks to the Lemma 2.2 the Kähler and Mori cones of such CY threefolds X can also be simply obtained via restriction. With these results in hand, the analysis is now

---

[8]Note that in fact *all* anticanonical hypersurfaces in $dP_r \times dP_s$ with $r = 0, \ldots 7$ and $s = r, \ldots, 7$ appear in the CICY list, however those not listed in table 1 have Kähler favorable descriptions with respect to an ambient product of projective spaces and their fibration structures are considered in section 4.

Ambient Space	CICY Id Numbers
$\mathbb{P}^1 \times \mathbb{P}^1 \times dP_3$	(7709, 7731)
$\mathbb{P}^1 \times \mathbb{P}^1 \times dP_4$	(7459)
$\mathbb{P}^1 \times \mathbb{P}^1 \times dP_5$	6826 (6829, 6925)
$\mathbb{P}^1 \times \mathbb{P}^1 \times dP_6$	5298
$\mathbb{P}^1 \times \mathbb{P}^1 \times dP_7$	2565
$dP_0 \times dP_3$	(7800, 7810)
$dP_0 \times dP_4$	(7665)
$dP_0 \times dP_5$	7232 (7233, 7298)
$dP_0 \times dP_6$	6021
$dP_0 \times dP_7$	3405 (6748, 6796)
$dP_1 \times dP_3$	(7716, 7743)
$dP_1 \times dP_4$	(7512)
$dP_1 \times dP_5$	6795
$dP_1 \times dP_6$	5282
$dP_1 \times dP_7$	2548
$dP_2 \times dP_3$	(7546, 7603)
$dP_2 \times dP_4$	(7126)
$dP_2 \times dP_5$	6291 (6292, 6369)
$dP_2 \times dP_6$	4473
$dP_2 \times dP_7$	1835
$dP_3 \times dP_3$	(7206, 7246, 7300)
$dP_3 \times dP_4$	(6533, 6619)
$dP_3 \times dP_5$	5254, 5300 (5121, 5257, 5306, 5440)
$dP_3 \times dP_6$	3388, 3406
$dP_3 \times dP_7$	1257, 1268
$dP_4 \times dP_4$	(5636)
$dP_4 \times dP_5$	4077 (3936, 4081)
$dP_4 \times dP_6$	2199
$dP_4 \times dP_7$	708
$dP_5 \times dP_5$	2564, 2566, 2638 (2568, 2641, 2837)
$dP_5 \times dP_6$	1266, 1267, 1289
$dP_5 \times dP_7$	381, 382, 384
$dP_6 \times dP_6$	536
$dP_6 \times dP_7$	206
$dP_7 \times dP_7$	95

Table 1. The 33 exceptional configurations which are not favorable with respect to the ambient product of projective spaces and which are not the Schoen manifold. Each of them turns out to be an anticanonical divisor of either $dP_r \times dP_s$ or $\mathbb{P}^1 \times \mathbb{P}^1 \times dP_s$, for $r = 0, \cdots, 7$ and $s = 5, 6, 7$. The configurations are labelled by their standard CICY ID numbers [3, 16]. In fact, there exist an additional 35 configurations which describe an anticanonical divisor in ambient spaces of the same form with possibly some smaller values of s. These are favorable but not Kähler-favorable with respect to the ambient product of projective spaces, and are also listed here in parentheses.

as tractable as those studied in previous sections, although they are not Kähler favorable with respect to the ambient product of projective spaces.

Given the explicit embeddings, all of the relevant topological properties of the Calabi-Yau hypersurfaces can be obtained by choosing a description of the space $H^{1,1}$ in terms of the $(1,1)$-forms descended from those of the del Pezzo surface factors. This can be illustrated via concrete configuration matrix (e.g., number 4077 in the CICY list [3, 16]):

$$X \sim \left[\begin{array}{c|cccc} \mathbb{P}^1 & 1 & 0 & 0 & 1 \\ \mathbb{P}^2 & 2 & 0 & 0 & 1 \\ \mathbb{P}^4 & 0 & 2 & 2 & 1 \end{array} \right] , \tag{5.3}$$

with Hodge numbers $(h^{1,1}(X), h^{2,1}(X)) = (11, 31)$. This configuration matrix is highly non-favorable with respect to the ambient product of projective spaces as is obvious from $h^{1,1}(X) - h^{1,1}(\mathcal{A}) = 11 - 3 = 8 > 0$ with $\mathcal{A} = \mathbb{P}^1 \times \mathbb{P}^2 \times \mathbb{P}^4$. On the other hand, the threefold X can also be thought of as an anticanonical divisor of the fourfold, $\mathcal{A}_{4,5} = dP_4 \times dP_5$, where the two del Pezzo surfaces are respectively given by the configurations,

$$dP_4 \sim \left[\begin{array}{c|c} \mathbb{P}^1 & 1 \\ \mathbb{P}^2 & 2 \end{array} \right] , \quad dP_5 \sim \left[\begin{array}{c|cc} \mathbb{P}^4 & 2 & 2 \end{array} \right] . \tag{5.4}$$

One can then easily see that the $h^{1,1}(\mathcal{A}_{4,5}) = 11$ Kähler forms of $\mathcal{A}_{4,5}$ descend to the $h^{1,1}(X) = 11$ independent Kähler forms of the Calabi-Yau hypersurface X and hence that X is favorably embedded in $\mathcal{A}_{4,5}$.

For any of the 35 geometries in table 1, a simple description of the divisors can be obtained from the ambient product of surfaces. Let us set the notation for such a basis here. Recall that the del Pezzo surface dP_r is constructed by blowing up a $\mathbb{P}^2$ at r generic points. The second homology group $H_2(dP_r, \mathbb{Z})$ is spanned by the hyperplane class L in $\mathbb{P}^2$ as well as the r exceptional divisors E_i, $i = 1, \cdots, r$, which intersect with one another as

$$L \cdot L = 1, \quad L \cdot E_i = 0, \quad E_i \cdot E_j = -\delta_{ij} . \tag{5.5}$$

In this basis, the Mori cone generators of the del Pezzo surfaces dP_r can be expressed as in table 2 and the first Chern class of dP_r is given by

$$c_1(dP_r) = 3L - \sum_{i=1}^{r} E_i . \tag{5.6}$$

See for example, [54] for more details on the geometry of the surface dP_r.

Equipped with such topological information, the triple intersections $d_{mnp}^{(r,s)}$ of the Calabi-Yau hypersurfaces, $X_{r,s} \subset \mathcal{A}_{r,s}$ can be straightforwardly computed as

$$d_{mnp}^{(r,s)} \equiv \int_{X_{r,s}} J_m \wedge J_n \wedge J_p = \int_{\mathcal{A}_{r,s}} J_m \wedge J_n \wedge J_p \wedge \left(3L - \sum_{i=1}^{r} E_i + 3L' - \sum_{i'=1}^{s} E'_{i'} \right), \tag{5.7}$$

where m, n, p are the indices labeling the $h^{1,1}(X) = r+s+2$ harmonic $(1,1)$-forms on $X_{r,s}$,

$$L, \quad E_{i=1,\dots,r}, \quad \text{and} \quad L', \quad E'_{i'=1,\dots,s} , \tag{5.8}$$

descending from those on dP_r and dP_s, respectively.

r	Generators ($i < j < \cdots \le r$)	Number
0	L	1
1	$E_1, L - E_1$	2
2	$E_i, L - E_i - E_j$	3
3	$E_i, L - E_i - E_j$	6
4	$E_i, L - E_i - E_j$	10
5	$E_i, L - E_i - E_j, 2L - E_i - E_j - E_k - E_l - E_m$	16
6	$E_i, L - E_i - E_j, 2L - E_i - E_j - E_k - E_l - E_m$	27
7	$E_i, L - E_i - E_j, 2L - E_i - E_j - E_k - E_l - E_m,$ $3L - 2E_i - E_j - E_k - E_l - E_m - E_n - E_o$	56
8	$E_i, \ L - E_i - E_j, \ 2L - E_i - E_j - E_k - E_l - E_m,$ $3L - 2E_i - E_j - E_k - E_l - E_m - E_n - E_o,$ $4L - 2(E_i + E_j + E_k) - \sum_{a=1}^{5} E_{m_a},$ $5L - E_i - E_j - 2\sum_{a=1}^{6} E_{m_a}, \ 6L - 3E_i - 2\sum_{a=1}^{7} E_{m_a}$	240
9	$f = 3L - \sum_{i=1}^{9} E_i, \ \text{and} \ \{y_a\} \ \text{such that} \ y_a^2 = -1, y_a \cdot f = 1$	∞

Table 2. The Mori cone generators for the del Pezzo surfaces dP_r, $r = 0, \cdots, 8$ and for the rational elliptic surface dP_9. The indices $i, j, \cdots \in \{1, \ldots, r\}$ appearing in each generator are distinct.

It is clear that a similar approach will also yield information on surfaces of the form $\mathcal{A}_s = \mathbb{P}^1 \times \mathbb{P}^1 \times dP_s$. Then

$$H, \quad \tilde{H} \quad \text{and} \quad L', \quad E'_{i'=1,\ldots,s}, \tag{5.9}$$

label the divisors on $X_s \subset \mathcal{A}_s$ descending from those on $\mathbb{P}^1 \times \mathbb{P}^1$ and dP_s. Furthermore, as in (5.7), the triple intersections $d_{mnp}^{(s)}$ of X_s can be obtained from

$$d_{mnp}^{(s)} \equiv \int_{X_s} J_m \wedge J_n \wedge J_p = \int_{\mathcal{A}_s} J_m \wedge J_n \wedge J_p \wedge \left(2H + 2\tilde{H} + 3L' - \sum_{i'=1}^{s} E'_{i'} \right), \tag{5.10}$$

where m, n, p label the $h^{1,1}(X) = s + 3$ $(1,1)$-forms on X_s.

Finally, the Mori (and the Kähler) cones of $\mathcal{A}_{r,s}$ and $\mathcal{A}_s$ can also be straightforwardly obtained from those of the individual del Pezzo factors (see table 2). Via Lemma 2.2 this information can then be interpreted as the Kähler/Mori data of the Calabi-Yau threefold $X_{r,s}$ or X_s [41].

5.1.2 Classification of genus-one fibrations

Recall that any divisors obeying the conditions (4.1) represent a genus-one fibration. In this subsection, we will classify such divisors for all the Calabi-Yau three-folds appearing in table 1, which we label as

$$X_{r,s} \subset \mathcal{A}_{r,s} \quad \text{and} \quad X_s \subset \mathcal{A}_s, \tag{5.11}$$

in terms of their four-fold ambient spaces, $\mathcal{A}_{r,s} = dP_r \times dP_s$ and $\mathcal{A}_s = \mathbb{P}^1 \times \mathbb{P}^1 \times dP_s$.

Let us start by analyzing $X_{r,s}$. Note first that divisors of $X_{r,s}$ can be parameterized as integer linear combinations,

$$\mathcal{D} = aL - \sum_{i=1}^{r} a_i E_i + a'L' - \sum_{i'=1}^{s} a'_{i'} E'_{i'}\,, \tag{5.12}$$

of the basis divisors $L, E_1, \ldots, E_r$ and $L', E'_1, \ldots, E'_s$. The triple intersection of $\mathcal{D}$ can then be expressed as

$$\int_{X_{r,s}} \mathcal{D}^3 = \int_{\mathcal{A}_{r,s}} \left(aL - \sum_{i=1}^{r} a_i E_i + a'L' - \sum_{i'=1}^{s} a'_{i'} E'_{i'} \right)^3 \wedge \left(3L - \sum_{i=1}^{r} E_i + 3L' - \sum_{i'=1}^{s} E'_{i'} \right) \tag{5.13}$$

$$= 3\left(a^2 - \sum_{i=1}^{r} a_i^2 \right)\left(3a' - \sum_{i'=1}^{s} a'_{i'} \right) + 3\left(a'^2 - \sum_{i'=1}^{s} a'^2_{i'} \right)\left(3a - \sum_{i=1}^{r} a_i \right)\,. \tag{5.14}$$

For the purpose of studying the geometries in table 1, let us restrict our analysis to $0 \leq r, s \leq 7$ in particular.

Note that the first of the Kollár criteria (4.1) for the divisor $\mathcal{D}$ of $X_{r,s}$ immediately leads to constraints on the divisors $D \equiv aL - \sum_{i=1}^{r} a_i E_i$ and $D' \equiv a'L' - \sum_{i'=1}^{s} a'_{i'} E'_{i'}$ of dP_r and dP_s, respectively. For example, for D considered as a divisor of dP_r, we should have $D \cdot C \geq 0$ for all curves C in dP_r.

We can, without loss of generality,[9] consider the case when the effective divisor $\mathcal{D}$ on $X_{r,s}$ descends from an effective divisor on $\mathcal{A}_{r,s}$. Since the first Chern class $c_1(dP_r) = 3L - \sum_{i=1}^{r} E_i$ is ample and D itself is to be a nef (and hence effective) divisor of dP_r, we have $D \cdot (3L - \sum_{i=1}^{r} E_i) \geq 0$ and $D \cdot D \geq 0$, which, respectively, lead to the inequalities,

$$3a - \sum_{i=1}^{r} a_i \geq 0\,, \tag{5.15}$$

$$a^2 - \sum_{i=1}^{r} a_i^2 \geq 0\,. \tag{5.16}$$

The situation where equality holds can then be described as follows (see appendix A.1 for the derivation): the first inequality saturates only for the zero vector $(a, a_1, \cdots, a_r) = 0$, while the second exhibits a more complicated solution set. This set contains not only the zero vector but also, depending on r, vectors of the form

$$(a, a_1, \cdots, a_r) = \alpha A_r^{(I)}\,, \quad \text{with } \alpha \in \mathbb{Z}_{>0}\,, \; I = 1, \cdots, N_r\,, \tag{5.17}$$

---

[9]Note that in general the cone of effective divisors on X (denoted Eff(X)) is larger than that of the ambient space, Eff($\mathcal{A}$), even for anticanonical hypersurfaces in Fano fourfolds. However, in the case at hand we are interested in divisors that are both effective and nef on X. That is the cone Nef(X) $\cap$ Eff(X). For the hypersurfaces in consideration here this intersection is maximal and equal to Nef(X) which descends fully from the ambient space $A_{r,s}$ (see [43] for a review of these issues).

where $A_r^{(I)}$ are the following vectors of length $r + 1$:

$$
\begin{aligned}
A_1^{(I)} &= (1,1), & I = 1 \,; \\
A_2^{(I)} &= (1,1,0),\ \cdots, & I = 1,2 \,; \\
A_3^{(I)} &= (1,1,0,0),\ \cdots, & I = 1,2,3 \,; \\
A_4^{(I)} &= (1,1,0,0,0),(2,1,1,1,1),\ \cdots, & 1 \le I \le 5 \,; \quad (5.18) \\
A_5^{(I)} &= (1,1,0,0,0,0),(2,1,1,1,1,0),\ \cdots, & 1 \le I \le 10 \,; \\
A_6^{(I)} &= (1,1,0,0,0,0,0),(2,1,1,1,1,0,0),(3,2,1,1,1,1,1),\ \cdots, & 1 \le I \le 27 \,; \\
A_7^{(I)} &= (1,1,0,0,0,0,0,0),(2,1,1,1,1,0,0,0),(3,2,1,1,1,1,1,0), \\
& \quad (4,2,2,2,1,1,1,1),(5,2,2,2,2,2,2,1),\ \cdots, & 1 \le I \le 126 \,.
\end{aligned}
$$

In (5.18), the ellipses represent all possible vectors obtained by permuting the $a_1, \cdots, a_r$ from any of the preceding vectors explicitly presented; e.g., with $r = 2$, one obtains an additional vector $A_2^{(2)} = (1,0,1)$ by permuting a_1 and a_2 from the $A_2^{(1)} = (1,1,0)$ presented above. Note that the counting, N_r, of the vectors $A_r^{(I)}$ for each $r = 0, \cdots, 7$ is given as

$$
N_0 = 0, \quad N_1 = 1, \quad N_2 = 2, \quad N_3 = 3, \quad N_4 = 5, \quad N_5 = 10, \quad N_6 = 27, \quad N_7 = 126 \,. \quad (5.19)
$$

Similarly, on dP_s, we also have

$$
3a' - \sum_{i'=1}^{s} a'_{i'} \ge 0 \,, \tag{5.20}
$$

$$
a'^2 - \sum_{i'=1}^{s} a'^2_{i'} \ge 0 \,, \tag{5.21}
$$

where the first inequality saturates only for the zero vector $(a', a'_1, \cdots, a'_s) = 0$, and the second, for the zero vector as well as for

$$
(a', a'_1, \cdots, a'_s) = \alpha' A_s^{(I')} \,, \text{ with } \alpha' \in \mathbb{Z}_{>0} \,, \ I' = 1, \cdots, N_s \,, \tag{5.22}
$$

where $A_s^{(I')}$ are the same length-$(s+1)$ vectors as in (5.18).

Given the constraints (5.15), (5.16), (5.20), and (5.21), together with the aforementioned equality conditions for them, the triple intersection (5.14) can only be set to zero in the following three cases.

Case 1: $(a, a_1, \cdots, a_r) = 0$. Each $(a', a'_1, \cdots, a'_s) \ne 0$ with D' nef in dP_s and $D'^2 \ne 0$ represents a genus-one fibration, where the base manifold is either dP_s or its blow down. For a generic choice of $(a', a'_1, \cdots, a'_s)$ the base is dP_s and the fibration is an OGF of the CICY configuration. For instance, in the configuration (5.3) with $(r,s) = (4,5)$, an OGF with the base $dP_{s=5} \sim \left[\mathbb{P}^4 \middle| 2\ 2 \right]$ is immediately found.

It should be noted that this same del Pezzo base can lead to other, related base geometries through the process of blowing down. Intuitively, any exceptional divisor in the del Pezzo base could be "grouped" with the fiber rather than the base geometry (leading

to a non-flat fiber over this locus). This phenomenon will be illustrated explicitly for a configuration matrix in Case 2 below. Such fibrations over the various blown-down bases can also be described by non-generic choices of $(a', a'_1, \cdots, a'_s)$, and these are not necessarily represented by an OGF. More details on these dP_s base geometries, the Kollár divisors (and how they relate to rational curves in the del Pezzo surface), as well as the enumeration of the distinct fibrations can be found in appendix C.

Case 2: $(a', a'_1, \cdots, a'_s) = 0$. Each $(a, a_1, \cdots, a_r) \neq 0$ with D nef in dP_r and $D^2 \neq 0$ represents a genus-one fibration, where the base is either dP_r or its blow down. For a generic $(a, a_1, \cdots, a_r)$ the base is dP_r and the fibration is an OFG. For instance, again in the configuration (5.3) with $(r, s) = (4, 5)$, an OGF with the base $dP_{r=4} \sim \begin{bmatrix} \mathbb{P}^1 & 1 \\ \mathbb{P}^2 & 2 \end{bmatrix}$ is immediately found.

This geometry provides an explicit illustration of the possible birational relationship of bases within this case distinction. Consider the configuration matrix in (5.3), re-written to make manifest the dP_4 base:

$$X \sim \begin{bmatrix} \mathbb{P}^4 & 0 & 2 & 2 & 1 \\ \mathbb{P}^1 & 1 & 0 & 0 & 1 \\ \mathbb{P}^2 & 2 & 0 & 0 & 1 \end{bmatrix} \quad . \tag{5.23}$$

This same configuration can also be re-grouped to make clear the fiber/base structure with a $\mathbb{P}^2$ base:

$$X \sim \begin{bmatrix} \mathbb{P}^4 & 0 & 2 & 2 & 1 \\ \mathbb{P}^1 & 1 & 0 & 0 & 1 \\ \mathbb{P}^2 & 2 & 0 & 0 & 1 \end{bmatrix} \quad . \tag{5.24}$$

Note that four exceptional divisors in the dP_4 base in (5.23) are now part of the fiber in (5.24). Consider the explicit form of the first defining equation associated to (5.24)

$$x_0 q_1(y) + x_1 q_2(y) = 0 \tag{5.25}$$

where x, y denote coordinates of $\mathbb{P}^1$ and $\mathbb{P}^2$ respectively. Over four points in the $\mathbb{P}^2$ base, the two quadratics q_1 and q_2 vanish, leading to a non-flat fiber over those points. In this case, the two bases are related by blowing up/down 4 points in $\mathbb{P}^2$. In general, similar base relationships can arise for *any choice of blow-downs for a del Pezzo base*, though not all may be visible as OGFs. In addition, these relationships can be seen via non-generic choices of the vectors $(a, a_1, \ldots, a_r)$ parameterizing Kollár divisors. Enumeration of all the blown-down bases is worked out in appendix C.

Case 3: $(a, a_1, \cdots, a_r) \neq 0$ and $(a', a'_1, \cdots, a'_s) \neq 0$. In this last case, $\mathcal{D}^3 = 0$ is only achieved for $\mathcal{D} = \mathcal{D}_{r,s}(\alpha, I; \alpha', I')$ of the form (5.12) with

$$\begin{aligned} (a, a_1, \cdots, a_r) &= \alpha A_r^{(I)}, & \alpha &\in \mathbb{Z}_{>0}, & I &= 1, \cdots, N_r, \\ (a', a'_1, \cdots, a'_s) &= \alpha' A_s^{(I')}, & \alpha' &\in \mathbb{Z}_{>0}, & I' &= 1, \cdots, N_s, \end{aligned} \tag{5.26}$$

where $A_r^{(I)}$ and $A_s^{(I')}$ are specified in (5.18). Regarding the counting of genus-one fibrations, two important observations follow. Firstly, although there are infinitely many such divisors

$\mathcal{D}_{r,s}(\alpha, I; \alpha', I')$, one can show that different choices of $\alpha, \alpha' \in \mathbb{Z}_{>0}$ for fixed I and I' lead to the same genus-one fibration. This can be observed by considering the redundancy criteria in section 1.1 and (1.12). In short, the fiber class $\mathcal{D}^2$ can be compared up to scaling for each member of the family. By intersecting $\mathcal{D}^2$ with the basis elements D_m for $m = 1, \cdots, h^{1,1}(X_{r,s})$ as in (1.13), one immediately observes that

$$\mathcal{D}_{r,s}^2(\alpha, I; \alpha', I') = \alpha\alpha' \mathcal{D}_{r,s}^2(1, I; 1, I'), \tag{5.27}$$

with $\mathcal{D}_{r,s}^2(1, I; 1, I') \neq 0$. Therefore, the fiber classes of the two possible fibrations are proportional (see the discussion in section 1.1). Hence, the bases of these two fibrations should differ only at non-generic points — for example, the two possible bases to the fibration are birational to each other (i.e. related by blowups in the base). On the other hand, it can also be shown that there are no curve classes which have a finite volume for one choice of α and α' but which shrink for another choice (see appendix A.2 for the details). This rules out possible disagreement of the fibrations. Secondly, having restricted ourselves to the divisors $\mathcal{D}_{r,s}(1, I; 1, I')$, one can prove that the $N_r N_s$ such divisors all lead to distinct genus-one fibrations. The following sufficient condition turns out to distinguish all those fibrations:

- If two divisors $\mathcal{D}_1$ and $\mathcal{D}_2$ each obey the conditions (4.1) while $\mathcal{D}_1 + \mathcal{D}_2$ does not, then $\mathcal{D}_1$ and $\mathcal{D}_2$ represent two distinct fibrations.

The above completes the classification of genus-one fibrations for all the CICYs in table 1 except for the first five geometries. For these cases, the general divisors of $X_s \subset \mathcal{A}_s$ are integer linear combinations of the form,

$$\mathcal{D} = hH + \tilde{h}\tilde{H} + a'L' - \sum_{i'=1}^{s} a'_{i'} E'_{i'}, \tag{5.28}$$

where H and $\tilde{H}$ are the two hyperplane classes of the $\mathbb{P}^1 \times \mathbb{P}^1$, appropriately pulled back to the Calabi-Yau threefold. We can now go through exactly the same steps as we did for $X_{r,s}$. Firstly, the triple intersection of $\mathcal{D}$ is given as

$$\int_{X_s} \mathcal{D}^3 = \int_{\mathcal{A}_s} \left(hH + \tilde{h}\tilde{H} + a'L' - \sum_{i'=1}^{s} a'_{i'} E'_{i'} \right)^3 \wedge \left(2H + 2\tilde{H} + 3L' - \sum_{i'=1}^{s} E'_{i'} \right) \tag{5.29}$$

$$= h\tilde{h}\left(3a' - \sum_{i'=1}^{s} a'_{i'} \right) + 2(h + \tilde{h})\left(a'^2 - \sum_{i'=1}^{s} a'^2_{i'} \right). \tag{5.30}$$

As in the $X_{r,s}$ cases, we can begin by assuming that each factor in the two terms of (5.30) are non-negative:

$$h \geq 0, \quad \tilde{h} \geq 0, \quad h + \tilde{h} \geq 0, \tag{5.31}$$

$$3a' - \sum_{i'=1}^{s} a'_{i'} \geq 0, \tag{5.32}$$

$$a'^2 - \sum_{i'=1}^{s} a'^2_{i'} \geq 0, \tag{5.33}$$

where the equality conditions for the last two inequalities have been described in the text around (5.22). It thus follows that the triple intersection of $\mathcal{D}$ can only be set to zero in the following four cases.

Case 1: $(h, \tilde{h}) = (0, 0)$. Each $(a', a'_1, \cdots, a'_s) \neq 0$ with D' nef in dP_s and $D'^2 \neq 0$ represents a genus-one fibration, where the base manifold is either dP_s or its blow down. Just as in the cases of $X_{r,s}$, for a generic $(a', a'_1, \cdots, a'_s)$ the base is dP_s and the fibration is an OGF. Enumeration of all the blown-down bases is worked out in appendix C.

Case 2: $(a', a'_1, \cdots, a'_s) = 0$. Each $(h, \tilde{h}) \neq 0$ corresponds to the genus-one fibration with the base $\mathbb{P}^1 \times \mathbb{P}^1$. Such a fibration is an OGF.

Case 3: $h = 0$, $\tilde{h} > 0$ and $(a', a'_1, \cdots, a'_s) \neq 0$. In this case, $\mathcal{D}^3 = 0$ is only achieved for $\mathcal{D} = \mathcal{D}_s(h = 0, h'; \alpha', I')$ of the form (5.28), with

$$(a', a'_1, \cdots, a'_s) = \alpha' A_s^{(I')}, \ \alpha' \in \mathbb{Z}_{>0}, \ I' = 1, \cdots, N_s, \tag{5.34}$$

where $A_s^{(I')}$ are specified in (5.18). Following exactly the same procedures as in the $X_{r,s}$ cases, we can confirm that $\mathcal{D}_s(0, h'; \alpha', I')$ represent the same genus-one fibration as $\mathcal{D}_s(0, 1; 1, I')$.

Case 4: $h > 0$ and $\tilde{h} = 0$ and $(a', a'_1, \cdots, a'_s) \neq 0$. In this case, $\mathcal{D}^3 = 0$ is only achieved for $\mathcal{D} = \mathcal{D}_s(h, h' = 0; \alpha', I')$ of the form (5.28), again with

$$(a', a'_1, \cdots, a'_s) = \alpha' A_s^{(I')}, \ \alpha' \in \mathbb{Z}_{>0}, \ I' = 1, \cdots, N_s. \tag{5.35}$$

We can confirm that $\mathcal{D}_s(h, 0; \alpha', I')$ represent the same genus-one fibration as $\mathcal{D}_s(1, 0; 1, I')$.

Finally, restricting ourselves to the $2N_s$ divisors, $\mathcal{D}_s(0, 1; 1, I')$ and $\mathcal{D}_s(1, 0; 1, I')$, we can prove, based on the aforementioned sufficient criterion for distinguishing fibrations, that the $2N_s$ such divisors all lead to distinct genus-one fibrations.

The counting of distinct genus-one fibrations for $X_{r,s} \subset \mathcal{A}_{r,s}$ and $X_s \subset \mathcal{A}_s$, with $r = 0, \ldots, 7$ and $s = 3, \ldots, 7$, is summarized in table 3. We also provide in table 4 another counting result that takes into account of some context-dependent potential redundancies (the permutations of the exceptional divisors of the del Pezzo factors, as well as the permutations of the two $\mathbb{P}^1$ factors in the X_s cases). Note, however, that such redundancies only arise from the topological view point. For the purpose of string dualities, a more relevant counting is the one given in table 3.

6 An infinite number of fibrations

In this section we analyze the CICY with Hodge numbers $(19, 19)$ which has long been known to have a number of unique and remarkable properties. This geometry proves to be the *only Kähler favorable CICY studied in this work which admits an infinite number*

Calabi-Yau	Number of Fibrations			
Space	Case 1	Case 2	All Others	Tot.
X_3	18	1	6	25
X_4	76	1	10	87
X_5	393	1	20	414
X_6	2764	1	54	2819
X_7	27094	1	252	27347
$X_{0,3}$	18	1	0	19
$X_{0,4}$	76	1	0	77
$X_{0,5}$	393	1	0	394
$X_{0,6}$	2764	1	0	2765
$X_{0,7}$	27094	1	0	27095
$X_{1,3}$	18	2	3	23
$X_{1,4}$	76	2	5	83
$X_{1,5}$	393	2	10	405
$X_{1,6}$	2764	2	27	2793
$X_{1,7}$	27094	2	126	27222
$X_{2,3}$	18	5	6	29
$X_{2,4}$	76	5	10	91
$X_{2,5}$	393	5	20	418
$X_{2,6}$	2764	5	54	2823
$X_{2,7}$	27094	5	252	27351
$X_{3,3}$	18	18	9	45
$X_{3,4}$	76	18	15	109
$X_{3,5}$	393	18	30	441
$X_{3,6}$	2764	18	81	2863
$X_{3,7}$	27094	18	378	27490
$X_{4,4}$	76	76	25	177
$X_{4,5}$	393	76	50	519
$X_{4,6}$	2764	76	135	2975
$X_{4,7}$	27094	76	630	27800
$X_{5,5}$	393	393	100	886
$X_{5,6}$	2764	393	270	3427
$X_{5,7}$	27094	393	1260	28747
$X_{6,6}$	2764	2764	729	6257
$X_{6,7}$	27094	2764	3402	33260
$X_{7,7}$	27094	27094	15876	70064

Table 3. The statistics of distinct genus-one fibrations for all the Calabi-Yau threefolds in table 1, where the Calabi-Yau hypersurfaces are embedded in the Fano fourfolds as $X_{r,s} \subset dP_r \times dP_s$ and $X_s \subset \mathbb{P}^1 \times \mathbb{P}^1 \times dP_s$, with $r = 0, \ldots, 7$ and $s = 3, \ldots, 7$. Case 1 and Case 2 denote those fibrations with the base surface being the second and the first ambient factor, respectively (incl. all their blow downs); this is consistent with the case distinctions in section 5.1.2.

Calabi-Yau	Number of Fibrations			
Space	Case 1	Case 2	All Others	Tot.
X_3	8	1	2	11
X_4	13	1	4	18
X_5	25	1	4	30
X_6	51	1	6	58
X_7	112	1	10	123
$X_{0,3}$	8	1	0	9
$X_{0,4}$	13	1	0	14
$X_{0,5}$	25	1	0	26
$X_{0,6}$	51	1	0	52
$X_{0,7}$	112	1	0	113
$X_{1,3}$	8	2	1	11
$X_{1,4}$	13	2	2	17
$X_{1,5}$	25	2	2	29
$X_{1,6}$	51	2	3	56
$X_{1,7}$	112	2	5	119
$X_{2,3}$	8	4	1	13
$X_{2,4}$	13	4	2	19
$X_{2,5}$	25	4	2	31
$X_{2,6}$	51	4	3	58
$X_{2,7}$	112	4	5	121
$X_{3,3}$	8	8	1	9
$X_{3,4}$	13	8	2	23
$X_{3,5}$	25	8	2	35
$X_{3,6}$	51	8	3	62
$X_{3,7}$	112	8	5	125
$X_{4,4}$	13	13	3	16
$X_{4,5}$	25	13	4	42
$X_{4,6}$	51	13	6	70
$X_{4,7}$	112	13	10	135
$X_{5,5}$	25	25	3	28
$X_{5,6}$	51	25	6	82
$X_{5,7}$	112	25	10	147
$X_{6,6}$	51	51	6	57
$X_{6,7}$	112	51	15	178
$X_{7,7}$	112	112	15	127

Table 4. The results from table 3 for genus-one fibrations for all the Calabi-Yau threefolds in table 1, grouped into families to reflect the symmetries of the del Pezzo ambient spaces. Case 1 and Case 2 denote those fibrations with the base surface being the second and the first ambient factor, respectively (incl. all their blow downs); this is consistent with the case distinctions in section 5.1.2. The families are defined by symmetries including: (a) for Case 1 and Case 2 the fibrations are only counted up to permutations of the exceptional divisors of the del Pezzo factors; (b) for All Others, up to the obvious permutation symmetries of the ambient space (i.e., permutations of the two $\mathbb{P}^1$ factors in the X_s cases and those of the two surface factors in the $X_{r,s}$ cases with $r = s$); (c) in the $X_{r,s}$ cases with $r = s$, the numbers for Case 1 and Case 2 do not add up for the Total counting as only one half of these is regarded as irredundant.

of genus one fibrations.[10] The existence of an infinite number of both genus one and $K3$-fibrations in this geometry has been observed in several contexts previously [27, 55], however we will provide here a new and explicit parameterization of one such infinite family.

6.1 The Schoen manifold

6.1.1 Topological data

As described in section D.1, of the 48 non-favorable configurations studied in section 5, there are 15 with Hodge numbers $(h^{1,1}, h^{2,1}) = (19, 19)$ and all can be proved to be equivalent to one another via splittings/contractions. Each is manifestly a fiber product of two generic rational elliptic surfaces (called dP_9 in the physics literature) identified over a common $\mathbb{P}^1$. Thus, they are all equivalent to the Schoen manifold.

One simple CICY configuration, similar in spirit to those studied in section 5 (i.e. a hypersurface in an ambient product of two surfaces) provides a particularly straightforward way to compute the topology — including all of the triple intersection numbers — of this manifold:

$$X_{\text{Schoen}} \sim \left[\begin{array}{c|ccc} \mathbb{P}^1 & 0 & 1 & 1 \\ \mathbb{P}^1 & 1 & 0 & 1 \\ \mathbb{P}^2 & 0 & 3 & 0 \\ \mathbb{P}^2 & 3 & 0 & 0 \end{array} \right] . \tag{6.1}$$

This configuration can be obtained by ineffectively splitting the configuration of the split bi-cubic (number 14 in the original CICY list [3, 16]),

$$\left[\begin{array}{c|cc} \mathbb{P}^1 & 1 & 1 \\ \mathbb{P}^2 & 0 & 3 \\ \mathbb{P}^2 & 3 & 0 \end{array} \right] . \tag{6.2}$$

The configuration (6.1) describes the Schoen manifold as an anticanonical divisor of $\mathcal{A}_{9,9} = dP_9 \times dP_9$, with

$$dP_9 \sim \left[\begin{array}{c|c} \mathbb{P}^1 & 1 \\ \mathbb{P}^2 & 3 \end{array} \right] . \tag{6.3}$$

As in the other del Pezzo surface cases, the second homology group $H_2(dP_9, \mathbb{Z})$ of dP_9 is spanned by the hyperplane class L in $\mathbb{P}^2$ as well as the, in this case 9, exceptional divisors $E_{i=1,\cdots,9}$. Their intersections and the first Chern class are as in (5.5) and (5.6). The twenty ambient divisors of $\mathcal{A}_{9,9}$ restrict to the anti-canonical hypersurface (i.e. X_{Schoen}) with one linear relation that reduces the number of independent divisors to the expected 19. Despite the fact that $h^{1,1}(\mathcal{A}_{9,9}) = 20 = 1 + h^{1,1}(X_{\text{Schoen}})$, X_{Schoen} is both favorable and (as we will see below) Kähler favorable, since its Picard group, Kähler, and Mori cones descend directly from $\mathcal{A}_{9,9}$, albeit in this case with a non-trivial redundancy.

The linear relationship reducing the 20 divisors of $\mathcal{A}_{9,9}$ to the 19 dimensional Picard group of X_{Schoen} can be seen in several ways. The first of these is to consider imposing

---

[10]Note, as discussed in previous sections, we are limited here to the study of Kähler favorable CICY threefolds. There could of course exist other geometries, not in this class, which also admit an infinite numbers of fibrations.

the third defining equation (given by the last column in (6.1)) first. From the well-known relation that

$$\left[\begin{array}{c|c} \mathbb{P}^1 & 1 \\ \mathbb{P}^1 & 1 \end{array} \right] \sim \mathbb{P}^1 \,, \tag{6.4}$$

it is clear that two distinct divisors (the hyperplanes of the first two $\mathbb{P}^1$ factors of the ambient space) are made linearly equivalent by imposing the third defining relation. Alternatively, this same relation can be observed by considering the long exact sequence in cohomology associated to the dual of the adjunction sequence:

$$0 \to TX_{\mathrm{Schoen}} \to T\mathcal{A}_{9,9}|_{X_{\mathrm{Schoen}}} \to \mathcal{N}|_{X_{\mathrm{Schoen}}} \to 0 \,, \tag{6.5}$$

where $\mathcal{N}|_{X_{\mathrm{Schoen}}}$ is the restriction of the normal bundle with the Chern class $c_1(\mathcal{N}) = 3L - \sum_{i=1}^9 E_i + 3L' - \sum_{i'=1}^9 E'_{i'}$. An explicit algebraic description of the following morphism (using the tools of [38, 39])

$$\phi : H^1(X_{\mathrm{Schoen}}, \mathcal{N}^*_{X_{\mathrm{Schoen}}}) \to H^1(X_{\mathrm{Schoen}}, T\mathcal{A}^*_{9,9}|_{X_{\mathrm{Schoen}}}) \tag{6.6}$$

demonstrates that $h^1(X_{\mathrm{Schoen}}, TX^*_{\mathrm{Schoen}}) = \dim(\mathrm{coker}(\phi)) = 19$ with the same linear relationship as in (6.4) imposed. Choosing the obvious basis of divisors descended from the ambient product of dP_9's:

$$L, E_{i=1,\ldots,9}, \quad \text{and} \quad L', E'_{i'=1,\ldots,9} \,, \tag{6.7}$$

the linear relationship takes the following form:

$$3L - \sum_{i=1}^9 E_i = 3L' - \sum_{i'=1}^9 E'_{i'} \,. \tag{6.8}$$

Having in mind of this redundancy, the Mori and the Kähler cones of X_{Schoen} can be immediately obtained by pulling back those of the ambient space $\mathcal{A}_{9,9}$ (though the argument is distinct in this case from that used in Lemma 2.2 since the ambient space is not Fano. Instead the same conclusion — that the Kähler and Mori cones descend from $\mathcal{A}_{9,9}$ — can be obtained by the results of [56]). The Mori cone generators of dP_9 are described in table 2.

With this favorable basis of divisors in hand, the triple intersection numbers of X_{Schoen} can be derived in the usual way as

$$d_{mnp}^{\mathrm{Schoen}} \equiv \int_{X_{\mathrm{Schoen}}} J_m \wedge J_n \wedge J_p = \int_{\mathcal{A}_{9,9}} J_m \wedge J_n \wedge J_p \wedge \left(3L - \sum_{i=1}^9 E_i + 3L' - \sum_{i'=1}^9 E'_{i'} \right) . \tag{6.9}$$

Here, m, n, p are the indices labeling the redundant (20-dimensional) basis of descended harmonic $(1,1)$-forms on X_{Schoen}. Such a description of the intersection numbers is symmetric in the two dP_9 factors. Note that the intersection numbers with the indices ranging from 1 to 19 already form a complete dataset themselves, given the redundancy (6.8) within the 20 $(1,1)$-forms.

6.1.2 A study of genus-one fibrations

In this section we will set-up a systematic study of the fibrations of X_{Schoen} and demonstrate that unlike the other cases investigated in section 5, the Schoen manifold manifestly admits an *infinite number* of genus one fibrations. Remarkably, it is the only such manifold we have encountered in the CICY list. We will not attempt to classify all such infinite classes here, but will instead illustrate the phenomenon with one explicit infinite family.

In order to classify genus-one fibrations within the Schoen manifold, we will take a similar approach to the one in subsection 5.1.2, based on Kollár's criteria. Even in the presence of the redundancy (6.8), the divisors of X_{Schoen} can be integrally parameterized as

$$\mathcal{D} = aL - \sum_{i=1}^{9} a_i E_i + a'L' - \sum_{i'=1}^{9} a'_{i'} E'_{i'} \,, \tag{6.10}$$

whose triple intersection is given by

$$\int_{X_{\text{Schoen}}} \mathcal{D}^3 = \int_{dP_9 \times dP_9} \left(aL - \sum_{i=1}^{9} a_i E_i + a'L' - \sum_{i'=1}^{s} a'_{i'} E'_{i'} \right)^3$$

$$\wedge \left(3L - \sum_{i=1}^{9} E_i + 3L' - \sum_{i'=1}^{9} E'_{i'} \right) \tag{6.11}$$

$$= 3\left(a^2 - \sum_{i=1}^{9} a_i^2 \right)\left(3a' - \sum_{i'=1}^{9} a'_{i'} \right) + 3\left(a'^2 - \sum_{i'=1}^{9} a'^{\,2}_{i'} \right)\left(3a - \sum_{i=1}^{9} a_i \right) \,. \tag{6.12}$$

In a search for fibrations, one of the Kollár criteria (4.1) says that $\mathcal{D} \cdot \mathcal{C} \geq 0$ for all curves $\mathcal{C}$ in X_{Schoen}. Given the description of the Mori and the Kähler cones of X_{Schoen} in the previous subsection, it follows that

$$\left(aL - \sum_{i=1}^{9} a_i E_i \right) \cdot C \geq 0 \quad \text{and} \quad \left(a'L' - \sum_{i'=1}^{9} a'_{i'} E'_{i'} \right) \cdot C' \geq 0 \,, \tag{6.13}$$

is required for all curves C and C' of the two dP_9 factors, respectively.

For simplicity, we will from now on denote the two pieces in $\mathcal{D}$ as

$$D = aL - \sum_{i=1}^{9} a_i E_i \,,$$

$$D' = a'L' - \sum_{i'=1}^{9} a'_{i'} E'_{i'} \,,$$

and due to the complete symmetry in the two dP_9 pieces, it is sufficient to analyze this constraint for a single piece, say, D. Since the fiber class $f = 3L - \sum_{i=1}^{9} E_i$ is a Mori cone generator and D must itself be a nef divisor of dP_9, we have $D \cdot f \geq 0$ and $D \cdot D \geq 0$,

which, respectively, lead to

$$3a - \sum_{i=1}^{9} a_i \geq 0 \tag{6.14}$$

$$a^2 - \sum_{i=1}^{9} a_i^2 \geq 0 . \tag{6.15}$$

In order to saturate (6.14), one must have

$$9a^2 = \left(\sum_{i=1}^{9} a_i \right)^2 \leq 9 \left(\sum a_i^2 \right) \leq 9a^2 , \tag{6.16}$$

where the first inequality comes from the Cauchy-Schwarz inequality and the second, from (6.15). Thus, both inequalities in (6.16) saturate, which can only happen when $(a, a_1, \cdots, a_9) \sim (3, 1, \cdots, 1)$, i.e., when D is a positive multiple of f. However, since the fiber classes f and f' on the two dP_9 factors are identified on X_{Schoen}, we may as well view this as $D = 0$ by shifting D' by f'.

Thus, as in subsection (5.1.2), we are naturally lead to the following three cases.

Case 1: $(a, a_1, \cdots, a_9) = 0$. In this case, $(a', a_1', \cdots, a_9') \neq 0$ so that $\mathcal{D}^2 \neq 0$, and each such divisor corresponds to the genus-one fibration with the base dP_9 (or its blow downs). Such a fibration is an OGF of the CICY configuration. For instance, in the configuration (6.2) of CICY 14, an OGF with the base $dP_9 \sim \begin{bmatrix} \mathbb{P}^1 & 1 \\ \mathbb{P}^2 & 3 \end{bmatrix}$ is immediately found, where, for instance, the $\mathbb{P}^2$ is that in the second row of the threefold configuration matrix.

Case 2: $(a', a_1', \cdots, a_9') = 0$. In this case, $(a, a_1, \cdots, a_9) \neq 0$ so that $\mathcal{D}^2 \neq 0$, and each divisor of this type corresponds to the genus-one fibration with the base being the other dP_9 (or its blow downs). Such a fibration is also an OGF. In the configuration (6.2), this corresponds to the OGF with the base $dP_9 \sim \begin{bmatrix} \mathbb{P}^1 & 1 \\ \mathbb{P}^2 & 3 \end{bmatrix}$, where the $\mathbb{P}^2$ is now taken from the third row of the threefold configuration.

Case 3: $(a, a_1, \cdots, a_r) \neq 0$ and $(a', a_1', \cdots, a_s') \neq 0$. Note first that the cases with D being a positive multiple of f and those with D' being a positive multiple of f' for D' have effectively been considered in the Case 2 and the Case 1 above, respectively. Therefore, we may strengthen the constraint (6.14) so that $(a, a_1, \cdots, a_9)$ obey

$$3a - \sum_{i=1}^{9} a_i > 0 , \tag{6.17}$$

and $(a', a_1', \cdots, a_9')$ obey the analogously strengthened constraint. For the triple intersection of $\mathcal{D}$ in (6.12) to vanish, we must thus have the inequality (6.15) saturated. Then, from the Riemann-Roch theorem, it follows that

$$0 < D \cdot f = D \cdot D - 2g + 2 = -2g + 2 \leq 2 , \tag{6.18}$$

and hence, the last inequality has to saturate. Therefore, we only need to classify the solutions to

$$3a - \sum_{i=1}^{9} a_i = 2 \,, \tag{6.19}$$

$$a^2 - \sum_{i=1}^{9} a_i^2 = 0 \,, \tag{6.20}$$

that describe certain rational curves of dP_9. Note that these two constraints for D arose from $D \cdot C \geq 0$ for particular curves C in dP_9 and as such they do not guarantee the inequality for every curve in dP_9 (i.e. the nef criterion).

Once we require that D should be nef, a somewhat lengthy argument (see appendix B.1 for details) demonstrates that the solutions can be characterized as

$$D = y + z \,, \tag{6.21}$$

where $y, z \,(\neq f)$ are any two (of the *infinite* number of) distinct Mori cone generators with $y \cdot z = 1$.

Given such a characterization, one can obtain a parametric family of infinitely many solutions for D (as described in (B.28)) by making use of specific parameterizations of the Mori cone generators of dP_9 (see appendix B.2 for details). An analogous parameterization is obtained for D' (as described in (B.29)) and hence, one can parametrically describe an infinite family of divisors $\mathcal{D} = D + D'$ of X_{Schoen}, each of which represents a genus-one fibration. Here, for simplicity, we will present and analyze an infinite, one-parameter subfamily[11] with

$$\begin{aligned} D &= 2(2 + k + k^2)f + 3E_1 - E_2 + E_3 + E_4 + 2kE_8 - 2(1+k)E_9 \,, \\ D' &= 4f' + 3E_1' - E_2' + E_3' + E_4' - 2E_9' \,, \end{aligned} \tag{6.22}$$

where $f = 3L - \sum_{i=1}^{9} E_i$ and $f' = 3L' - \sum_{i'=1}^{9} E_{i'}'$ have been used for a simpler description and $k \in \mathbb{Z}$. It is straightforward to verify that $\mathcal{D}$ is nef (via the criteria in (4.1)) and satisfies $\mathcal{D}^3 = 0$ and $\mathcal{D}^2 \neq 0$ as required.

Finally, it remains to verify that for each value of k these are in fact *inequivalent* Kollár divisors. For this we will utilize the criteria laid out in (1.12) (i.e. that two Kollár divisors are equivalent if they lead to proportional fiber classes in X) in section 1.1. Using the triple intersection numbers (6.9) of X_{Schoen}, the fiber class (up to a proportional constant) can be obtained as the following vector of length 19,

$$\begin{aligned} \{\mathcal{D}^2 \cdot J_m\}_{m=1}^{10} &= \{48 + 3\kappa, 4 + \kappa, 20 + \kappa, 12 + \kappa, 12 + \kappa, 16 + \kappa, \\ &\qquad 16 + \kappa, 16 + \kappa, 16 + 8k^2, 24 + \kappa + 8k\} \quad (6.23) \\ \{\mathcal{D}^2 \cdot J_m\}_{m=11}^{19} &= \{48, 4, 20, 12, 12, 16, 16, 16, 16\} \,, \end{aligned}$$

---

[11]This subfamily is obtained by turning off all but one parameter $k_8 \equiv k$ from the 14-parameter family described in (B.28), (B.29), and (B.31). See appendix B.2.

where $\kappa = 8k + 8k^2$ and the 19 (1,1)-forms J_m are the first 19 of those in (6.7) except the E_9'. It is therefore obvious that the fibers can never be the same for different values of k and hence, all of the divisors $\mathcal{D}$ described by (6.22) represent distinct genus-one fibrations. Thus, $\mathcal{D} = D + D'$ with (6.22) defines a true infinite family of genus one fibrations in X_{Schoen}.

It may seem somewhat surprising that an infinite number of genus one fibrations can arise for any CICY threefold. In addition, the fact that this infinite structure appears to occur for only one geometry is also remarkable. However, the Schoen manifold has a number of special features that set the stage for this infinite structure. First, as remarked above, the Kähler and Mori cones of X_{Schoen} are infinitely generated. This alone was perplexing in the context of mirror symmetry and was the subject of a detailed study by Morrison and Grassi in [56]. There they observed that although the Kähler cone of X_{Schoen} is infinitely generated, the action of the automorphism group of X_{Schoen} on the Kähler cone has a rationally polyhedral fundamental domain (Morrison has conjectured[12] that this must hold for any CY manifold with such an infinitely generated Kähler cone [57]). Like our constructions above, the automorphism action descends from the two ambient space copies of the rational elliptically fibered surface, dP_9, and the associated action on the Kähler/Mori cones of dP_9. Although it is beyond the scope of the present work to explore, it is reasonable to surmise that this automorphism action could collapse the infinite families parameterized above into a finite (physically distinct) set.

Finally, realizing the Schoen manifold as the blow up of the toroidal orbifold $T^6/\mathbb{Z}_2 \times \mathbb{Z}_2$ [27] has lead to the observation that X_{Schoen} must contain an infinite number of both elliptic and $K3$ fibrations (see [27] and [58] for details). Moreover, the physical consequences of this infinite fibration structure for string dualities (in particular for heterotic/Type IIA or heterotic/F-theory duality) were explored in [55], where an argument was made that such infinite families could be realized as U-duality symmetries [59] in the dual pairs. It would be interesting to find additional examples of such infinite fibration structures in other constructions of CY manifolds and to more explicitly explore their consequences for string dualities.

7 Conclusions and future directions

As summarized in section 1.2, the goal of this work was to undertake a comprehensive survey of genus-one fibrations in the data set of CICY threefolds. We find that not only do more than 99% of the 7890 configuration matrices in this dataset lead to a genus-one fibered geometry, but that this simple set of CY manifolds yields a vast number (indeed an infinite number) of distinct genus one fibrations. We have approached this survey using two tools: 1) A study of so-called "obvious" fibrations manifestly realized in the algebraic form of the manifolds and 2) An exhaustive search for genus-one fibrations using the Kollár criteria outlined in section 1.1. We explicitly provide examples of geometries for which these methods of enumerating fibrations agree (see section 4) and those for which OGFs vastly undercount the possible fibration structures (see sections 5 and 6).

---

[12]For a more precise definition of the Morrison-Kawamata Cone Conjecture see [43] for a recent review.

– 40 –

The Kollár criteria provides a means of classifying *all genus-one fibrations* within the set of CICY threefolds. However, a complete classification is dependent on having explicit descriptions of the full Kähler and Mori cones of each manifold. In general, tools to determine this data had been lacking in the literature to date and we substantially expand these methodologies here. By means of splitting/contracting configuration matrices as outlined in section 2 we have found new, favorable descriptions of 2946 CICYs and moreover determined the full Kähler/Mori cone structure of 4957 "Kähler favorable" geometries. Thus, the survey completed here is a complete classification of genus-one fibrations for 4957 out of the 7868 CICYs that are not direct products. If new tools are developed to complete the Kähler/Mori data of the remaining CICY geometries, the techniques outlined here could be readily applied to the remainder of the CICY dataset. Such systematic scans for Kollár divisors/fibrations in toric hypersurfaces could also be readily carried out. We leave such explorations for future work.

The enhanced CICY list [3] described above now contains the full topology of each manifold (the so-called "Wall's theorem data" [60] that can be used to distinguish these threefold geometries as real manifolds), and also, thanks to the OGF survey, many descriptions of them as genus one fibered geometries. It is our expectation that this data will provide a useful playground for the study of string compactifications, model building, and string dualities. For example, this set of CY geometries has already provided a fruitful arena for heterotic model building [32, 61–68] (see also toric approaches in [69–71]) and simple geometries in which to explore new approaches to moduli stabilization [38, 72–77]. The study of fibration structures completed here could yield valuable new approaches to the study of heterotic string and F-theory compactifications, as well as string dualities — including providing novel backgrounds for 6-dimensional compactifications of F-theory. For example, CICY threefolds have been observed to generically lead to higher rank Mordell-Weil groups [2, 29] and have been used as compactification geometries for heterotic/F-theory duality for $\mathcal{N} = 1$, 4-dimensional solutions.

The results of the fibration survey completed here indicate that even existing data sets of CY geometries may contain many more genus-one fibrations than previously realized. Indeed, genus one fibrations have long provided intriguing structure that suggests a possible route to classifying all CY threefolds. The work of [5, 7] establishing that the set of all genus-one fibered CY manifolds is finite was motivated in no small part by the hope that this result could be used to bound the number of *all CY geometries*. The essential idea is as follows: many studies of CY threefold geometry have indicated that as $h^{1,1}$ increases, the topology and triple intersection numbers of the threefold take on more specific forms [78, 79]. This fact, coupled to the ubiquitous presence of genus-one fibrations at large $h^{1,1}$ in known data sets of CY threefolds, has lead to speculation that perhaps all CY threefolds with large enough $h^{1,1}$ admit an elliptic fibration — and hence their topology may be bounded by the classification of [5] (see also [80–84] for a recent program of work explicitly enumerating such fibrations). In that spirit, the results of this systematic survey seem to provide more evidence for this conjecture (indeed every CICY threefold is fibered for $h^{1,1} > 4$). We are hopeful that the approaches outlined here may be applied to further these ideas and study fibration structures in CY geometries more generally in the future.

Acknowledgments

A Details of the Diophantine system for del Pezzo surfaces

In this section we provide the details of the arguments leading to a complete fibration count for the 68 CICY configurations analyzed in section 5, which correspond to an anticanonical hypersurface in an ambient product of two del Pezzo surfaces (see table 1 for the CICY ID numbers).

A.1 Saturation of the inequalities

Here, we will derive the equality conditions for the two inequalities (5.15) and (5.16),

$$3a - \sum_{i=1}^{r} a_i \geq 0 \,, \tag{A.1}$$

$$a^2 - \sum_{i=1}^{r} a_i^2 \geq 0 \,, \tag{A.2}$$

that should hold for a divisor $D = aH - \sum_{i=1}^{r} a_i E_i$ of dP_r obeying $D \cdot C \geq 0$ for all curves C in dP_r, where $r = 0, \cdots, 7$. Without loss of generality, we may assume that a_i's are ordered so that

$$a_1 \geq \cdots \geq a_r \geq 0 \,, \tag{A.3}$$

where the last inequality can be seen from the fact that E_r, being a Mori cone generator, is effective. Further, when $r \geq 1$, $a \geq a_1$ since $L - E_1 - E_2$ (or $L - E_1$ in the $r = 1$ case) is also effective as a Mori cone generator.

Let us start with the inequality (A.1). We will prove that a vanishes (and hence so do a_i's) when it saturates, i.e., when $3a = \sum_{i=1}^{r} a_i$. This can easily be seen for each $r = 0, \cdots, 7$ as follows:

- $r = 0$: Vacuously true.

- $r = 1$: $a_1 = 3a \geq a \geq a_1$ (as $L - E_1$ is effective) $\Rightarrow$ $a = 0$.

- $r = 2$: $a_1 + a_2 = 3a \geq a \geq a_1 + a_2$ (as $L - E_1 - E_2$ is effective) $\Rightarrow$ $a = 0$.

- $r = 3$: $\sum_{i=1}^{3} a_i = 3a \geq 2a \geq (a_1 + a_2) + (a_1 + a_3)$ (as $L - E_i - E_j$ are effective) $\geq \sum_{i=1}^{3} a_i \Rightarrow a = 0$.

– 42 –

- $r = 4$: $\sum_{i=1}^{4} a_i = 3a \geq 2a \geq (a_1 + a_2) + (a_3 + a_4)$ (as $L - E_i - E_j$ are effective) $\geq \sum_{i=1}^{4} a_i \Rightarrow a = 0$.

- $r = 5$: $\sum_{i=1}^{5} a_i = 3a \geq 2a \geq \sum_{i=1}^{5} a_i$ (as $2L - \sum_{i=1}^{5} E_i$ is effective) $\Rightarrow a = 0$.

- $r = 6$: $\sum_{i=1}^{6} a_i = 3a = \frac{1}{2}(2a + 2a + 2a) \geq \frac{3}{2} \sum_{i=1}^{5} a_i$ (as $2L - \sum_{i=1}^{5} E_i$ is effective) $\geq \sum_{i=1}^{5} a_i + (\frac{1}{2}a_1 + \frac{1}{2}a_2 + \frac{3}{2}a_6) \geq \sum_{i=1}^{6} a_i \Rightarrow a_1 = 0 \Rightarrow a = 0$.

- $r = 7$: $\sum_{i=1}^{7} a_i = 3a = \frac{1}{2}(2a + 2a + 2a) \geq \frac{3}{2} \sum_{i=1}^{5} a_i$ (as $2L - \sum_{i=1}^{5} E_i$ is effective) $\geq \sum_{i=1}^{5} a_i + (\frac{1}{2}a_1 + \frac{2}{2}a_6 + \frac{2}{2}a_7) \geq \sum_{i=1}^{7} a_i \Rightarrow a_1 = 0 \Rightarrow a = 0$.

Next, saturation of the second inequality (A.2) can be immediately analyzed on a computer, for each $r = 1, \cdots, 7$ (when $r = 0$, the inequality can not be saturated unless $a = 0$). Practically, upon setting $a = 1$, we can show that $g(a_i) \equiv \sum_{i=1}^{r} a_i^2 \leq 1$ and the maximum value 1 can only be achieved when a_i's take values from (5.18) (up to an appropriate rescaling of a). Note that the region for the values of the r parameters $(1 \geq) a_1 \geq \cdots \geq a_r (\geq 0)$ is further restricted by the Mori cone generators of table 2 as follows,

- $r = 1$: $a_1 \leq 1$

- $r = 2, 3, 4$: $a_1 + a_2 \leq 1$

- $r = 5, 6$: $a_1 + a_2 \leq 1$, $\sum_{i=1}^{5} a_i \leq 2$

- $r = 7$: $a_1 + a_2 \leq 1$, $\sum_{i=1}^{5} a_i \leq 2$, $a_1 + \sum_{i=2}^{7} a_i \leq 3$,

and the maximum of g may only occur at the critical points on the boundary of the bounded region defined as such. A quick computer analysis based on this leads to the aforementioned result.

A.2 Shrinking curves

To a divisor $\mathcal{D}$ of the Calabi-Yau threefold $X \subset \mathcal{A}$ obeying the criteria (4.1), there exists a corresponding genus-one fibration $\pi : X \to B$. Let us suppose that we are given another such divisor $\tilde{\mathcal{D}}$ and the corresponding fibration $\tilde{\pi} : X \to \tilde{B}$ such that $c\mathcal{D}^2 = \tilde{c}\tilde{\mathcal{D}}^2$ for some $c, \tilde{c} \in \mathbb{Z}_{>0}$. In general there is still a possibility of π and $\tilde{\pi}$ being a different projection with B and $\tilde{B}$ being only birational.

In this subsection, we consider the divisors of a given Calabi-Yau threefold $X_{r,s} \subset \mathcal{A}_{r,s}$,

$$\mathcal{D}(\alpha, \alpha') \equiv D_{r,s}(\alpha, I; \alpha', I'), \tag{A.4}$$

described in (5.26), for fixed I and I'. They obey (5.27) and may in principle represent different fibrations. The purpose of this subsection is to rule out such a possibility.

Let us begin by choosing one such divisor, $\mathcal{D} = \mathcal{D}(\alpha, \alpha')$, associated with the corresponding fibration $\pi : X_{r,s} \to B$. In the following, we will first characterize the Picard lattice of B. Note that any pulled-back divisors $\mathcal{D}_B = D_B + D'_B$ from the base B must obey $\mathcal{D}^2 \cdot \mathcal{D}_B = 0$ on $X_{r,s}$, where D_B and D'_B are the pieces pulled back from the dP_r

and dP_s under their own projections, respectively. Similarly decomposing the divisor $\mathcal{D}$ as $D + D'$, we thus have

$$
\begin{aligned}
0 &= \int_{X_{r,s}} \mathcal{D}^2 \wedge \mathcal{D}_B \\
&= \int_{\mathcal{A}_{r,s}} (D + D')^2 \wedge (D_B + D'_B) \wedge \left(3L - \sum_{i=1}^r E_i + 3L' - \sum_{i'=1}^s E'_{i'} \right) \quad (A.5) \\
&= 4\alpha' \int_{dP_r} D \wedge D_B + 4\alpha \int_{dP_s} D' \wedge D'_B \,, \quad (A.6)
\end{aligned}
$$

where in the last step we have used the properties of D that $D^2 = 0$ and $D \cdot (3L - \sum_{i=1}^r E_i) = 2\alpha$ on dP_r, as well as the analogous properties of D' on dP_s. Now, restricting to those divisors $\mathcal{D}_B$ that are pull-backs of ample divisors of B, we must have the two integrals in (A.6) both non-negative since D_B and D'_B are effective curves of dP_r and dP_s, in particular, and hence, each integral should vanish. In terms of the expansion coefficients in $D = aL - \sum_{i=1}^r a_i E_i$ and $D_B = bL - \sum_{i=1}^r b_i E_i$, we have

$$
\int_{dP_r} D \wedge D_B = ab - \sum_{i=1}^r a_i b_i \geq ab - \left(\sum_{i=1}^r a_i^2 \right)^{1/2} \left(\sum_{i=1}^r b_i^2 \right)^{1/2} \geq 0 \,, \quad (A.7)
$$

where we have used the Cauchy-Schwarz inequality, as well as the intersections $D \cdot D = 0$ (by construction) and $D_B \cdot D_B \geq 0$ (as D_B is ample) on dP_r. For the saturation of inequalities, we conclude that D_B is proportional to D, and similarly, D'_B to D'. Thus, ample cone of B, when pulled-back to $X_{r,s}$, should lie in the two-dimensional plane spanned by D and D'. Therefore, the Picard lattice of B also lies in that plane, and effective curves C of B can be expanded as $C = \lambda D + \lambda' D'$ for some rational numbers λ and λ'. Note that we are not distinguishing the $(1,1)$-forms in B from their pull-backs to $X_{r,s}$, having in mind of the obvious injection.

For the rest of this subsection, we will show that there do not exist zero-volume effective curves of B when Kähler forms are taken from the interior of the positive cone spanned by D and D'. This, if proven, will guarantee that different choice of α and α' still represents the same genus-one fibration. For this purpose, let us consider a Kähler form J and an effective curve C of the form,

$$
J = \mu D + \mu' D' \quad (\mu, \mu' > 0) \qquad \text{and} \quad C = \lambda D + \lambda' D' \,, \quad (A.8)
$$

in the base B and demand

$$
\text{Vol}(C) = J \cdot C = 0 \,. \quad (A.9)
$$

This, when pulled-back to $X_{r,s}$, implies the vanishing triple intersection,

$$
J \cdot C \cdot e = 0 \,, \quad (A.10)
$$

in the threefold $X_{r,s}$ where e is an arbitrary divisor of $X_{r,s}$, and hence, leads to

$$
J \cdot C \cdot e \cdot \left(3L - \sum_{i=1}^r E_i + 3L' - \sum_{i'=1}^s E'_{i'} \right) = 0 \,, \quad (A.11)
$$

in the fourfold $\mathcal{A}_{r,s}$. Upon some algebras, this gives

$$\lambda : \lambda' = \mu : -\mu', \tag{A.12}$$

and hence,

$$C = c\mu D - c\mu' D', \tag{A.13}$$

where $D = aL - \sum_{i=1}^{r} a_i E_i$ with $(a, a_1, \cdots, a_r) = \alpha A_r^{(I)}$ and similarly, $D' = a'L' - \sum_{i'=1}^{s} a'_{i'} E'_{i'}$ with $(a', a'_1, \cdots, a'_s) = \alpha' A_s^{(I')}$. Since C is an effective divisor of B, so is its pull-back $\pi^* C$ in $X_{r,s}$. Denoting the line bundle on $\mathcal{A}_{r,s}$ of degree $c\mu D - c\mu' D'$ by $\mathcal{L}$, let us now consider the Koszul sequence,

$$0 \to \mathcal{L} \otimes \mathcal{N}^* \to \mathcal{L} \to \mathcal{L}|_{X_{r,s}} \to 0, \tag{A.14}$$

where $\mathcal{N} = \mathcal{O}(3L - \sum_{i=1}^{r} E_i + 3L' - \sum_{i'=1}^{s} E'_{i'})$. Using the explicit formulae for the line bundle cohomologies on del Pezzo surfaces (see e.g. appendix of ref. [85]), one can then show that $H^0(\mathcal{A}_{r,s}, \mathcal{L}) = 0 = H^1(\mathcal{A}_{r,s}, \mathcal{L} \otimes \mathcal{N}^*)$, and hence, that $H^0(X_{r,s}, \mathcal{L}|_{X_{r,s}}) = 0$. However, this contradicts the effectiveness of $\pi^* C$, and therefore, no zero-volume effective curves exist in B for any Kähler forms. This completes the proof that the divisors $\mathcal{D}(\alpha, \alpha')$ of $X_{r,s}$ represent the same fibration for any positive α and α'.

B Details of the Diophantine system for dP_9

In this section we provide further details on the characterization of the infinite family of genus one fibrations found for the Schoen manifold in section 6.

B.1 A non-trivial fact

Here, we will show that nef divisors D of rational elliptic surface dP_9 (i.e., $D \cdot C \geq 0$ for every curve C in dP_9) that obey

$$D \cdot f = 2, \tag{B.1}$$
$$D \cdot D = 0, \tag{B.2}$$

for the fiber class f, can be classified as

$$D = y + z, \tag{B.3}$$

where $y, z \, (\neq f)$ are two distinct Mori cone generators with $y \cdot z = 1$.

With the Mori cone generators described in table 2, D can be expanded as

$$D = c\,f + \sum_a c_a\, y_a, \tag{B.4}$$

where c and c_a's are non-negative integers. (B.1) then demands that at most two of the c_a can be non-zero and only leaves the two possibilities: (a) $D = c\,f + 2\,y$ for a Mori cone generator $y \, (\neq f)$; (b) $D = c\,f + y + z$ for distinct Mori cone generators $y, z \, (\neq f)$. In the former case, $D \cdot D = 4c - 4 = 0$ and hence $c = 1$. For D to be nef, $D \cdot y' = 2y \cdot y' + 1 \geq 0$

for all the Mori cone generators y', which implies that $y \cdot y' \geq 0$ for all y'. Therefore, y also has to be nef but this contradicts that y is a Mori cone generator itself. In the latter case, $D \cdot D = -2 + 4c + 2y \cdot z = 0$ and hence $y \cdot z = 1 - 2c$. On the other hand, since y and z are distinct irreducible effective curves, they must intersect non-negatively and hence $y \cdot z = 1$ and $c = 0$.

Having derived the desired form (B.3), to complete the proof, let us now show that such a divisor D is necessarily nef. Note first that the only non-nef irreducible effective curves of dP_9 are the rational (-1)-curves, i.e. the Mori cone generators y_a described in table 2 (see the argument of Donagi et al. in ref. [86]). Since $D \cdot D = 0$, it is enough to show that D is irreducible. For the rest of this subsection, therefore, we will show that

$$h^0(dP_9, \mathcal{O}(y)) = 1 = h^0(dP_9, \mathcal{O}(z)), \qquad h^0(dP_9, \mathcal{O}(y + z)) = 2, \qquad (B.5)$$

which guarantee that $D = y + z$ is indeed irreducible.

Note that the Mori cone generators y_a with $y_a \cdot y_a = -1$ and $y_a \cdot f = 1$ are sections of the elliptic fibration and vice versa. We may thus rely on the Leray spectral sequence to compute the line bundle cohomologies in (B.5); see e.g. appendix A of ref. [20] for a self-contained description of the Leray spectral sequence.

Given the elliptic fibration,

$$\pi : dP_9 \to \mathbb{P}^1, \qquad (B.6)$$

it is straightforward to demonstrate that the push-forward functors act on the trivial bundle as

$$R^0\pi_*(\mathcal{O}) = \mathcal{O}_{\mathbb{P}^1}, \qquad R^1\pi_*(\mathcal{O}) = \mathcal{O}_{\mathbb{P}^1}(-1). \qquad (B.7)$$

Firstly, for a single section, y, the Koszul sequence,

$$0 \to \mathcal{O} \to \mathcal{O}(y) \to \mathcal{O}(y \cdot y)|_y \to 0, \qquad (B.8)$$

can be push-forwarded to

$$0 \to \mathcal{O}_{\mathbb{P}^1} \to R^0\pi_*\mathcal{O}(y) \to \mathcal{O}_{\mathbb{P}^1}(-1) \qquad (B.9)$$

$$\to \mathcal{O}_{\mathbb{P}^1}(-1) \to R^1\pi_*\mathcal{O}(y) \to 0. \qquad (B.10)$$

This leads to

$$R^0\pi_*\mathcal{O}(y) = \mathcal{O}_{\mathbb{P}^1}, \qquad R^1\pi_*\mathcal{O}(y) = 0, \qquad (B.11)$$

and hence, $h^0(dP_9, \mathcal{O}(y)) = h^0(\mathbb{P}^1, \mathcal{O}_{\mathbb{P}^1}) = 1$. Similarly, for two distinct sections y and z with $y \cdot z = 1$, we can twist the Koszul sequence (B.8) as

$$0 \to \mathcal{O}(z) \to \mathcal{O}(y + z) \to \mathcal{O}((y + z) \cdot y)|_y \to 0, \qquad (B.12)$$

which can be push-forwarded to

$$0 \to \mathcal{O}_{\mathbb{P}^1} \to R^0\pi_*\mathcal{O}(y + z) \to \mathcal{O}_{\mathbb{P}^1} \qquad (B.13)$$

$$\to 0 \to R^1\pi_*\mathcal{O}(y + z) \to 0. \qquad (B.14)$$

This leads to

$$R^0\pi_*\mathcal{O}(y + z) = \mathcal{O}_{\mathbb{P}^1}^{\oplus 2}, \qquad R^1\pi_*\mathcal{O}(y + z) = 0, \qquad (B.15)$$

and hence, $h^0(dP_9, \mathcal{O}(y + z)) = h^0(\mathbb{P}^1, \mathcal{O}_{\mathbb{P}^1}^{\oplus 2}) = 2$.

B.2 An infinite family of solutions

From the specific form (B.3) of the general solutions, we are led to classify pairs of distinct sections,

$$y = aL - \sum_{i=1}^{9} a_i E_i \,, \tag{B.16}$$

$$z = bL - \sum_{i=1}^{9} b_i E_i \,, \tag{B.17}$$

with

$$y \cdot z = ab - \sum_{i=1}^{9} a_i b_i = 1 \,. \tag{B.18}$$

In this subsection, instead of attempting a complete classification, we will impose an additional (rather artificial) constraint $a = b$ and will solve the corresponding restricted Diophantine system.

Note first that

$$\sum_{i=1}^{9}(a_i-b_i)^2 = \sum_{i=1}^{9}a_i^2+\sum_{i=1}^{9}b_i^2-2\sum_{i=1}^{9}a_ib_i = (a^2+1)+(b^2+1)-2(ab-1) = (a-b)^2+4, \tag{B.19}$$

where $y \cdot y = z \cdot z = -1$ as well as (B.18) have been used. Under the additional constraint that $a = b$, we thus have

$$\sum_{i=1}^{9}(a_i - b_i)^2 = 4 \,, \tag{B.20}$$

which leads to the two possibilities: (a) $|a_i - b_i|$ is 2 for one i and 0 for the others; (b) $|a_i - b_i|$ is 1 for four i's and 0 for the others. On the other hand, since $a = b$,

$$\left(\sum_{i=1}^{9} a_i\right) - \left(\sum_{i=1}^{9} b_i\right) = z \cdot f - y \cdot f = 0 \,, \tag{B.21}$$

and hence, case (a) is ruled out and case (b) is further restricted to the condition that $|a_i - b_i|$ is 1 for two i's, -1 for another two i's, and 0 for the others. Upon permutation of the exceptional divisors, we may assume that

$$b_{1,2} = a_{1,2} + 1 \,, \quad b_{3,4} = a_{3,4} - 1 \,, \quad b_i = a_i \text{ for } i = 5, \dots, 9 \,. \tag{B.22}$$

Since z is a section, we must have

$$\begin{aligned}
-1 = z \cdot z &= b^2 - \sum_{i=1}^{9} b_i^2 \\
&= a^2 - \sum_{i=1}^{9} a_i^2 + 2(a_3 + a_4 - a_1 - a_2) - 4 \\
&= -1 + 2(a_3 + a_4 - a_1 - a_2) - 4 \,,
\end{aligned} \tag{B.23}$$

where in the last step $y \cdot y = -1$ has been used. Therefore, for any section $y = aL - \sum_{i=1}^{9} a_i E_i$ such that

$$a_1 + a_2 + 2 = a_3 + a_4 , \qquad (B.24)$$

we can construct another section,

$$z = aL - (a_1 + 1)E_1 - (a_2 + 1)E_2 - (a_3 - 1)E_3 - (a_4 - 1)E_4 - a_5 E_5 - \cdots - a_9 E_9 , \quad (B.25)$$

and $D = y + z$ is the general solution to the restricted Diophantine system.

Let us now use the following result for the classification of sections y in terms of 8 integer parameters k_i, $i = 1, \ldots, 8$ (see ref. [87] for the details),

- $a \equiv 0 \pmod 3$: $a = 3d$, $a_i = d - k_i$ for $i = 1, \ldots, 8$, and $a_9 = d + s - 1$

- $a \equiv 1 \pmod 3$: $a = 3d + 4 + 9s$, $a_i = d - k_1 + 1 + 3s$ for $i = 1, \ldots, 8$, and $a_9 = d + 4s + 3$

- $a \equiv 2 \pmod 3$: $a = 3d + 32 + 18s$, $a_i = d - k_i + 10 + 6s$ for $i = 1, \ldots, 8$, and $a_9 = d + 7s + 15$

where

$$d = \sum_{i=1}^{8} k_i^2 + \sum_{1 \le i < j \le 8} k_i k_j - \sum_{i=1}^{8} k_i \qquad \text{and} \qquad s = \sum_{i=1}^{8} k_i . \qquad (B.26)$$

Here, we will choose y from the first category with $a \equiv 0 \pmod 3$ (one can proceed in exactly the same way for the other two categories). The only constraint that y is required to obey is (B.24). Thus, $k_1 + k_2 - 2 = k_3 + k_4$ and the general solution for D is give as

$$
\begin{aligned}
D &= y + z \\
&= 2aL - (2a_1 + 1)E_1 - (2a_2 + 1)E_2 - (2a_3 - 1)E_3 - (2a_4 - 1)E_4 \\
&\quad - 2a_5 E_5 - \cdots - 2a_9 E_9 , \\
&= \alpha - \sum_{i=1}^{9} \alpha_i E_i ,
\end{aligned}
\qquad (B.27)
$$

where

$$\alpha = 6d , \qquad \alpha_{i=1,2} = 2d - 2k_i + 1, \qquad \alpha_{i=3,4} = 2d - 2k_i - 1 ,$$
$$\alpha_{i=5,\ldots,8} = 2d - 2k_i , \qquad \alpha_9 = 2d + 2s - 2 . \qquad (B.28)$$

Here, s and d are again functions of k_i's as in (B.26) and $k_1 = k_3 + k_4 - k_2 + 2$ is to be substituted so that the solutions (B.28) actually form a seven-parameter family of divisors with arbitrary integer parameters, $k_2, \cdots, k_8 \in \mathbb{Z}$.

Similarly, the restricted Diophantine system can also be solved for the other dP_9 factor and leads to the following parameterization for $D' = \alpha' L' - \sum_{i'=1}^{9} \alpha'_{i'} E'_{i'}$ with

$$\alpha' = 6d' , \qquad \alpha'_{i'=1,2} = 2d' - 2l_{i'} + 1, \qquad \alpha'_{i'=3,4} = 2d' - 2l_{i'} - 1 ,$$
$$\alpha'_{i'=5,\ldots,8} = 2d' - 2l_{i'} , \qquad \alpha'_9 = 2d' + 2s' - 2 , \qquad (B.29)$$

where d' and s' are defined as

$$d' = \sum_{i'=1}^{8} l_{i'}^2 + \sum_{1 \le i' < j' \le 8} l_{i'} l_{j'} - \sum_{i'=1}^{8} l_{i'} \qquad \text{and} \qquad s' = \sum_{i'=1}^{8} l_{i'} . \tag{B.30}$$

Here, as for the k_i's, $l_1 = l_3 + l_4 - l_2 + 2$ is to be substituted and $l_2, \cdots, l_8$ are the seven free integer parameters. Combining (B.28) and (B.29), we thus obtain an infinite family of divisors

$$\mathcal{D} = D + D' = \alpha - \sum_{i=1}^{9} \alpha_i E_i + \alpha' - \sum_{i'=1}^{9} \alpha'_{i'} E'_{i'} , \tag{B.31}$$

meeting the criteria of Kollár's, in terms of the 14 free integer parameters, $k_2, \ldots, k_8$ and $l_2, \ldots, l_8$.

C Enumerating the blow-downs of del Pezzo surfaces

In this section, we provide our methodology for enumerating various blow downs of del Pezzo surfaces. The enumeration result is used in counting Kollár divisors in section 5.

For an illustration, let us consider blowing down dP_3, which is the simplest del Pezzo surface with a non-simplicial Kähler cone. Note first that the (non-simplicial) Kähler cone of dP_3 is spanned by the following 5 generators,[13]

$$\mathcal{K} = \langle L, L - E_1, L - E_2, L - E_3, 2L - E_1 - E_2 - E_3 \rangle , \tag{C.1}$$

which can be seen as the dual description of the Mori cone in table 2 (see [44] for the complete list of Kähler cone generators for all del Pezzo surfaces). We will now consider possible chains of blow downs of the irreducible exceptional curves, $E_1, E_2, E_3, L - E_1 - E_2,$ $L - E_2 - E_3$ and $L - E_3 - E_1$.

If the curve E_1 is blown down first, we may delete the generators of $\mathcal{K}(dP_3)$ that do not intersect with E_1 and are led to the following three-dimensional boundary component,

$$\mathcal{K}_{E_1} = \langle L, L - E_2, L - E_3 \rangle , \tag{C.2}$$

where the subscript denotes the blown down curve. The cone $\mathcal{K}_{E_1}$ should thus be seen as the Kähler cone of dP_2. Next, all of its two-dimensional boundaries,

$$\mathcal{K}_{E_1,E_2} = \langle L, L - E_3 \rangle , \tag{C.3}$$

$$\mathcal{K}_{E_1,E_3} = \langle L, L - E_2 \rangle , \tag{C.4}$$

$$\mathcal{K}_{E_1,L-E_2-E_3} = \langle L - E_2, L - E_3 \rangle , \tag{C.5}$$

can be approached by a further blow down. Here, the first two are the Kähler cones of dP_1 surfaces, which can be further blown down to $\mathbb{P}^2$ with the Kähler cones,

$$\mathcal{K}_{E_1,E_2,E_3} = \langle L \rangle = \mathcal{K}_{E_1,E_3,E_2} , \tag{C.6}$$

---

[13]In this appendix, we phrase the blown down bases in terms of their Kähler cone generators. One can consider a generic divisor positively spanned by those generators and pull it back to the Calabi-Yau three-fold. That way, a divisor of the three-fold is reconstructed from the Kähler cone information.

while the third is the Kähler cone of $\mathbb{P}^1 \times \mathbb{P}^1$, which cannot be blown down any further. A similar analysis can be made for the cases where E_2 or E_3 is blown down first. Taking into account of all such blow downs, one ends up with the following descriptions of the base surfaces in terms of their Kähler cones,

$$dP_2 : \langle L, L - E_i, L - E_j \rangle \,, \tag{C.7}$$

$$dP_1 : \langle L, L - E_i \rangle \,, \tag{C.8}$$

$$\mathbb{P}^1 \times \mathbb{P}^1 : \langle L - E_i, L - E_j \rangle \,, \tag{C.9}$$

$$\mathbb{P}^2 : \langle L \rangle \,, \tag{C.10}$$

where i and j are distinct indices from $\{1, 2, 3\}$.

If the curve $L - E_1 - E_2$ is first blown down on the other hand, a different pattern is found for the resulting Kähler cones. At the first step, we obtain a dP_2 surface with the Kähler cone,

$$\mathcal{K}_{L-E_1-E_2} = \langle L - E_1, L - E_2, 2L - E_1 - E_2 - E_3 \rangle \,, \tag{C.11}$$

of which boundaries can be approached as

$$\mathcal{K}_{L-E_1-E_2,E_3} = \langle L - E_1, L - E_2 \rangle \,, \tag{C.12}$$

$$\mathcal{K}_{L-E_1-E_2,L-E_2-E_3} = \langle L - E_2, 2L - E_1 - E_2 - E_3 \rangle \,, \tag{C.13}$$

$$\mathcal{K}_{L-E_1-E_2,L-E_3-E_1} = \langle L - E_1, 2L - E_1 - E_2 - E_3 \rangle \,. \tag{C.14}$$

Of these three, the first is the Kähler cone of $\mathbb{P}^1 \times \mathbb{P}^1$, which cannot be blown down any further, while the other two are the Kähler cones of dP_1 surfaces, which can be further blown down to $\mathbb{P}^2$ with the Kähler cones,

$$\mathcal{K}_{L-E_1-E_2,L-E_2-E_3,L-E_3-E_1} = \langle 2H - E_1 - E_2 - E_3 \rangle = \mathcal{K}_{L-E_1-E_2,L-E_3-E_1,L-E_2-E_3} \,. \tag{C.15}$$

A similar analysis can be made for the cases where $L - E_2 - E_3$ or $L - E_3 - E_1$ is blown down first and one ends up adding to the list in (C.7)–(C.10) the following new types of base surfaces:

$$dP_2 : \langle L - E_i, L - E_j, 2L - E_1 - E_2 - E_3 \rangle \,, \tag{C.16}$$

$$dP_1 : \langle L - E_i, 2L - E_1 - E_2 - E_3 \rangle \,, \tag{C.17}$$

$$\mathbb{P}^2 : \langle 2L - E_1 - E_2 - E_3 \rangle \,, \tag{C.18}$$

where, once again, i and j are distinct indices from $\{1, 2, 3\}$.

This completes the classification of the blown down bases. In summary, we have a total of 18 different base surfaces: (a) the dP_3 with which we start; (b) 6 types of dP_2 surfaces in (C.7) and (C.16); (c) 6 types of dP_1 surfaces in (C.8) and (C.17); (d) 3 types of $\mathbb{P}^1 \times \mathbb{P}^1$ in (C.9); (e) 2 types of $\mathbb{P}^2$ in (C.10) and (C.18).

Along the same line, we have classified all the blown down bases by starting from each of the del Pezzo base surfaces dP_r, $r = 0, \cdots, 7$, that are relevant to this work. In table 5, we summarize the counting of different types of blown down bases. We also provide in table 6 another counting result that takes into account of the permutation redundancies of the exceptional divisors of the del Pezzo factors, although, for the purpose of string dualities, a more relevant counting is the one given in table 5.

r	dP_0	$\mathbb{P}^1 \times \mathbb{P}^1$	dP_1	dP_2	dP_3	dP_4	dP_5	dP_6	dP_7	Tot.
0	1	—	—	—	—	—	—	—	—	1
1	1	—	1	—	—	—	—	—	—	2
2	1	1	2	1	—	—	—	—	—	5
3	2	3	6	6	1	—	—	—	—	18
4	5	10	20	30	10	1	—	—	—	76
5	16	40	80	160	80	16	1	—	—	393
6	72	216	432	1080	720	216	27	1	—	2764
7	576	1974	4025	12104	3745	3857	756	56	1	27094

Table 5. The statistics of different blow downs of the dP_r surfaces, $r = 0, \cdots, 7$. The numbers in parentheses count the fibrations up to permutations of the exceptional divisors of the del Pezzo factors.

r	dP_0	$\mathbb{P}^1 \times \mathbb{P}^1$	dP_1	dP_2	dP_3	dP_4	dP_5	dP_6	dP_7	Tot.
0	1	—	—	—	—	—	—	—	—	1
1	1	—	1	—	—	—	—	—	—	2
2	1	1	1	1	—	—	—	—	—	4
3	2	1	2	2	1	—	—	—	—	8
4	2	2	3	3	2	1	—	—	—	13
5	3	3	5	6	4	3	1	—	—	25
6	5	6	9	12	9	6	3	1	—	51
7	10	12	18	24	18	16	9	4	1	112

Table 6. A redundancy removed version of the statistics of different blow downs of the dP_r surfaces, $r = 0, \cdots, 7$; here, the blow downs are counted up to permutations of the exceptional divisors of the del Pezzo factors.

D A class of CICY redundancies via base surface splittings/contractions

In this section, we give a brief overview of a simple method for identifying equivalent CICY threefold configurations. Suppose that a given configuration matrix can be written, upon row and column permutations, in the following block form,

$$X \sim \left[\begin{array}{c|cc} \mathcal{A}_1 & \mathbf{0} & \mathcal{F} \\ \mathcal{A}_2 & \mathcal{B} & \mathcal{T} \\ \mathcal{A}_3 & \mathcal{C} & \mathbf{0} \end{array} \right] , \tag{D.1}$$

where the $\mathbf{0}$'s are zero matrices of appropriate sizes and the upper-right corner,

$$F \sim \left[\begin{array}{c|c} \mathcal{A}_1 & \mathcal{F} \end{array} \right] , \tag{D.2}$$

represents a curve of complex dimension one. Given that X is a Calabi-Yau threefold, one observes the obvious genus-one fibration (OGF) structure [1], in which F necessarily represents an elliptic curve fibered over the surface base,

$$B \sim \left[\begin{array}{c|c} \mathcal{A}_2 & \mathcal{B} \\ \mathcal{A}_3 & \mathcal{C} \end{array} \right] , \tag{D.3}$$

with the twist described by $\mathcal{T}$.

Let us now consider varying the configuration (D.1) via a chain of splittings and contractions [16], so that $\mathcal{A}_3$ may lose and/or gain some projective space factors together with the associated rows of the configuration matrix, while the columns involving $\mathcal{F}$ and $\mathcal{T}$ are kept intact. In the end, the chain will relate the two configurations,

$$X \sim \left[\begin{array}{c|cc} \mathcal{A}_1 & \mathbf{0} & \mathcal{F} \\ \mathcal{A}_2 & \mathcal{B} & \mathcal{T} \\ \mathcal{A}_3 & \mathcal{C} & \mathbf{0} \end{array} \right] \quad \longleftrightarrow \quad X' \sim \left[\begin{array}{c|cc} \mathcal{A}_1 & \mathbf{0} & \mathcal{F} \\ \mathcal{A}_2 & \mathcal{B}' & \mathcal{T} \\ \mathcal{A}_3' & \mathcal{C}' & \mathbf{0} \end{array} \right] \; . \tag{D.4}$$

The observation to made here is that all such splittings and contractions are *ineffective* [16]; in particular, the two configurations in (D.4) are equivalent.

To see this, note first that it is sufficient to show the equivalence for a single splitting/contraction transition and we may restrict to the case where $\mathcal{A}_3$ is a single projective space. For example, suppose that $\mathcal{A}_3 = \mathbb{P}^1$ and $\dim_{\mathbb{C}} \mathcal{A}_2 = 3$ (the generalization to the cases with $\mathcal{A}_3 = \mathbb{P}^n$ and $\dim_{\mathbb{C}} \mathcal{A}_2 = m$ is straightforward) and consider the $\mathbb{P}^1$ contraction,

$$X \sim \left[\begin{array}{c|ccc} \mathcal{A}_1 & \mathbf{0} & \mathbf{0} & \mathcal{F} \\ \mathcal{A}_2 & u & v & \mathcal{T} \\ \mathbb{P}^1 & 1 & 1 & \mathbf{0} \end{array} \right] \quad \rightsquigarrow \quad X' \sim \left[\begin{array}{c|cc} \mathcal{A}_1 & \mathbf{0} & \mathcal{F} \\ \mathcal{A}_2 & u+v & \mathcal{T} \end{array} \right] \; . \tag{D.5}$$

X is guaranteed to be smooth, given a generic complex structure, and we denote the two defining equations of X associated to the first two columns of its configuration by

$$\begin{pmatrix} P & Q \\ R & S \end{pmatrix} \begin{pmatrix} a_0 \\ a_1 \end{pmatrix} = \begin{pmatrix} 0 \\ 0 \end{pmatrix} , \tag{D.6}$$

where P, Q, R, and S are generic polynomials in $\mathcal{A}_2$ with $\deg P = \deg Q = u$, $\deg R = \deg S = v$ and $(a_0 : a_1)$ are the homogeneous coordinates of $\mathbb{P}^1$. The first defining equation of X' can then be written as

$$PS - QR = 0 \; . \tag{D.7}$$

It is then immediately seen that as long as at least one of P, Q, R, and S is non-vanishing so that

$$\mathrm{rk} \begin{pmatrix} P & Q \\ R & S \end{pmatrix} = 1 , \tag{D.8}$$

there exists a local isomorphism between X and X', and hence, the only source of singularities in X' is the locus where $P = Q = R = S = 0$. For a generic complex structure of X, however, there is no solution to such a simultaneous vanishing since $\dim_{\mathbb{C}} \mathcal{A}_2 = 3$. Therefore, the $\mathbb{P}^1$ contraction, (D.5), does not involve singularities and is necessarily ineffective.

Note that such a redundancy for the configurations of CICY threefolds, (D.4), arises essentially from those of the base surfaces,

$$B \sim \left[\begin{array}{c|c} \mathcal{A}_2 & \mathcal{B} \\ \mathcal{A}_3 & \mathcal{C} \end{array} \right] \quad \longleftrightarrow \quad B' \sim \left[\begin{array}{c|c} \mathcal{A}_2 & \mathcal{B}' \\ \mathcal{A}_3' & \mathcal{C}' \end{array} \right] , \tag{D.9}$$

and can easily be spotted by comparing the latter. We will thus call the CICY threefold redundancies of this type a *surface redundancy*.

D.1 Illustration

An example of this CICY configuration matrix redundancy can be illustrated with the following example of two configurations,

$$
\left[\begin{array}{c|cc}
\mathbb{P}^1 & 1 & 1 \\
\mathbb{P}^2 & 0 & 3 \\
\mathbb{P}^2 & 3 & 0
\end{array}\right]
\quad \text{and} \quad
\left[\begin{array}{c|cccc}
\mathbb{P}^1 & 1 & 1 & 0 & 0 \\
\mathbb{P}^2 & 3 & 0 & 0 & 0 \\
\mathbb{P}^4 & 0 & 1 & 2 & 2
\end{array}\right],
\tag{D.10}
$$

labelled respectively as #14 and #16 in the original CICY threefold dataset [16]. We first permute the rows and columns of each configuration appropriately so that the two configurations are written respectively as

$$
\left[\begin{array}{c|c|c}
\mathbb{P}^2 & 0 & 3 \\ \hline
\mathbb{P}^1 & 1 & 1 \\ \hline
\mathbb{P}^2 & 3 & 0
\end{array}\right]
\quad \text{and} \quad
\left[\begin{array}{c|ccc|c}
\mathbb{P}^2 & 0 & 0 & 0 & 3 \\ \hline
\mathbb{P}^1 & 1 & 0 & 0 & 1 \\ \hline
\mathbb{P}^4 & 1 & 2 & 2 & 0
\end{array}\right].
\tag{D.11}
$$

Such permutations only correspond to an appropriate relabeling of the defining equations as well as the ambient homogeneous coordinates and hence never affect the geometry. Here, the horizontal and the vertical lines have been added to manifestly distinguish the six blocks as in (D.4). Note that the two configurations (D.11) are exactly of the form (D.4) and the following is a relevant chain of base surface equivalences,

$$
\left[\begin{array}{c|c}
\mathbb{P}^1_{\mathbf{x}} & 1 \\
\mathbb{P}^2_{\mathbf{y}} & 3
\end{array}\right]
\underset{sp.}{\overset{\mathbf{a}}{\leftrightsquigarrow}}
\left[\begin{array}{c|cc}
\mathbb{P}^1_{\mathbf{x}} & 1 & 0 \\
\mathbb{P}^2_{\mathbf{y}} & 2 & 1 \\
\mathbb{P}^1_{\mathbf{a}} & 1 & 1
\end{array}\right]
\underset{sp.}{\overset{\mathbf{b}}{\leftrightsquigarrow}}
\left[\begin{array}{c|ccc}
\mathbb{P}^1_{\mathbf{x}} & 1 & 0 & 0 \\
\mathbb{P}^2_{\mathbf{y}} & 1 & 1 & 1 \\
\mathbb{P}^1_{\mathbf{a}} & 1 & 0 & 1 \\
\mathbb{P}^1_{\mathbf{b}} & 1 & 1 & 0
\end{array}\right]
\underset{cont.}{\overset{\mathbf{y}}{\leftrightsquigarrow}}
\left[\begin{array}{c|c}
\mathbb{P}^1_{\mathbf{x}} & 1 \\
\mathbb{P}^1_{\mathbf{a}} & 2 \\
\mathbb{P}^1_{\mathbf{b}} & 2
\end{array}\right]
$$

$$
\underset{sp.}{\overset{\mathbf{w}}{\leftrightsquigarrow}}
\left[\begin{array}{c|ccccc}
\mathbb{P}^1_{\mathbf{x}} & 1 & 0 & 0 & 0 & 0 \\
\mathbb{P}^1_{\mathbf{a}} & 0 & 1 & 1 & 0 & 0 \\
\mathbb{P}^1_{\mathbf{b}} & 0 & 0 & 0 & 1 & 1 \\
\mathbb{P}^4_{\mathbf{w}} & 1 & 1 & 1 & 1 & 1
\end{array}\right]
\underset{cont.}{\overset{\mathbf{b}}{\leftrightsquigarrow}}
\left[\begin{array}{c|cccc}
\mathbb{P}^1_{\mathbf{x}} & 1 & 0 & 0 & 0 \\
\mathbb{P}^1_{\mathbf{a}} & 0 & 1 & 1 & 0 \\
\mathbb{P}^4_{\mathbf{w}} & 1 & 1 & 1 & 2
\end{array}\right]
\tag{D.12}
$$

$$
\underset{cont.}{\overset{\mathbf{a}}{\leftrightsquigarrow}}
\left[\begin{array}{c|ccc}
\mathbb{P}^1_{\mathbf{x}} & 1 & 0 & 0 \\
\mathbb{P}^4_{\mathbf{w}} & 1 & 2 & 2
\end{array}\right].
$$

Here, the bold subscripts for the projective spaces label their homogeneous coordinates and the symbol "*sp.*" (resp., "*cont.*") below each arrow indicates that the configuration on the right is obtained by splitting (resp., by contracting) the one on the left along the projective space with homogeneous coordinates denoted above the arrow. This then leads to the equivalence between the two CICY threefold configurations (D.10) according to the arguments in the previous subsection.

In fact, there are total of 15 configurations in the original dataset that are shown to be equivalent exactly for the families of surfaces described above (numbers 14; 16, . . . , 21; 23, . . . , 30). They all represent the Schoen manifold, in particular. See section 6 for further details on this geometry.

D.1.1 The complete network of base surface splitting/contraction redundancies

It is possible to search for such redundancies in the entire dataset of 7890 CICY threefolds. In turns out that this class of redundancies arise only with the base surfaces, dP_3, dP_5 and dP_9.[14] The statistics for each of the three base types can be summarized as follows.

- dP_3: there arise 16 pairs involving the surface equivalence,

$$
\left[\begin{array}{c|cc} \mathbb{P}^2 & 1 & 1 \\ \mathbb{P}^2 & 1 & 1 \end{array} \right] \longleftrightarrow \left[\begin{array}{c|cccc} \mathbb{P}^2 & 1 & 0 & 1 & 0 \\ \mathbb{P}^2 & 0 & 1 & 0 & 1 \\ \mathbb{P}^1 & 0 & 0 & 1 & 1 \\ \mathbb{P}^1 & 1 & 1 & 0 & 0 \end{array} \right] , \tag{D.13}
$$

  as well as 15 pairs involving

$$
\left[\begin{array}{c|c} \mathbb{P}^1 & 1 \\ \mathbb{P}^1 & 1 \\ \mathbb{P}^1 & 1 \end{array} \right] \longleftrightarrow \left[\begin{array}{c|ccc} \mathbb{P}^1 & 1 & 0 & 0 \\ \mathbb{P}^1 & 0 & 1 & 0 \\ \mathbb{P}^1 & 0 & 0 & 1 \\ \mathbb{P}^2 & 1 & 1 & 1 \end{array} \right] . \tag{D.14}
$$

  Thus, total of 62 configurations are grouped into 31 classes. The pair of CICY configurations in each class are equivalent.

- dP_5: total of 666 configurations are grouped into 119 classes via the surface equivalence,

$$
\left[\begin{array}{c|c} \mathbb{P}^1 & 1 \\ \mathbb{P}^1 & 1 \\ \mathbb{P}^1 & 2 \end{array} \right] \longleftrightarrow \left[\begin{array}{c|cc} \mathbb{P}^1 & 1 & 0 \\ \mathbb{P}^1 & 0 & 1 \\ \mathbb{P}^2 & 1 & 2 \end{array} \right] . \tag{D.15}
$$

  The maximal number of equivalent threefold configurations in a class is 24.

- dP_9: the 15 configurations discussed in the previous subsection are all that involves a dP_9 surface redundancy; they are grouped into a single class that describes the Schoen manifold.

E   A guide to the new CICY data set and fibration data

The new favorable CICY configurations, and their obvious fibrations, are publicly available and can be found here: www1.phys.vt.edu/cicydata. The website includes two files. The first is a new version of the CICY list, with as many configuration matrices replaced by favorable examples as possible. The second contains the obvious fibrations of the CICYs.

An example of the format of the entries of the CICY list is given in figure 4. The first entry gives the number labeling the CICY, which are compatible with the numbers in the original CICY list [16] obtainable here. The next two entries specify the Hodge data of the

---

[14]We believe that this is an artifact of the particular algorithm based on which the original dataset of CICY threefolds was generated in [16].

```
{Num → 7732, H11 → 5, H21 → 53, C2 → {24, 36, 24, 36, 44},
 Conf → {{1, 1, 0, 0, 0, 0}, {0, 1, 1, 0, 1, 0}, {0, 0, 1, 1, 0, 0}, {1, 0, 0, 1, 0, 1},
    {0, 0, 0, 0, 3, 1}}, Favour → True, KahlerPos → False, IsProduct → False}
```

Figure 4. An example entry in the new maximally favorable CICY list.

threefold. The fourth entry gives the second Chern class of the manifold. The format here is as follows. Express the second Chern class in the form

$$c_2(TX) = C^{ij} J_i \wedge J_j \tag{E.1}$$

where the J_i are the Kähler forms of the projective space factors restricted to the Calabi-Yau and the C's are some numerical coefficients. One can then contract the C's with the intersection form for the manifold to get the numbers given (no information is lost in performing this operation). The fifth entry in the list is simply the configuration matrix. In this case we have the following.

$$X_{7732} = \left[\begin{array}{c|cccccc} \mathbb{P}^1 & 1 & 1 & 0 & 0 & 0 & 0 \\ \mathbb{P}^2 & 0 & 1 & 1 & 0 & 1 & 0 \\ \mathbb{P}^1 & 0 & 0 & 1 & 1 & 0 & 0 \\ \mathbb{P}^2 & 1 & 0 & 0 & 1 & 0 & 1 \\ \mathbb{P}^3 & 0 & 0 & 0 & 0 & 3 & 1 \end{array} \right] \tag{E.2}$$

The sixth entry says whether the description provided is favorable, the seventh says whether the naive ambient space Kähler cone descends to give that of the Calabi-Yau and the final entry indicates whether the configuration matrix describes a direct product manifold.

The obvious fibrations of the maximally favorable CICY list described above are provided in a second download file available at [3]. In this instance a list of 7868 cases is provided, one for each CICY threefold excluding manifolds that are direct products (i.e. those for which "IsProduct → True" in the above CICY list). Each list entry has four components. The first entry is simply the relevant CICY number. The second entry lists the obvious genus one fibrations of the configuration, the third entry lists the obvious K3 fibrations of the configuration and the final entry describes how the K3 and torus fibrations are nested.

The list of torus fibrations for each configuration contains one entry per fibration. An example for CICY 7732 is the following (this is the first genus one fibration listed).

$$\{\{5\}, \{5, 6\}\} \tag{E.3}$$

This means that the fiber in this example is described by the 5th row and 5th and 6th columns, with reference back to the configuration provided in the maximally favorable CICY list. Referring back to the configuration matrix (E.2), we see that the fibration (E.3)

can be presented in our usual format as follows.

$$X'_{7732} = \begin{bmatrix} \mathbb{P}^3 & 0 & 0 & 0 & 0 & 3 & 1 \\ \hline \mathbb{P}^1 & 1 & 1 & 0 & 0 & 0 & 0 \\ \mathbb{P}^2 & 0 & 1 & 1 & 0 & 1 & 0 \\ \mathbb{P}^1 & 0 & 0 & 1 & 1 & 0 & 0 \\ \mathbb{P}^2 & 1 & 0 & 0 & 1 & 0 & 1 \end{bmatrix}$$

(E.4)

This abbreviated formatting is used to keep the fibration list to a manageable size.

The list of K3 fibrations in the third entry for each configuration follows the same format. So for example, for CICY 7732, the first entry in the K3 fibration list is the following.

$$\{\{1, 2, 4, 5\}, \{1, 2, 3, 4, 5, 6\}\}$$

(E.5)

This corresponds to the following K3 fibration in our usual notation (again referring back to (E.2)).

$$X''_{7732} = \begin{bmatrix} \mathbb{P}^1 & 1 & 1 & 0 & 0 & 0 & 0 \\ \mathbb{P}^2 & 0 & 1 & 1 & 0 & 1 & 0 \\ \mathbb{P}^2 & 1 & 0 & 0 & 1 & 0 & 1 \\ \mathbb{P}^3 & 0 & 0 & 0 & 0 & 3 & 1 \\ \hline \mathbb{P}^1 & 0 & 0 & 1 & 1 & 0 & 0 \end{bmatrix}$$

(E.6)

As mentioned above, the fourth and final entry in the list provided for each configuration matrix describes how these fibrations are nested. Each case in this fourth entry is a list of two numbers. The first number specifies a K3 fibration from the previous list and the second a genus one fibration from the second entry for that configuration matrix. If a given pair exists, then those two fibrations are compatible (that is, the genus one fibers are also fibers of the K3 of the K3 fibration). For example, in the case of CICY 7732, the first case we have is simply the following.

$$\{1, 1\}$$

(E.7)

This just states that the first genus one fibration (E.4) is nested in the first K3 fibration (E.6) in a compatible way. This can be confirmed by performing row and column permutations on those two matrices that are compatible with both fibration structures. That is, we only consider permutations that do not mix the matrix blocks of the form (3.1). In the case at hand, we can obtain the following in this manner.

$$X'''_{7732} = \begin{bmatrix} \mathbb{P}^3 & 0 & 0 & 0 & 0 & 3 & 1 \\ \hline \mathbb{P}^1 & 1 & 1 & 0 & 0 & 0 & 0 \\ \mathbb{P}^2 & 0 & 1 & 1 & 0 & 1 & 0 \\ \mathbb{P}^2 & 1 & 0 & 0 & 1 & 0 & 1 \\ \hline \mathbb{P}^1 & 0 & 0 & 1 & 1 & 0 & 0 \end{bmatrix} \quad .$$

(E.8)

References

[1] J. Gray, A.S. Haupt and A. Lukas, *Topological invariants and fibration structure of complete intersection Calabi-Yau four-folds*, *JHEP* **09** (2014) 093 [`arXiv:1405.2073`] [ɪɴSPIRE].

[2] L.B. Anderson, X. Gao, J. Gray and S.-J. Lee, *Multiple Fibrations in Calabi-Yau Geometry and String Dualities*, *JHEP* **10** (2016) 105 [`arXiv:1608.07555`] [ɪɴSPIRE].

[3] L. Anderson, X. Gao, J. Gray and S.J. Lee, *The favorable CICY List and its fibrations*, http://www1.phys.vt.edu/cicydata/.

[4] C. Vafa, *Evidence for F-theory*, *Nucl. Phys.* **B 469** (1996) 403 [`hep-th/9602022`] [ɪɴSPIRE].

[5] M. Gross, *A finiteness theorem for elliptic Calabi-Yau threefolds*, *Duke Math. J.* **74** (1993) 271 [`alg-geom/9305002`] [ɪɴSPIRE].

[6] G. Di Cerbo and R. Svaldi, *Log birational boundedness of Calabi-Yau pairs*, `arXiv:1608.02997`.

[7] A. Grassi, *On minimal models of elliptic threefolds*, *Math. Ann.* **290** (1991) 287.

[8] F. Rohsiepe, *Fibration structures in toric Calabi-Yau fourfolds*, `hep-th/0502138` [ɪɴSPIRE].

[9] S.B. Johnson and W. Taylor, *Calabi-Yau threefolds with large $h^{2,1}$*, *JHEP* **10** (2014) 023 [`arXiv:1406.0514`] [ɪɴSPIRE].

[10] S.B. Johnson and W. Taylor, *Enhanced gauge symmetry in $6D$ F-theory models and tuned elliptic Calabi-Yau threefolds*, *Fortsch. Phys.* **64** (2016) 581 [`arXiv:1605.08052`] [ɪɴSPIRE].

[11] P. Candelas, A. Constantin and H. Skarke, *An abundance of $K3$ fibrations from polyhedra with interchangeable parts*, *Commun. Math. Phys.* **324** (2013) 937 [`arXiv:1207.4792`] [ɪɴSPIRE].

[12] D.R. Morrison, D.S. Park and W. Taylor, *Non-Higgsable abelian gauge symmetry and F-theory on fiber products of rational elliptic surfaces*, `arXiv:1610.06929` [ɪɴSPIRE].

[13] N. Nakayama, *On Weierstrass models*, *Alg. Geom. Comm. Alg.* (1987) 405.

[14] J. Gray, A.S. Haupt and A. Lukas, *All complete intersection Calabi-Yau four-folds*, *JHEP* **07** (2013) 070 [`arXiv:1303.1832`] [ɪɴSPIRE].

[15] J. Gray, A. Haupt and A. Lukas, *Calabi-Yau fourfolds in products of projective space*, *Proc. Symp. Pure Math.* **88** (2014) 281.

[16] P. Candelas, A.M. Dale, C.A. Lütken and R. Schimmrigk, *Complete intersection Calabi-Yau manifolds*, *Nucl. Phys.* **B 298** (1988) 493 [ɪɴSPIRE].

[17] M. Kreuzer and H. Skarke, *Complete classification of reflexive polyhedra in four-dimensions*, *Adv. Theor. Math. Phys.* **4** (2002) 1209 [`hep-th/0002240`] [ɪɴSPIRE].

[18] V. Braun, *Toric elliptic fibrations and F-theory compactifications*, *JHEP* **01** (2013) 016 [`arXiv:1110.4883`] [ɪɴSPIRE].

[19] L.B. Anderson, F. Apruzzi, X. Gao, J. Gray and S.-J. Lee, *A new construction of Calabi–Yau manifolds: Generalized CICYs*, *Nucl. Phys.* **B 906** (2016) 441 [`arXiv:1507.03235`] [ɪɴSPIRE].

[20] L.B. Anderson, F. Apruzzi, X. Gao, J. Gray and S.-J. Lee, *Instanton superpotentials, Calabi-Yau geometry and fibrations*, *Phys. Rev.* **D 93** (2016) 086001 [arXiv:1511.05188] [INSPIRE].

[21] P. Berglund and T. Hubsch, *On Calabi-Yau generalized complete intersections from Hirzebruch varieties and novel K3-fibrations*, arXiv:1606.07420 [INSPIRE].

[22] P. Berglund and T. Hubsch, *A generalized construction of Calabi-Yau models and mirror symmetry*, arXiv:1611.10300 [INSPIRE].

[23] A. Garbagnati and B. van Geemen, *A remark on generalized complete intersections*, arXiv:1708.00517 [INSPIRE].

[24] V. Braun, *On free quotients of complete intersection Calabi-Yau manifolds*, *JHEP* **04** (2011) 005 [arXiv:1003.3235] [INSPIRE].

[25] A. Constantin, J. Gray and A. Lukas, *Hodge numbers for all CICY quotients*, *JHEP* **01** (2017) 001 [arXiv:1607.01830] [INSPIRE].

[26] J. Kollar, *Deformations of elliptic Calabi-Yau manifolds*, arXiv:1206.5721 [INSPIRE].

[27] K. Oguiso, *On algebraic fiber space structures on a Calabi-Yau 3-fold*, *Int. J. Math.* **4** (1993) 439, with an appendix by N. Nakayama [MR-1228584 (94g:14019)].

[28] P.M.H. Wilson, *The existence of elliptic fibre space structures on Calabi-Yau threefolds*, *Math. Ann.* **300** (1994) 693 [MR-1314743 (96a:14047)].

[29] L.B. Anderson, X. Gao, J. Gray and S.-J. Lee, *Tools for CICYs in F-theory*, *JHEP* **11** (2016) 004 [arXiv:1608.07554] [INSPIRE].

[30] P.M.H. Wilson, *The existence of elliptic fibre space structures on Calabi-Yau threefolds II*, *Math. Proc. Cambridge Philos. Soc.* **123** (1998) 259.

[31] A.M. He and P. Candelas, *On the number of complete intersection Calabi-Yau manifolds*, *Commun. Math. Phys.* **135** (1990) 193 [INSPIRE].

[32] L.B. Anderson, Y.-H. He and A. Lukas, *Monad bundles in heterotic string compactifications*, *JHEP* **07** (2008) 104 [arXiv:0805.2875] [INSPIRE].

[33] C. Schoen, *On fiber products of rational elliptic surfaces with section*, *Math. Zeit.* **197** (1988) 177.

[34] T. Hubsch, *Calabi-Yau manifolds: A Bestiary for physicists*, World Scientific, Singapore (1992).

[35] P.S. Green, T. Hubsch and C.A. Lütken, *All Hodge numbers of all complete intersection Calabi-Yau manifolds*, *Class. Quant. Grav.* **6** (1989) 105 [INSPIRE].

[36] P. Candelas, P.S. Green and T. Hubsch, *Rolling among Calabi-Yau vacua*, *Nucl. Phys.* **B 330** (1990) 49 [INSPIRE].

[37] P. Candelas, X. de la Ossa, Y.-H. He and B. Szendroi, *Triadophilia: a special corner in the landscape*, *Adv. Theor. Math. Phys.* **12** (2008) 429 [arXiv:0706.3134] [INSPIRE].

[38] L.B. Anderson, J. Gray, A. Lukas and B. Ovrut, *Vacuum varieties, holomorphic bundles and complex structure stabilization in heterotic theories*, *JHEP* **07** (2013) 017 [arXiv:1304.2704] [INSPIRE].

[39] L.B. Anderson, *Heterotic and M-theory compactifications for string phenomenology*, arXiv:0808.3621 [INSPIRE].

[40] P. Green and T. Hubsch, *Calabi-Yau manifolds as complete intersections in products of complex projective spaces*, *Commun. Math. Phys.* **109** (1987) 99 [INSPIRE].

[41] C. Borcea, *Homogeneous vector bundles and families of Calabi-Yau threefolds. II*, *Proc. Symp. Pure Math.* **52** (1991), with appendix by J. Kollár.

[42] K. Oguiso and T. Peternell, *Calabi-Yau threefolds with positive second Chern class*, *Comm. Anal. Geom.* **6** (1998) 153.

[43] V. Lazić, K. Oguiso and T. Peternell, *The Morrison-Kawamata cone conjecture and abundance on Ricci flat manifolds*, arXiv:1611.00556.

[44] M. Cvetič, J. Halverson, D. Klevers and P. Song, *On finiteness of Type IIB compactifications: Magnetized branes on elliptic Calabi-Yau threefolds*, *JHEP* **06** (2014) 138 [arXiv:1403.4943] [INSPIRE].

[45] S. Hosono, A. Klemm, S. Theisen and S.-T. Yau, *Mirror symmetry, mirror map and applications to Calabi-Yau hypersurfaces*, *Commun. Math. Phys.* **167** (1995) 301 [hep-th/9308122] [INSPIRE].

[46] S. Hosono, A. Klemm, S. Theisen and S.-T. Yau, *Mirror symmetry, mirror map and applications to complete intersection Calabi-Yau spaces*, *Nucl. Phys.* **B 433** (1995) 501 [*AMS/IP Stud. Adv. Math.* **1** (1996) 545] [hep-th/9406055] [INSPIRE].

[47] P. Candelas, X.C. De La Ossa, P.S. Green and L. Parkes, *A pair of Calabi-Yau manifolds as an exactly soluble superconformal theory*, *Nucl. Phys.* **B 359** (1991) 21 [*AMS/IP Stud. Adv. Math.* **9** (1998) 31].

[48] H. Clemens, *Some results about Abel-Jacobi mappings*, in *Topics in transcendental algebraic geometry*, Ann. of Math. Stud. volume 106, Princeton University Press, Princeton U.S.A. (1984).

[49] S. Katz, *On the finiteness of rational curves on quintic threefolds*, *Compos. Math.* **60** (1986) 151.

[50] R. Pandharipande and R.P. Thomas, *13/2 ways of counting curves*, *Lond. Math. Soc. Lect. Note Ser.* **411** (2014) 282 [arXiv:1111.1552] [INSPIRE].

[51] E. Buchbinder, A. Lukas, B. Ovrut and F. Ruehle, *Heterotic instanton superpotentials from complete intersection Calabi-Yau manifolds*, *JHEP* **10** (2017) 032 [arXiv:1707.07214] [INSPIRE].

[52] D.R. Morrison and C. Vafa, *Compactifications of F-theory on Calabi-Yau threefolds. 1*, *Nucl. Phys.* **B 473** (1996) 74 [hep-th/9602114] [INSPIRE].

[53] P. Green and T. Hubsch, *Calabi-Yau hypersurfaces in products of semiample surfaces*, *Commun. Math. Phys.* **115** (1988) 231 [INSPIRE].

[54] R. Donagi, Y.-H. He, B.A. Ovrut and R. Reinbacher, *The particle spectrum of heterotic compactifications*, *JHEP* **12** (2004) 054 [hep-th/0405014] [INSPIRE].

[55] P.S. Aspinwall and M. Gross, *Heterotic-heterotic string duality and multiple K3 fibrations*, *Phys. Lett.* **B 382** (1996) 81 [hep-th/9602118] [INSPIRE].

[56] A. Grassi and D.R. Morrison, *Automorphisms and the Kähler cone of certain Calabi-Yau manifolds*, *Duke Math. J.* **71** (1993) 831.

[57] D.R. Morrison, *Compactifications of moduli spaces inspired by mirror symmetry*, in *Journées de Géométrie Algébrique d'Orsay (Juillet 1992)*, A. Beauville et al. eds., Astérisque volume 218,, Société Mathématique de France, France (1993), alg-geom/9304007.

[58] I. I. Piateckiii-Shapiro and I. R. Shafarevich, *A Torelli theorem for algebraic surfaces of type K3*, *Math. USSR Izv.* **5** (1971) 547.

[59] C.M. Hull and P.K. Townsend, *Unity of superstring dualities*, *Nucl. Phys.* **B 438** (1995) 109 [hep-th/9410167] [INSPIRE].

[60] C.T.C. Wall, *Classification problems in differential topology V. On certain 6-manifolds*, *Invent. Math.* **1** (1966) 355.

[61] L.B. Anderson, A. Constantin, S.-J. Lee and A. Lukas, *Hypercharge flux in heterotic compactifications*, *Phys. Rev.* **D 91** (2015) 046008 [arXiv:1411.0034] [ɪɴSPIRE].

[62] L.B. Anderson, A. Constantin, J. Gray, A. Lukas and E. Palti, *A comprehensive scan for heterotic* SU(5) *GUT models*, *JHEP* **01** (2014) 047 [arXiv:1307.4787] [ɪɴSPIRE].

[63] L.B. Anderson, J. Gray, A. Lukas and E. Palti, *Heterotic line bundle standard models*, *JHEP* **06** (2012) 113 [arXiv:1202.1757] [ɪɴSPIRE].

[64] L.B. Anderson, J. Gray, A. Lukas and E. Palti, *Two hundred heterotic standard models on smooth Calabi-Yau threefolds*, *Phys. Rev.* **D 84** (2011) 106005 [arXiv:1106.4804] [ɪɴSPIRE].

[65] L.B. Anderson, J. Gray, Y.-H. He and A. Lukas, *Exploring positive monad bundles and a new heterotic standard model*, *JHEP* **02** (2010) 054 [arXiv:0911.1569] [ɪɴSPIRE].

[66] L.B. Anderson, Y.-H. He and A. Lukas, *Heterotic compactification, an algorithmic approach*, *JHEP* **07** (2007) 049 [hep-th/0702210] [ɪɴSPIRE].

[67] E.I. Buchbinder, A. Constantin, J. Gray and A. Lukas, *Yukawa unification in heterotic string theory*, *Phys. Rev.* **D 94** (2016) 046005 [arXiv:1606.04032] [ɪɴSPIRE].

[68] S. Blesneag, E.I. Buchbinder, P. Candelas and A. Lukas, *Holomorphic Yukawa couplings in heterotic string theory*, *JHEP* **01** (2016) 152 [arXiv:1512.05322] [ɪɴSPIRE].

[69] Y.-H. He, S.-J. Lee and A. Lukas, *Heterotic models from vector bundles on toric Calabi-Yau manifolds*, *JHEP* **05** (2010) 071 [arXiv:0911.0865] [ɪɴSPIRE].

[70] Y.-H. He, M. Kreuzer, S.-J. Lee and A. Lukas, *Heterotic bundles on Calabi-Yau manifolds with small Picard number*, *JHEP* **12** (2011) 039 [arXiv:1108.1031] [ɪɴSPIRE].

[71] Y.-H. He, S.-J. Lee, A. Lukas and C. Sun, *Heterotic model building:* 16 *special manifolds*, *JHEP* **06** (2014) 077 [arXiv:1309.0223] [ɪɴSPIRE].

[72] L.B. Anderson, J. Gray, A. Lukas and B. Ovrut, *The Atiyah class and complex structure stabilization in heterotic Calabi-Yau compactifications*, *JHEP* **10** (2011) 032 [arXiv:1107.5076] [ɪɴSPIRE].

[73] L.B. Anderson, J. Gray, A. Lukas and B. Ovrut, *Stabilizing all geometric moduli in heterotic Calabi-Yau vacua*, *Phys. Rev.* **D 83** (2011) 106011 [arXiv:1102.0011] [ɪɴSPIRE].

[74] L.B. Anderson, J. Gray and B.A. Ovrut, *Transitions in the web of heterotic vacua*, *Fortsch. Phys.* **59** (2011) 327 [arXiv:1012.3179] [ɪɴSPIRE].

[75] L.B. Anderson, J. Gray, A. Lukas and B. Ovrut, *Stabilizing the complex structure in heterotic Calabi-Yau vacua*, *JHEP* **02** (2011) 088 [arXiv:1010.0255] [ɪɴSPIRE].

[76] L.B. Anderson, J. Gray, A. Lukas and B. Ovrut, *Stability walls in heterotic theories*, *JHEP* **09** (2009) 026 [arXiv:0905.1748] [ɪɴSPIRE].

[77] L.B. Anderson, J. Gray, A. Lukas and B. Ovrut, *The edge of supersymmetry: stability walls in heterotic theory*, *Phys. Lett.* **B 677** (2009) 190 [arXiv:0903.5088] [ɪɴSPIRE].

[78] A. Kanazawa and P.M.H. Wilson, *Trilinear forms and Chern classes of Calabi-Yau threefolds*, arXiv:1201.3266.

[79] P.M.H. Wilson, *Calabi-Yau manifolds with large Picard number*, *Invent. Math.* **98** (1989) 139.

[80] D.R. Morrison and W. Taylor, *Classifying bases for* 6D *F-theory models*, *Central Eur. J. Phys.* **10** (2012) 1072 [arXiv:1201.1943] [ɪɴSPIRE].

[81] D.R. Morrison and W. Taylor, *Toric bases for* 6D *F-theory models*, *Fortsch. Phys.* **60** (2012) 1187 [arXiv:1204.0283] [ɪɴSPIRE].

[82] W. Taylor, *On the Hodge structure of elliptically fibered Calabi-Yau threefolds*, *JHEP* **08** (2012) 032 [arXiv:1205.0952] [INSPIRE].

[83] G. Martini and W. Taylor, *6D F-theory models and elliptically fibered Calabi-Yau threefolds over semi-toric base surfaces*, *JHEP* **06** (2015) 061 [arXiv:1404.6300] [INSPIRE].

[84] W. Taylor and Y.-N. Wang, *Non-toric bases for elliptic Calabi-Yau threefolds and 6D F-theory vacua*, arXiv:1504.07689 [INSPIRE].

[85] R. Blumenhagen, S. Moster, R. Reinbacher and T. Weigand, *Massless spectra of three generation* U(N) *heterotic string vacua*, *JHEP* **05** (2007) 041 [hep-th/0612039] [INSPIRE].

[86] R. Donagi, A. Grassi and E. Witten, *A nonperturbative superpotential with E_8 symmetry*, *Mod. Phys. Lett.* **A 11** (1996) 2199 [hep-th/9607091] [INSPIRE].

[87] I. Morrison and U. Persson, *The group of sections on a rational elliptic surface*, in *Algebraic geometry — Open problems*, C. Ciliberto et al. eds., Lecture Notes in Mathematics volume 997, Springer, Berlin Germany (1983).